



University of
Stavanger

Faculty of Science and Technology

MASTER'S THESIS

Study program/ Specialization:

Offshore Technology / Marine and Subsea
Technology

Spring semester, 2015
Open / ~~Restricted~~ access

Writer:

Muthuraman Nagarathinam

(Writer's signature)

Faculty supervisor: Sverre Kristian Haver, Professor, University of Stavanger

External supervisor(s): Xinying Zhu, Discipline Lead-Analysis, Ocean Installer AS

Thesis title:

Installation Analyses of a Subsea Structure

Credits (ECTS): 30

Key words:

Subsea Structure, Installation analysis, dynamic
analysis, Vessel motions, RAO, Transfer functions,
Heave compensation, Limiting sea state, Marine
operations, Haltenbanken, Scatter diagram,
Hindcast, Weather window

Pages: 78 + enclosure: 66 pages

Stavanger, June 12th, 2015

MASTER THESIS IN MARINE AND SUBSEA TECHNOLOGY

Spring 2015

For

Sverre Kristian Haver

Installation Analyses of a Subsea Structure

Marine operations do generally require rather good weather for a certain time in order to be executed by a reasonable safety margin. If operation is done using a certain vessel, the vessel motions are the parameters that determine whether or not an operation can be performed. The critical vessel motion will vary from operation to operation, but often the heave motion will be the important motion. Slowly varying motions like surge and yaw is often limited by applying dynamic positioning devices. Thus emphasis is in most often given to the wave frequent motions.

Although it is vessel motions (or response function caused by vessel motions) that is limiting the execution of an operation, it is for planning and execution very useful to establish the limiting wave conditions for a given operation. In the thesis limiting weather condition shall be identified for a given operation – an actual operation or a generic operation. The vessel motions can be assumed to be linear functions of the wave process. This will be inaccurate for rolling and it will only be valid for small rolling angles.

In the thesis the focus will be on the early planning of a marine operation. The purpose is to investigate the feasibility of the planned operation in various seasons. Variability in number of available weather windows for each month and the variability from year to year shall be investigated. As a base case, the sea state is characterized by the significant wave height and spectral peak period in combination with a JONSWAP spectrum. Results shall be assessed for at least two vessels. If time permits results regarding feasibility can be compared for another offshore area.

The necessary weather information will be given by the Norwegian hindcast data base, NORA10, giving weather characteristics every 3 hours from September 1st 1957 – June 30th 2011.

Below a possible division into sub-tasks is given.

1. Describe the offshore operation you planned to study. The critical response parameter shall be specified together the accept criteria for this parameter, e.g. the b-percentile of the 3-hour extreme value distribution. The duration of operation should also be given.
2. Prepare the hindcast data file by:
 - “correcting” the wind speed for cases with mean wind speed in excess of 15m/s.
 - Randomize the spectral peak period.A reference describing how this can be done will be provided.
Present monthly and annual scatter diagrams for Hs and Tp.
3. Determine the values of significant wave height and spectral peak period for which the sea state is acceptable for the marine operation. Determine the percentage of time sea states are below the accept level for all year and month by month. This can be done by screening the hindcast data file. A window referring to a given month should start in the month, but it may in in the following month.
4. For the weather limit and the required window length for the operation, establish the number of possible operation windows for the whole period 1957 – 2014. Determine the no. of window for the

various months show variability from year to year.

5. Investigate sensitivity of the feasibility to the length of the operation of 50% and 200 % of the duration required for operation above.
6. In most practical cases heave compensation is introduced for cranes used for marine operation. Discuss the consequences of heave compensation on feasibility of a selected operation.
7. Show sensitivity of crossing sea regarding the feasibility of a given operation. Use the wind sea and swell sea characteristics as provided by NORA10. Use a JONSWAP spectrum with peakedness equal to 1 both for the wind sea and the swell sea. Assume that ship is heading into the wind sea and calculate the maximum rolling during the operation period. Assume in this connection that rolling is a linear function of the wave process. Discuss this assumption. Introduce a rolling amplitude of 4σ as unacceptable for operation and investigate if crossing sea is of importance regarding planning of operations.
8. For an operation requiring 72 hours of acceptable weather in order to be completed in one go, investigate if there is a gain of redesigning it so it can performed in two phases. Duration of first phase is 48 hours and the last 36 hours. This can be done by estimating the expected duration until operation is completed for each month for the two designs of the operation.

The candidate may of course select another scheme as the preferred approach for solving the requested problem.

The work may show to be more extensive than anticipated. Some topics may therefore be left out after discussion with the supervisor without any negative influence on the grading.

The candidate should in his report give a personal contribution to the solution of the problem formulated in this text. All assumptions and conclusions must be supported by mathematical models and/or references to physical effects in a logical manner. The candidate should apply all available sources to find relevant literature and information on the actual problem.

The report shall be well organised and give a clear presentation of the work and all conclusions. It is important that the text is well written and that tables and figures are used to support the verbal presentation. The report should be complete, but still as short as possible.

The final report must contain this text, an acknowledgement, summary, main body, conclusions, suggestions for further work, symbol list, references and appendices. All figures, tables and equations must be identified by numbers. References should be given by author and year in the text, and presented alphabetically in the reference list. The report must be submitted in two copies unless otherwise has been agreed with the supervisor.

The supervisor may require that the candidate should give a written plan that describes the progress of the work after having received this text. The plan may contain a table of content for the report and also assumed use of computer resources. As an indication such a plan should be available by mid March.

From the report it should be possible to identify the work carried out by the candidate and what has been found in the available literature. It is important to give references to the original source for theories and experimental results.

The report must be signed by the candidate, include this text, appear as a paperback, and - if needed - have a separate enclosure (binder, diskette or CD-ROM) with additional material.

Supervisor:

Sverre Haver, University of Stavanger.

PREFACE

After all the theoretical subjects are learnt for a while, writing a thesis which is a part of curriculum, with the learnt knowledge has been an interesting task. The curiosity on the research has never stopped. Every day passes with a new learning and understanding. Going through the Master Programme at University of Stavanger is a great experience and improved my technical working life. Especially, the curriculum for the Master programme in Marine and Subsea Technology which covers a variety of subjects, did change the perception of looking at the Oil and Gas Industry where I have a decade of experience.

It has been a really great experience doing my Masters at University of Stavanger!

ACKNOWLEDGEMENT

I am grateful to Sverre Haver for guiding me on this thesis topic by his questioning skills, helping tendency, motivation skills. Whenever I have been frustrated during this study, his motivation and support boost me to go along. He is a great example in my life as he has shown how to teach or guide a student. This will certainly help in my work life.

I would like to thank my external supervisor Xinying Zhu for her guidance on understanding the SIMA software and technical details. She helped me to retrieve the needed information during this study, despite her busy work schedule.

Besides the supervisors, there are many people helped me at Ocean Installer AS by having good discussion, lending study materials or sharing their experience. In this regard, I would like to thank Jin Ping Zhan, Abdilahi Qayre, Shiva Gowda and Tau Nielsen.

Also, I would like to thank Randi Moe, Engineering Manager, Ocean Installer AS for getting internal approval inside the company to carry out this task.

Thanks to Jason Dunlap for proof reading of this thesis and lending his support with various technical documents.

Finally, I would like to thank my family members and friends for their moral support during this study.

Stavanger, June 2015

Muthuraman Nagarathinam

ABSTRACT

A typical installation of a subsea structure with mono hull offshore construction vessel is studied. Focus has been on the vessel motions, lifting arrangement and the planning of this operation.

The behaviour of vessel motions are studied with the available transfer functions of the vessel at centre of gravity. The key transfer functions for Heave, Pitch and Roll are discussed when the wave propagates in head and beam seas. The transfer functions used are qualitatively verified for their correctness and usage in this study. Then, the heave motion at two different points far away from the CoG of the vessel are studied to see the difference in heave motion. Transfer functions at cranetip are derived, as this is the main excitation for the dynamics on the crane wire. The derived transfer function at the crane tip is verified against the results from SIMA software.

In the lifting arrangement study, transfer functions for the vertical motion of the suspended load are derived by assuming linear relationship between crane tip motion and motion of the mass. Then, using that transfer function, the transfer function for the dynamic tension on the crane wire is derived for the wave in head sea and beam sea. To improve the lifting arrangement system, the heave compensation system is introduced with a discussion about its efficiency.

To obtain the limiting sea state for this operation, a deterministic and a stochastic approach have been followed. In the stochastic method, JONSWAP spectrum is used for the total sea case which propagated in head sea and beam sea respectively. Then, combined sea spectrum i.e. double peak spectrum for the wind sea with head sea direction introduced and swell sea which here is simplified to always propagate between the direction of head and beam seas, is used to obtain limiting sea state accounting the effect of crossing sea approximately. Respective response spectrum is then derived based on linearity of the response and assumption that response of swell sea is not effected by the wind sea from a different direction and vice versa. The discussion is made about the comparison of the approaches followed to obtain the limiting sea state. Sensitivity study on the probability of exceedance of critical response is shown as well.

For planning of this operation, 60 years of hindcast data are used. The hindcast data taken are corrected based on the wind speed measurement available. And the discrete values of the spectral peak period in the data are uniformly distributed. After randomization of T_p , annual and monthly scatter tables of H_s and T_p , and plots have been produced to see the percentage of times available for a sea state during a year and monthly. Likewise, for $H_s \leq 2\text{m}$, the average percentages of non-exceedance of this sea state are produced for various months. Since the scatter table do not give any info regarding the duration of the sea state, the average durations of sea state for $H_s \leq 1\text{ m}$, 2 m , and 3 m are calculated. Then, since number of available windows are useful for planning an operation, the average number of windows available for $H_s \leq 2\text{m}$, and duration 6, 12, 24, 48, 72 hours are screened through the hindcast data and presented. Finally, dividing an operation into smaller phases, here 72 hours operations divided into 48+24 hours, 24+24+24 hours, are studied and discussed about the change in percentage of successful operation and average number of days to complete that operation, in a month using the 60 years of hindcast data.

Table of Contents

1.	Introduction.....	12
2.	Installation Methods	13
2.1.	Traditional method.....	13
2.2.	Submerged towing	13
2.3.	Pencil Buoy Method.....	13
3.	Phases of lifting	14
3.1.	Lifting in Air	14
3.2.	Lifting through splash zone.....	14
3.3.	Lowering through water column.....	14
3.4.	Landing on seabed	14
4.	Description of operations.....	15
4.1.	Subsea Structure details	15
4.2.	Durations.....	15
5.	Vessel Information	16
5.1.	Vessel Parameters	16
5.2.	Crane data	16
6.	Limiting Criteria	18
7.	Description of Waves	19
7.1.	Regular Waves	19
7.2.	Irregular Waves.....	20
7.2.1.	JONSWAP Spectra	21
7.2.2.	Crossing Sea Spectrum	22
8.	Transfer functions.....	23
8.1.	Co-ordinate system	23
8.2.	Motion transfer function of Vessel at CoG.....	23
8.2.1.	Heave Motion Transfer functions	24
8.2.2.	Pitch Motion Transfer functions	27
8.2.3.	Roll Motion Transfer functions.....	29
8.2.4.	RAO Quality Check.....	31
8.3.	Motion transfer function of Crane-tip.....	33
8.4.	Motion transfer function of Equipment.....	38
8.5.	Dynamic tension transfer function of Equipment	40

9. Response Spectrum	42
9.1. Response Spectrum of Total Sea	42
9.2. Combined Response Spectrum of Wind and Swell Sea.....	43
10. Heave Compensation	45
10.1. Passive Heave Compensation	45
10.2. Active Heave Compensation.....	49
11. Limiting Sea-state	50
11.1. Deterministic approach	50
11.2. Stochastic Approach	51
12. Planning of Marine Operations	56
12.1. Wind Speed Correction.....	56
12.2. Randomizing spectral peak periods	57
12.3. Annual and Monthly Scatter Table	62
12.4. Percentage of times non-exceedance of sea-state	65
12.5. Average duration of a sea state	66
12.6. Number of possible Weather Window	68
12.7. Sensitivity of weather window with respect to duration	71
12.8. Benefits of dividing the operation into phases	72
13. Conclusion	75
14. References.....	78
Appendix -1: Crossing Sea Spectral Parameters	79
Appendix -2: Monthly Scatter Tables.....	82
Appendix -3: Total No. of Windows in Month wise.....	95
Appendix -4: Duration to complete a operation in Month wise	101
Appendix -5: Matlab Scripts.....	105

Abbreviations

AHC	Active Heave Compensation
DAF	Dynamic Amplification Factor
FOW	Full of Water
H _s	Significant Wave Height
LOA	Length of Overall of Vessel
LPP	Length between perpendiculars
MRU	Motion Reference Unit
OG21	Oil and Gas in 21 Century
PHC	Passive Heave Compensators
RAO	Response Amplitude Operator
SWL	Safe Working Load
t / Ton	1000 kg
T _p	Spectral Peak Period
WD	Water Depth

1. Introduction

The subsea field development is moving towards to bring all the top side equipment to the sea floor. In addition, the industry is going larger water depth and harsher environments such as the arctic to meet the demand of oil and gas. OG21 association listed installing the subsea equipment with cost effective method as challenging in the industry.

Marine operations can be defined as any activity carried out offshore, related to any installation, lifting, towing and laying. In general, the success of marine operations depends on the vessel behaviour, lifting arrangement and planning of marine operations. In this study, installing a subsea equipment is considered. This equipment is installed by an onboard crane on the mono hull construction vessel over the side of the vessel.

The selection of the vessel which is not too sensitive to the weather is an important thing for the success of the operation. A vessel sensitive to the waves needs much lower limiting sea state to install which is expensive in terms of cost. The dynamics of the selected vessel (Normand Vision) is discussed in chapter §8.

There are many limiting conditions for installing an equipment. The capacities of the lifting arrangements, clearances between the vessel and equipment and landing velocity are some of them. In this study, it is considered that dynamic capacity of the crane wire is the only limiting criteria. To find out the dynamic tension, the dynamics of the lifting arrangement are to be calculated as presented in chapter §8. In order to calculate the limiting sea state for an operation by stochastic approach, the response spectrum are to be obtained as discussed in chapter § 9.

The limiting sea state for an operation is the highest sea state in which the installation can be performed safely. This is usually obtained by simulating the propagation of waves in different directions towards the vessel. Sometimes, the waves can propagate from two different directions such as wind and swell seas. In order to simulate these irregular waves, the wave spectrum is used as described in chapter § 7.

The lifting arrangement is a key arrangement to have the success of an operation. In this aspects, the heave compensation can be used to improve the effectiveness of the lifting system and thereby the limiting sea state. In the chapter §10.Heave Compensation, different types of heave compensation and their effectiveness are discussed.

The un-planned operations are expensive due to the waiting of vessel for the suitable weather conditions. If the operations could be planned for a period of a year in which the probability of successful installation is high and waiting time for the suitable weather conditions are lesser, then that operation becomes economical. For this purpose of planning an operation, weather statistics made from weather measurements from the past years are required. The weather statistics of 60 years of hindcast data for the Haltenbanken area are used for the planning in this study. These aspects of planning an operation is discussed in chapter §12. However, for the actual execution of marine operations, a reliable weather forecast is needed.

2. Installation Methods

Choosing a relevant installation method based on their limiting conditions is a strategy to improve the probability of success of an operation, with shorter duration of installation time including the waiting period. There are three methods discussed below which have their own advantages and disadvantages. In this study, the traditional method is focused as most of the subsea equipment in the industry are installed by the traditional method. It is evident that, the industry is focusing on methods of installation that are more cost effective and efficient.

2.1. Traditional method

A subsea structure is traditionally transported on the deck of a crane vessel or on a barge. The traditional method consists of stages of lifting the structure from barge or crane vessel, slew around to the side of the vessel, lowering through splash zone, lowering through water column, at last landing on the sea floor or on top of another piece of equipment.

2.2. Submerged towing

The submerged towing is an alternative method to traditional installations, when no heavy lift vessels are available. This method of installation has a wider operational window due to the avoidance of stages such as lift in air and lift through splash zone. However, the disadvantage of this method is, transit time takes longer than the traditional installation due to the towing through water column. (Kenneth, Aarset; Sarkar, Arunjyoti; Karunakaran, Daniel;, 2011, January 1)

2.3. Pencil Buoy Method

The pencil buoy method is patented by Aker Marine Contractors. This method is similar to the submerged towing concept mentioned above except the pencil buoy. In this method, a subsea equipment is suspended from pencil buoy during towing to an offshore field. The offshore operation is performed as a winch operation rather than lowering through splash zone. (Risoey, Mork, Johnsgard, & Gramnaes, 2007, January 1)

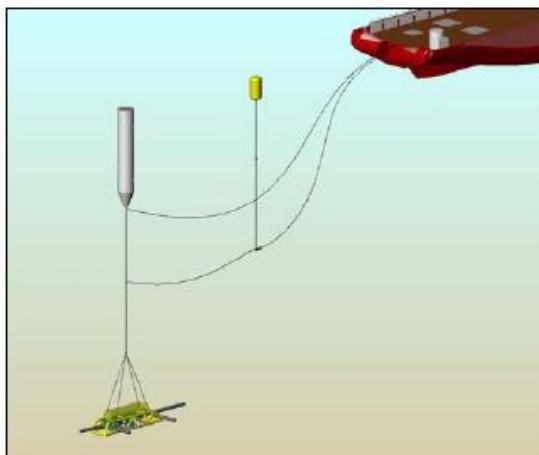


Figure 2-1: Lifting arrangement of Pencil Buoy Method (Risoey, Mork, Johnsgard, & Gramnaes, 2007, January 1)

3. Phases of lifting

There are four different phases of installation in the traditional method of installation. In each phase, there are some limiting factors which influence the installation criteria. Those limiting factors are discussed below. But in this study, the first phase of the operation is mainly focused.

3.1. Lifting in Air

The phase of lifting an object in air is the first phase of the operation in the traditional method of installation. This phase experiences the pendulum motion and spring action due to the stiffness in the wire. The pendulum motions can be controlled by arrangement of tugger winches or any other innovative systems. When the equipment is lifted off from the vessel deck or barge, there will be a dynamic tension variation on the crane wire due to transient response. This transient response due to the initial conditions are not considered for this study. Only steady state response of the crane wire is considered.

3.2. Lifting through splash zone

Passing of an equipment through the splash zone is challenging, most of the times, it is the limiting factor for the seastate. There are few methods evolved to get rid of this zonal lifting. The loads are varying with respect to time in this zone. The wave profile on the surface of equipment changes with respect to time, hence the load due to them also. The buoyancy also varies. This is the phase where the dangerous snap load on the wire would happen. The snap load occurs when the tension on the wire increase from zero to full in very short period. The snap load will be equal to twice as the actual static load. Slamming on the equipment is also an important concern in this stage.

3.3. Lowering through water column

In this phase, the pendulum motion is not any more a problem as the surrounding water acts as a damper. As the length of crane wire increases, the stiffness of the wire decreases, therefore, the natural frequency of the lifting system also decreases. So, the change in natural frequency of the lifting system with respect to water depth could have lead to resonance between crane tip motion and the motion of equipment. The dynamic loading is mainly caused by the crane tip motion of the vessel. It is also a concern that, if there is a current present on the field, the module will be drifted in the direction of the current.

3.4. Landing on seabed

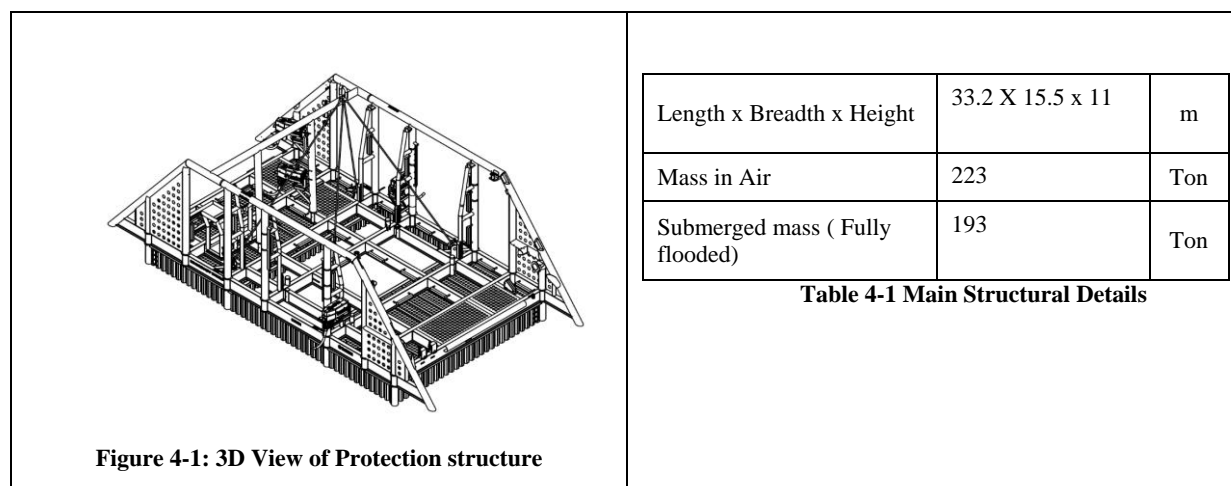
The landing on the seabed may be restricted by the velocity or acceleration of the equipment. This is due to avoid any damage to the equipment or disturbance of the soil condition. The installation aid such as Passive Heave Compensation can be used to reduce the landing velocity. In this phase, care should be taken to transfer the load to the seabed slowly with the simultaneous operation of de-ballasting if there is a counter weight on the ballast tank to avoid uneven keel of the vessel, when the suspended weight is on the side of the vessel. Abrupt landing on the seabed with the counter weight leads to high rolling of vessel on the opposite direction.

4. Description of operations

As a part of the Draugen field development, a subsea boosting pump station has to be installed in order to improve the recovery rate by pressurising. The pump station installed as two heavy lifts, one with Pump protection structure and the second one is pump itself. This study deals with the installation of the pump protection structure. This structure is lift-off from the deck, slewed and lowered through the port side of the vessel as shown in Figure 5-2. In case of weather deterioration, the structure will be abandoned at a pre-defined emergency location on the seabed.

4.1. Subsea Structure details

The protection structure is designed to be an overtrawable structure, also to accommodate the pump station. The protection structure is illustrated in Figure 4-1. The primary structural elements consist of circular steel members and I section members. The skirt foundation made of steel corrugated plates. There are perforated plates, which welded to the “I section” steel members. The centre of gravity of the structure is to be in-line with the hook point during lifting to avoid instability. The constant tension winch is used to avoid any pendulum motions on the air. There are 4 numbers of lifting points on the structure; each has the capacity of 160 ton.



As the actual mass of the structure (223 ton) did not influence the dynamic tension on the wire significantly in the air for the steady state response, the mass has been assumed to be 10 times the actual mass i.e. 2230 ton for the academic illustration purpose of this study.

4.2. Durations

The operation is planned for 8 hours (T_{POP}). Since this kind of operation has extensive experience, the contingency time (T_C) is chosen as 50% of planned operation period (T_{POP}). The duration of the marine operations shall be defined by Operation reference period (T_R) (DNV-OS-H101, 2011)

$$T_R = T_{POP} + T_C = 8 + 4 = 12 \text{ hours}$$

The above-mentioned duration is typical for this kind of marine operations.

5. Vessel Information

The Offshore Construction Support Vessel “Normand Vision” is installing the protection structure. The vessel has good see keeping capability as it has a state of the art of DP3 dynamic positioning system. The dynamic positioning system will be in active mode during this lifting operation.

5.1. Vessel Parameters

The main particulars of the vessel are shown in Table 5-1 (Vessel Info, 2015).

Vessel Name	Normand Vision	
Length Overall (LOA)	156.7	m
Length between perpendiculars (LPP)	144.6	m
Maximum Draught	8.5	m
Moulded Breadth	27	m
Moulded Depth	12	m
Dead weight	12000	Ton

Table 5-1 Vessel Properties

5.2. Crane data

The capacity of the crane to install a subsea structure is one of the limiting factors to decide, if the structure could be installed. The vessel has 400 Ton main crane with Active Heave Compensation (AHC). The mentioned capacity will be varying depending on the boom tip height and working radius based on mechanical and structural strength of the crane. The operational limit of wind speed is 20 m/s for this crane. In addition, the heel of the vessel shall be less than 5° to avoid high moment on the pedestal during heavy lift. Otherwise, this will lead to stability issue of the vessel. Also the maximum pitch limitation is 2°. The working radius for the crane is chosen as 18 m from the centre of pedestal. The crane centre on the main deck is located (-35.8 m, 11m, 5 m) with respect to the global origin defined in §8.1.

- Working radius of crane = 18 m
- Crane tip height from the deck = 51 m

The crane has two lift modes for heavy structure installation. The internal lift mode is described as the stage from the module is lifted from the deck to before the splash zone. Whereas subsea lift is defined as from splash zone to the seabed.

Dynamic amplification factor is defined as,

$$\text{Dynamic Amplification Factor (DAF)} = \frac{\text{Static} + \text{Dynamic Tension}}{\text{Static Tension}}$$

The DAF value shown below are assumed for this lifting operation.

- Maximum allowable SWL (Safe Working Load) = 225 t for subsea lift (DAF=1.3)
- Maximum allowable SWL = 250 t for internal lift (DAF=1.3)
 - Maximum allowable dynamic tension in the wire = 1.3 *250 - 250 = 75 t

For the illustration of variation of crane wire weight with water depth, the below data are used.

Mass of crane wire in air = 77.8 kg/m

Mass of crane wire in submerged condition = $0.87 * 77.8 = 67.7$ kg/m (assumed)

Mass of crane block = 12 t

Assuming, the height of wire from crane tip and the still water level is 20 m, then the variation of the wire weight with respect to water depth is shown Figure 5-1. The static wire weight at the crane tip is linearly increasing with respect to the water depth. It can be seen that considerable amount of allowable crane capacity is taken by the weight of the wire itself. At the water depth of 1200 m, the weight of wire occupies the 35 % of the maximum allowable crane capacity. In deep water and ultra-deep water fields, one of the restrictions for installing the heavy weight subsea equipment is due to the weight of the crane wire.

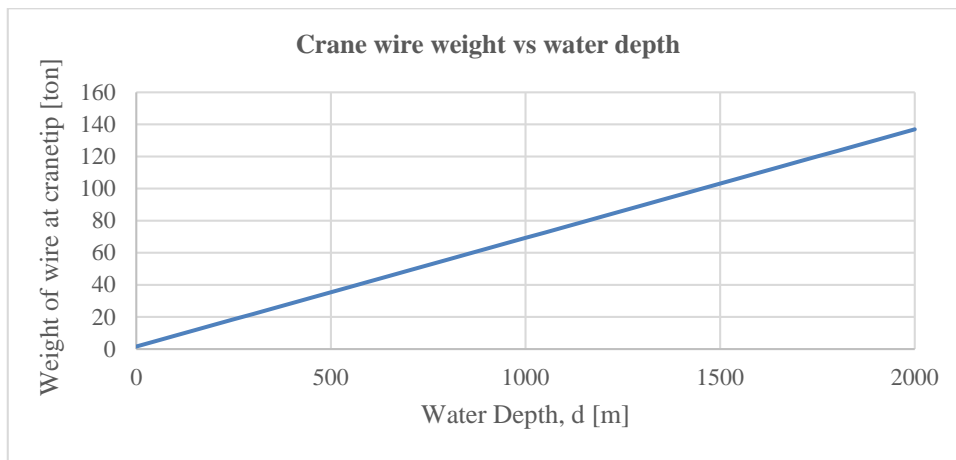


Figure 5-1: Crane wire weight at crane tip vs water depth

The lifting system consists of elements such as crane steel structure, crane wire, soft slings, master links, etc as shown in Figure 5-2. Each element has its own stiffness value. The combined stiffness value of these elements are needed for analysis. As these elements in series connection, the equivalent stiffness value, k_{eq} is calculated by,

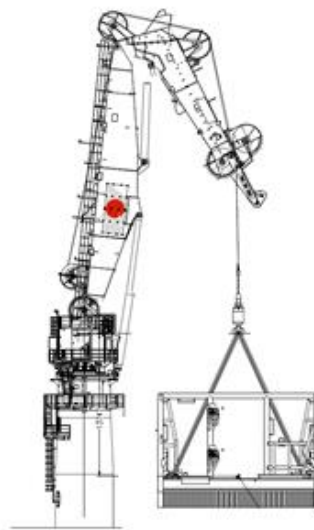


Figure 5-2: Illustrating the typical lifting arrangement

$$\frac{1}{k_{eq}} = \frac{1}{k_{crane\ steel\ structure}} + \frac{1}{k_{wire}} + \frac{1}{k_{others}}$$

For this study, the crane structure is assumed as rigid. That means the stiffness of the crane structure is infinite. Only, the stiffness of the crane wire is considered.

$$k_{wire} = \frac{EA}{L} = 7690\text{ kN/m}$$

EA – Axial stiffness of the wire (430000 kN, assumed); L – Length of wire (56 m)

It can be seen that, the stiffness of wire is inversely proportional to its length. Hence, in the deep water case, the stiffness of the system reduced, thus natural frequency as well. This may lead to resonance with the crane tip motion, when oscillation frequency match with the natural frequency of the lifting system.

6. Limiting Criteria

The limiting parameters for ta installation can be many. They can be overall dimensions and weight of lifted object, vessel limitations such as dynamic hook load capacity and weather limitations.

The overall dimension of a structure is one of the parameter which will decide an installation program by choosing the right vessel to accommodate them. This should be foreseen during the planning of field development concept. So that, the structural size can be decided based on the installation program. During lowering through the splash zone, the hydrodynamic forces depends on the shape of the structure. This will also limit the operational conditions.

The transportation of lifted object can also influence the installation programme. If the crane vessel has not have enough deck capacity to transport, then the structure should be transported via either barge or another bigger vessel, which has the sufficient deck capacity.

The lifting equipment can also be a limiting factor, if the capacities are not suitable to carry the load imposed on them. Especially, the lifting pad eyes on the structure, which are usually designed before the dynamic analysis is carried out. In some cases, the sling between pad eye and hook limits, if they are not chosen according the calculated dynamic forces. The capacities of lifting equipment are given as

- Lift point capacity on the structure = 160 ton = 1570 kN
- Sling capacity MBL of 600 ton, Length = 16.2 m

When it comes to critical limiting criteria, the dynamic hook load and the slack on the sling are the most important things. The dynamic hook load depends upon the working radius and boom tip height. In this study, the dynamic hook load is considered as the only limiting criteria. Other factors mentioned above is assumed to have sufficient capacity in order to carry the installation with the seastate considered for the analysis.

- Maximum allowable SWL = 225 t for subsea lift
- Maximum allowable SWL = 250 t for internal lift

7. Description of Waves

7.1. Regular Waves

The simplest wave theory is airy wave theory or sinusoidal wave theory which assumes linearized boundary conditions. It ends with the derivation similar to sinusoidal wave which can be termed as regular wave.

The parameters of regular waves are shown in Figure 7-1. The wave height (H) is the distance between crest and trough of wave in vertical direction. Wave period (T) is the time taken to complete a cycle starting from a crest i.e. interval time between successive crests. Inverse of wave period is defined as wave frequency in Hz. Angular wave frequency in rad/s can be estimated by $2\pi/T$.

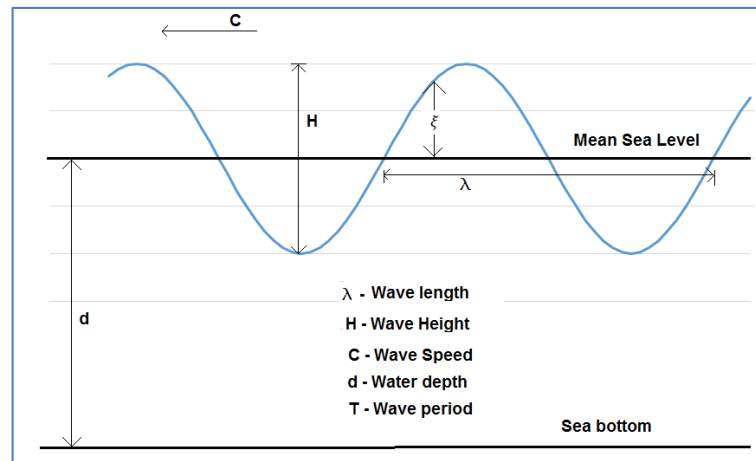


Figure 7-1 Definition of Wave Parameters

The wave surface elevation process for regular waves can be described as a harmonic motion. The wave amplitude elevation for regular wave can be written in the form of

$$\xi(x, t) = \xi_0 \operatorname{Re}[e^{i(\omega t - kx)}] = \xi_0 \cos(\omega t - kx) \quad \text{----Eq. 7.1.1}$$

Where, ω – wave angular frequency in rad/s; t – time in seconds; k – wave number; x is the distance from the origin to the point of interest in X direction.

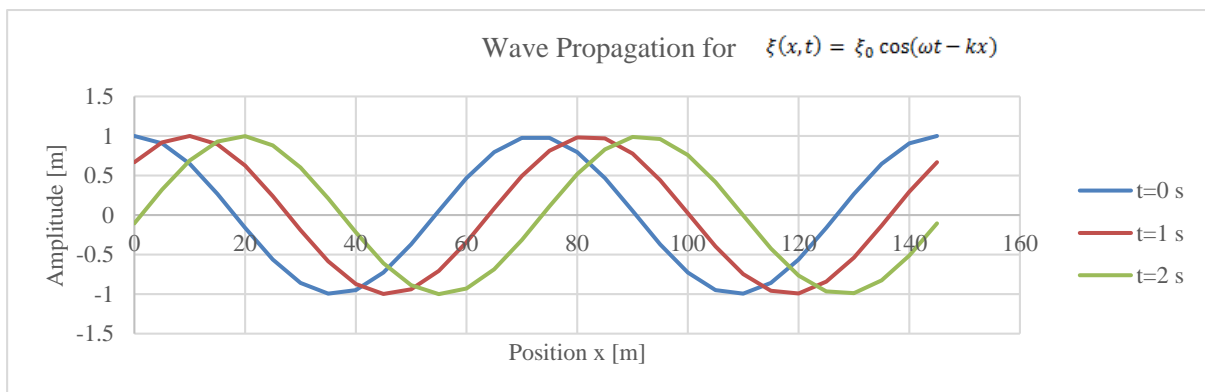


Figure 7-2 Illustration of wave propagation in positive x direction with respect to time and position for a wave $H=2$ m, $T = 7.5$ s

The expression given in Eq.7.1.1 for the wave surface process is propagating in positive X direction as shown in Figure 7-2. If the expression is considered with “+” sign in front of wave number

“k”, the wave will propagate in negative X direction as shown in Figure 7-3. This linear wave theory is referred from (Gudmestad, 2014).

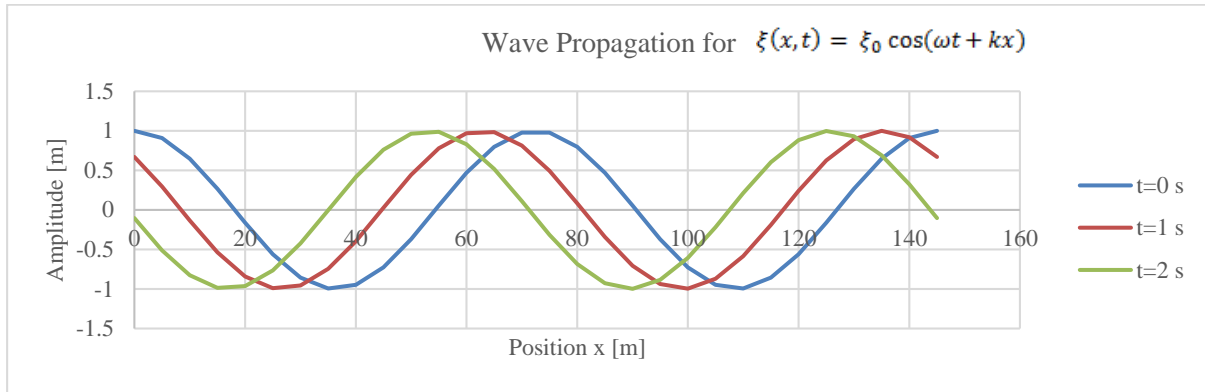


Figure 7-3 Illustration of wave propagation with respect to time and position for a wave $H=2$ m, $T = 7.5$ s

7.2. Irregular Waves

Waves are irregular and random natural phenomena on the surface of the sea. The irregular sea can be described by superimposing many regular waves with different wave heights and wave periods. The phasing angle between each regular waves are also different. As the waves are random in reality, the wave spectrum is introduced to capture the randomness by assuming the sea state is stationary for few hours, typically 3 hours. Stationary means the statistical properties of the sea state such as mean, variance are constant; they don't vary with time.

In the wave spectrum, Significant wave height (H_s) and Spectral Peak Period (T_p) are the key spectral parameters. Two different definitions exist for the Significant wave height. In one way, this can be defined as the mean of the one third of the highest wave heights taken during spectral stationary time (3 hours or 6 hours). In another way, this can be defined as 4 times the square root of variance of the spectrum ($4\sqrt{M_0}$). Variance which is equal to 0th spectral moment can be calculated by taking the area under the spectrum. Spectral peak period is the period where the spectral energy is maximum.

$$\text{The } k^{\text{th}} \text{ spectral moment} \quad M_k = \int_0^{\infty} \omega^k S_{\xi\xi}(\omega) d\omega$$

$$\text{Variance of spectrum} \quad M_0 = \sigma_{\xi\xi}^2 = \sum_{i=1}^N S_{\xi\xi}(\omega_i) \cdot \Delta\omega$$

$$\Delta\omega = \frac{\omega_N - \omega_1}{N - 1}$$

$$\text{Second order spectral moment} \quad M_2 = \sum_{i=1}^N \omega_i^2 S_{\xi\xi}(\omega_i) \cdot \Delta\omega$$

$$\text{Average zero up crossing period} \quad T_z = 2\pi \sqrt{\frac{M_0}{M_2}}$$

If the spectrum is estimated with wave frequency in Hz, then the spectrum shape will vary from the spectrum derived from the angular wave frequency in rad/s as shown in Figure 7-4. However, the variance of the spectrum should be same. The spectrum can be converted from frequency in Hz to radians/sec by,

$$S_{\xi\xi}(\omega) = \frac{S_{\xi\xi}(f)}{2\pi}$$

7.2.1. JONSWAP Spectra

The JONSWAP spectrum is the modified spectrum from Pierson-Moskowitz (PM) spectrum which is given by the expression

$$S_J(\omega) = A_\gamma S_{PM}(\omega) \gamma \exp\left(-0.5\left(\frac{\omega-\omega_p}{\sigma\omega_p}\right)^2\right)$$

ω – wave angular frequency in rad/s

$$A_\gamma = 1 - 0.287 \ln(\gamma)$$

γ – non-dimensional peak shape parameter, ($\gamma = 2$) is considered

$$S_{PM}(\omega) = \frac{5}{16} H_s^2 \omega_p^4 \omega^{-5} \exp\left(-\frac{5}{4}\left(\frac{\omega}{\omega_p}\right)^{-4}\right)$$

$S_{PM}(\omega)$ - Pierson-Moskowitz (PM) spectrum

H_s - Significant wave height in m

ω_p - Angular spectral frequency = $\frac{2\pi}{T_p}$ (rad/s)

T_p - Spectral peak period in seconds

σ – spectral width parameter, $\sigma = \sigma_a = 0.07$ for $\leq \omega_p$, else , $\sigma = \sigma_b = 0.09$. Average values of experimental data is considered.

The Jonswap spectra is reasonable model when, $3.6 < T_p/\sqrt{H_s} < 5$, (DNV-RP-C205, 2010). Based on this condition, the relevant spectral peak periods are 7 s to 11 s for the significant wave height up to 8 m.

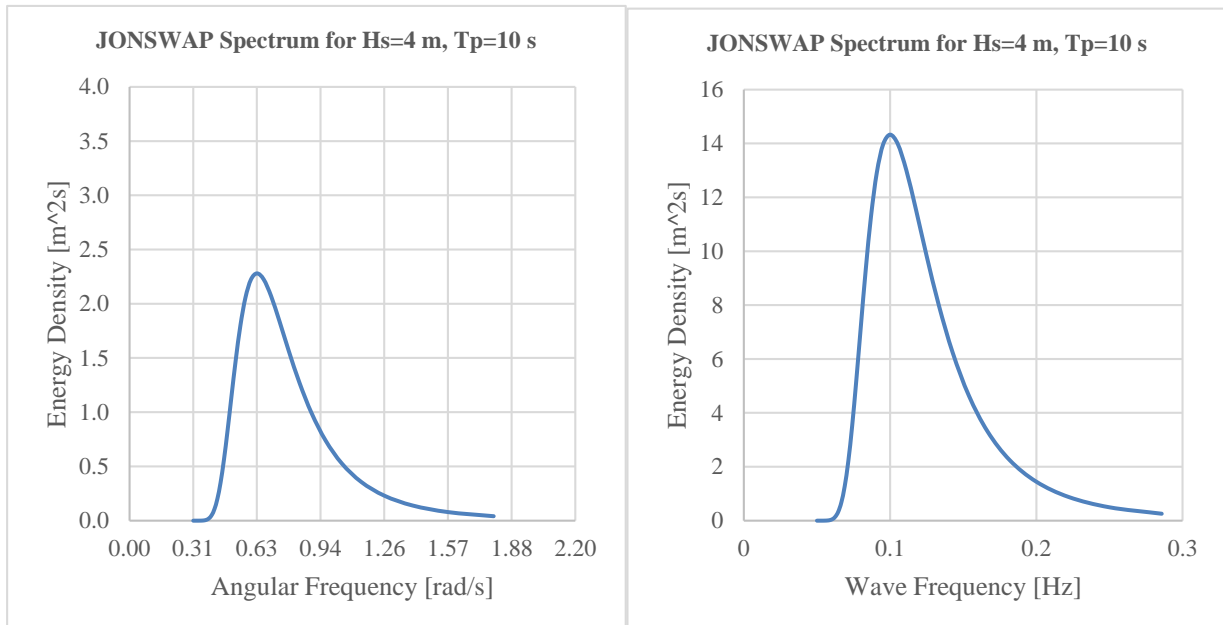


Figure 7-4 JONSWAP Energy Spectrum for Hs =4m, Tp=10 s, gamma =1

7.2.2. Crossing Sea Spectrum

The combined sea spectrum is more relevant to see the effects from wind and swell components. It is derived here by superimposing the JONSWAP spectrum for wind sea and swell sea. The combined spectrum will have the spectral parameters H_s & T_p . In order to create JONSWAP spectrum for wind sea and swell sea, the H_s & T_p of crossing sea spectrum should be split. The procedure for the split is shown in Appendix -1: Crossing Sea Spectral Parameters. The spectral parameters for wind and swell sea spectrum are obtained from combined spectrum parameter H_s , T_p based on the reference (Torsethaugen & Haver, 2004).

The directionality of the wind and swell sea is not taken into account in this combination. In actual case, they propagate from different directions.

The spectral energy peak in Figure 7-5 is in the region of high frequency range, hence this sea state is dominated by wind. There is a secondary peak in the low frequency range due to the swell sea.

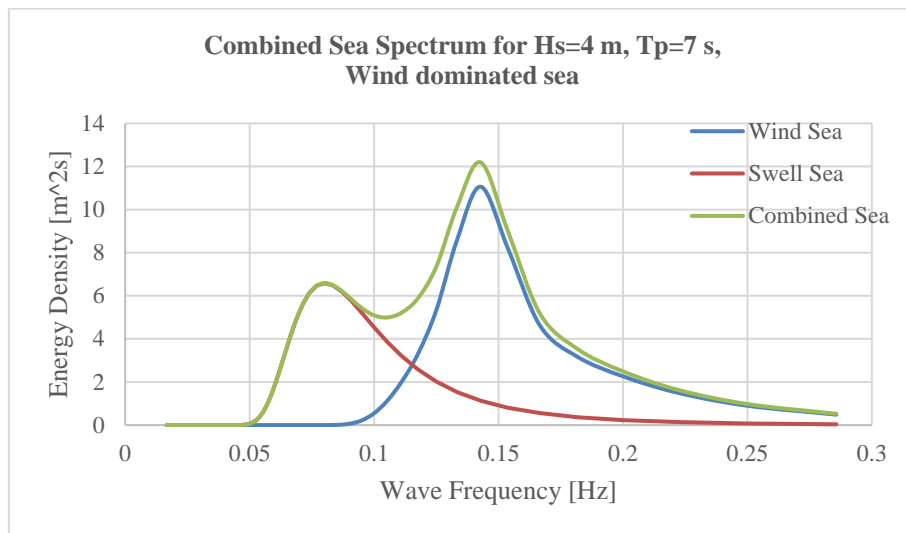


Figure 7-5 Combined Energy Spectrum for $H_s=4$ m, $T_p=7$ s for wind dominated sea

In the swell dominated sea state, the primary peak is in the low frequency range and secondary peak in the high frequency wind dominated region. This can be seen in Figure 7-6.

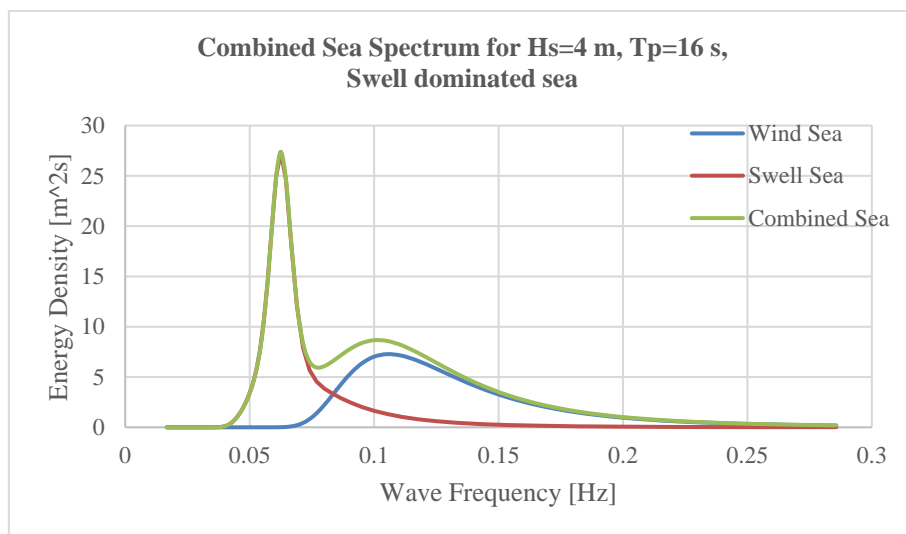


Figure 7-6 Combined Energy Spectrum for $H_s=4$ m, $T_p=16$ s for swell dominated sea

8. Transfer functions

8.1. Co-ordinate system

The notations for the vessel motions are followed based on Right handed co-ordinate system as shown in Figure 8-1.

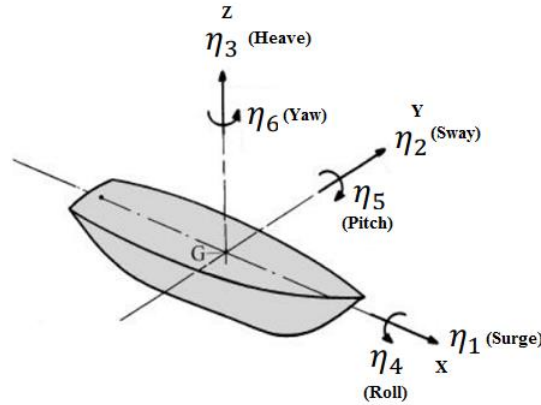


Figure 8-1 Ship motion notations-modified (Journee & Adegeest, 2003)

X-axis is pointing towards bow. X=0 at LPP/2; Y axis is pointing towards port, Y=0 at centreline of the vessel; Z axis upwards, Z=0 at still water level; Wave propagation direction is 180°, when the waves are coming on head sea; 90° for beam sea along positive Y axis. The CoG of the ship is located at -2.55m, 0 m , 3.87m. The RAOs used, are respective to this CoG co-ordinate.

8.2. Motion transfer function of Vessel at CoG

Vessel motions are represented by motion transfer functions. This is also called as RAOs (Response Amplitude Operator). RAO can be defined as response of a vessel in its six degree of freedom due to the wave amplitude. The RAO can be estimated based on tank model experiment or by the proprietary numerical software such as WADAM, WAMIT. The RAO consists of two parameters. One is a response amplitude of the vessel per amplitude of the wave; the second one is a phase angle between the vessel motion and wave motion.

The motion amplitude of a vessel at any degree of freedom can be estimated by multiplying the RAO with respect to relevant wave direction and degree of freedom by the wave amplitude.

The displacement of the vessel η_k is calculated as follows,

$$\begin{aligned} \eta_k(t) &= \text{Re} [H_k(\omega) \cdot \xi_0 e^{i\omega t}] \\ &= |H_k(\omega)| \xi_0 \cos(\omega t + \phi_k), \end{aligned}$$

$$k = 1, 2, \dots, 6$$

where, η_k - the vessel displacement at k^{th} degrees of freedom,

$|H_k(\omega)|$ – absolute value of motion amplitude per unit wave amplitude

ω – wave frequency in rad/s, t – time in seconds

ϕ_k – phase angle in radians, ξ_0 - wave amplitude (in length units)

The phase angle gives the relationship between vessel motion and wave. If the phase angle is zero, then the vessel and the wave are in same phase; whereas 180° gives the out of phase in opposite direction. Positive value of the phase represents the maximum vessel motion occurs before the maximum wave elevation at the longitudinal centre of gravity of vessel. Negative value means the maximum vessel motion occurs after the maximum wave elevation as shown in Figure 8-2.

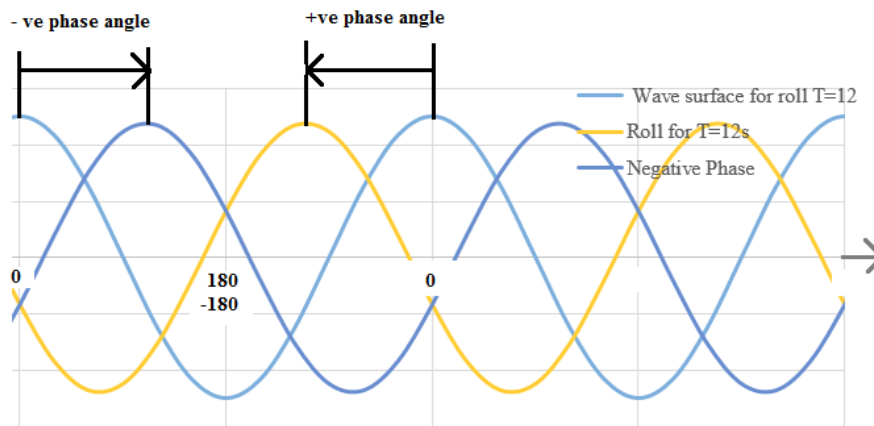


Figure 8-2 Phase Angle Definition

The transfer functions in § 8.2.1, 8.2.2 & 8.2.3 are applicable, when the vessel does not have the forward speed. That means the vessel is just floating on the open sea without any anchoring.

8.2.1. Heave Motion Transfer functions

Heave motion of the vessel is a very critical motion for the lifting operations. The heave motion of the vessel in head sea depends on the wave length with respect to the length of ship. When the wave length is more than the twice of the vessel length (LOA), the heave amplitude is equal to wave amplitude. In order to have the heave amplitude equal to wave amplitude in head sea for this vessel, the relevant wave frequency should be less than 0.07 Hz. This limit is calculated by considering the wave length equal to twice the ship's length and deep water dispersion relation. When the wave frequency increases further i.e. the wave length decreases, the heave amplitude is reducing, because the varying vertical wave excitation force on the ship along the longitudinal direction cancels each other. The gradual drop in heave amplitude in head sea shown in Figure 8-3 is disturbed by the peak due to the natural frequency of the vessel, 0.13 Hz ($T=8$ s) in heave. The heave amplitude in beam sea increases towards the natural frequency region and then it drops when the wave frequency increases beyond the natural frequency of heave.

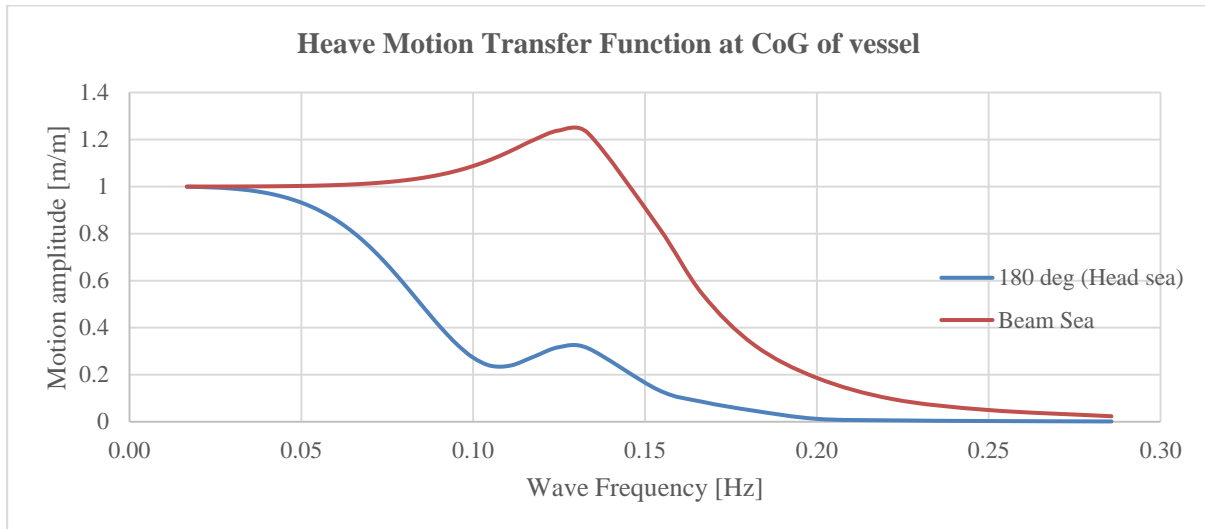


Figure 8-3: Heave Motion transfer function at COG of vessel

The heave motion of the vessel in head sea and beam sea follows the wave motion for low frequency waves, as the phase angle is zero. In head sea, the phase angle varies $0 < \phi < 120$ for the wave frequency less than the heave natural frequency. That means, the maximum heave vessel motion happens before the maximum wave elevation. Then, it varies between $120 < \phi < 180$, $-180 < \phi < 0$ for the frequencies higher than natural frequency as shown in Figure 8-4. The phase angle should end in a particular angle with high frequencies as per single degree of freedom system. The deviation of phase angle in given RAO after the high frequency 0.2 Hz is not important parameter compared to the lesser motion amplitude which is close to zero.

In beam sea, the phase angle for heave motion vary by $-30 < \phi < 0$ deg for $\omega \leq \omega_n$, and $-60 < \phi < -30$ degrees for the condition $\omega \geq \omega_n$,

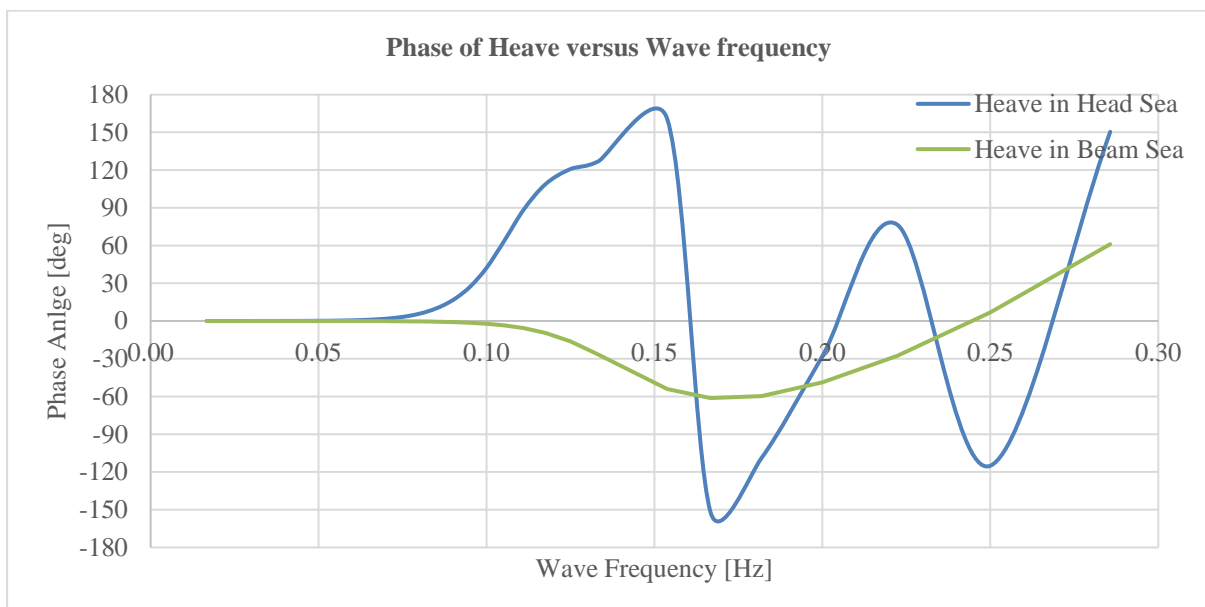


Figure 8-4: Phase angle of Heave Motion transfer function at COG of vessel

For smaller period ($T=7.5$ s which is equal to 0.13 Hz), the maximum heave displacement in head sea occurs before the wave elevation reaches its maximum. The phase angle for the wave frequency 0.13 Hz is + 150 deg. The heave displacement of the vessel in head sea for longer wave periods shall

follow the wave elevation as the vessel is surfing on the waves. This means the vessel motion and wave motion are in-phase, i.e. phase angle is zero. This has been verified with the RAO considered and can be seen in motion plot. The harmonic motion of the wave propagation in head sea and heave motion of the vessel for the wave periods 7.5 s, 12 s, 20s (0.13 Hz, 0.08 Hz, 0.05 Hz respectively) are shown in Figure 8-5.

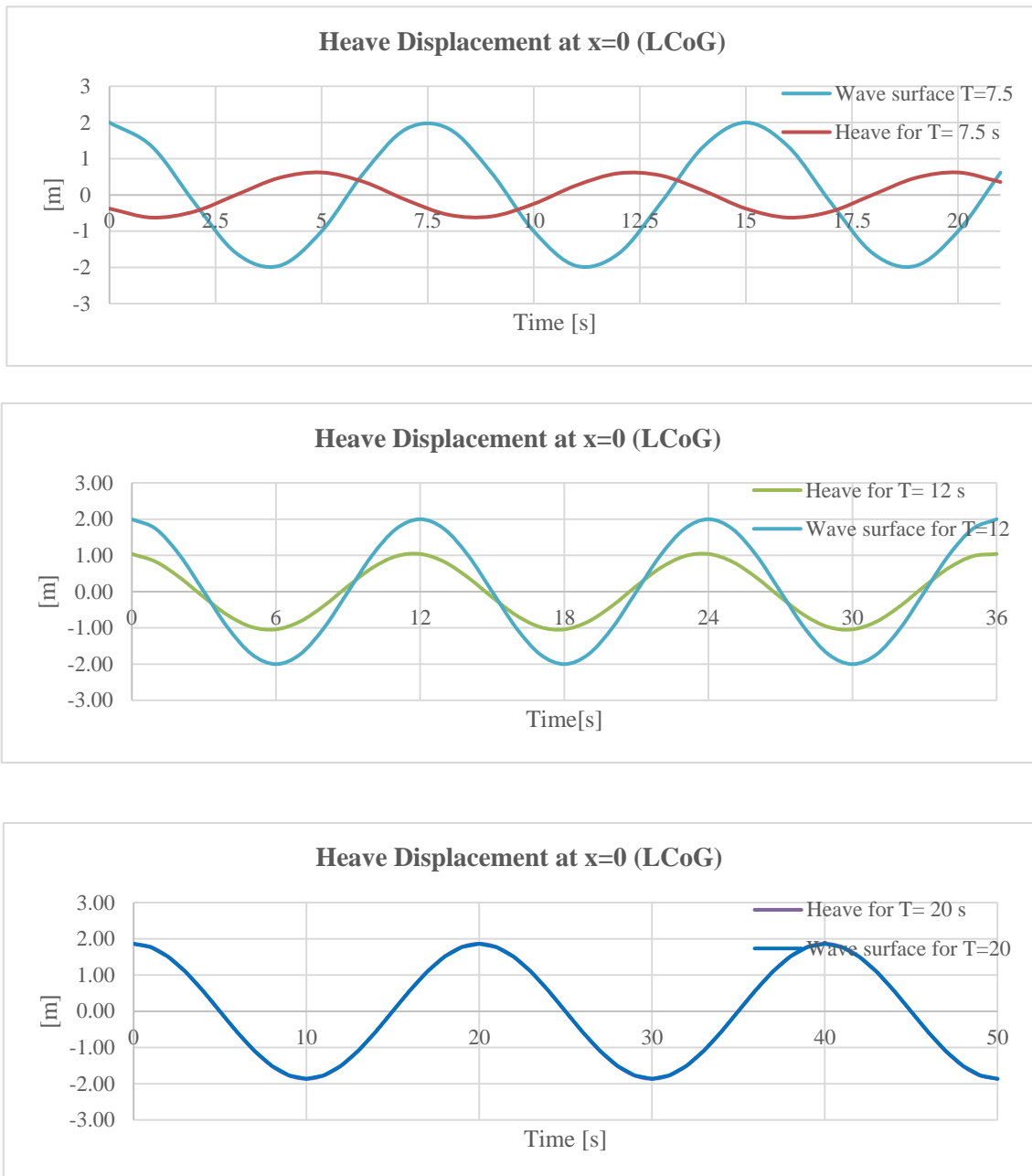


Figure 8-5 Illustrating the phase difference between wave and heave response for different wave periods in head sea; wave propagation in '-ve x direction (left side) in the graph

8.2.2. Pitch Motion Transfer functions

The pitch motion is a rotational motion about the transverse axis of the ship. The pitch motion in head sea with low frequency waves are lesser, because the slope of wave surface in higher wave length is smaller. The pitch motion increases up to the maximum where the wave length is twice as the ship length, where the slope is maximum. Then, it decreases due to cancellation effects. The pitch motion in beam sea is very minimum. The secondary peak at wave frequency at 0.15 Hz as shown in Figure 8-6 is due to the resonance with the natural frequency of the vessel ($T=6.5$ s) in pitch motion.

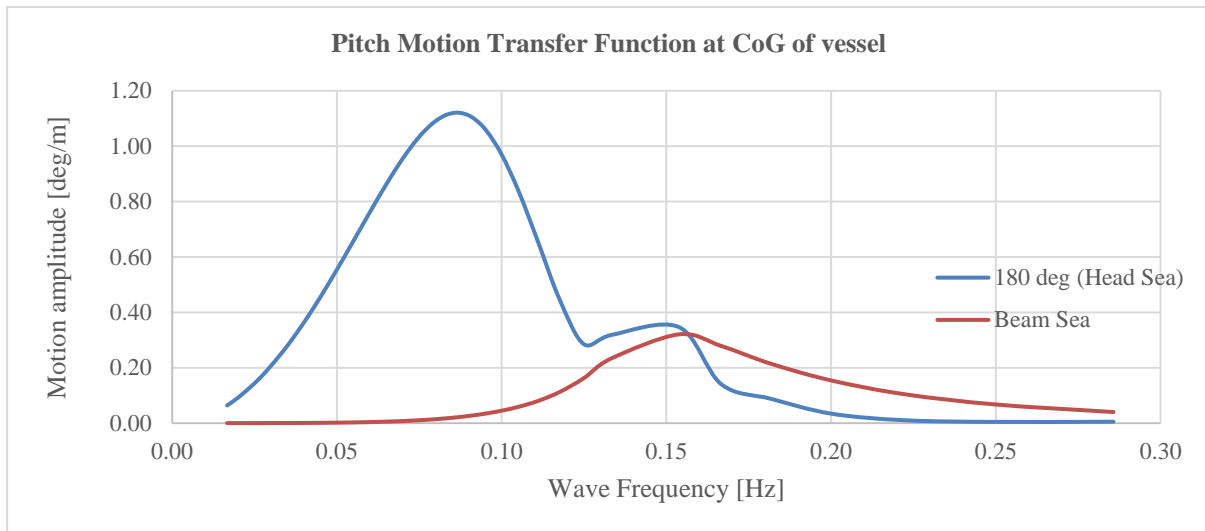


Figure 8-6: Pitch Motion transfer function at COG of vessel

In head sea, the phase angle between pitch motion and wave motion is varying $-107^\circ < \phi_5 < 12^\circ$, when the wave frequency is less than the natural frequency in pitch (0.15 Hz). The phase angle varies $12^\circ < \phi_5 < 180^\circ$ for the wave frequencies higher than the natural frequency in pitch. There are some non-uniform behaviour on the phase taken from RAO for the frequencies higher than 0.2 Hz as shown in Figure 8-7. This can be ignored by comparing with the response amplitude which is very small.

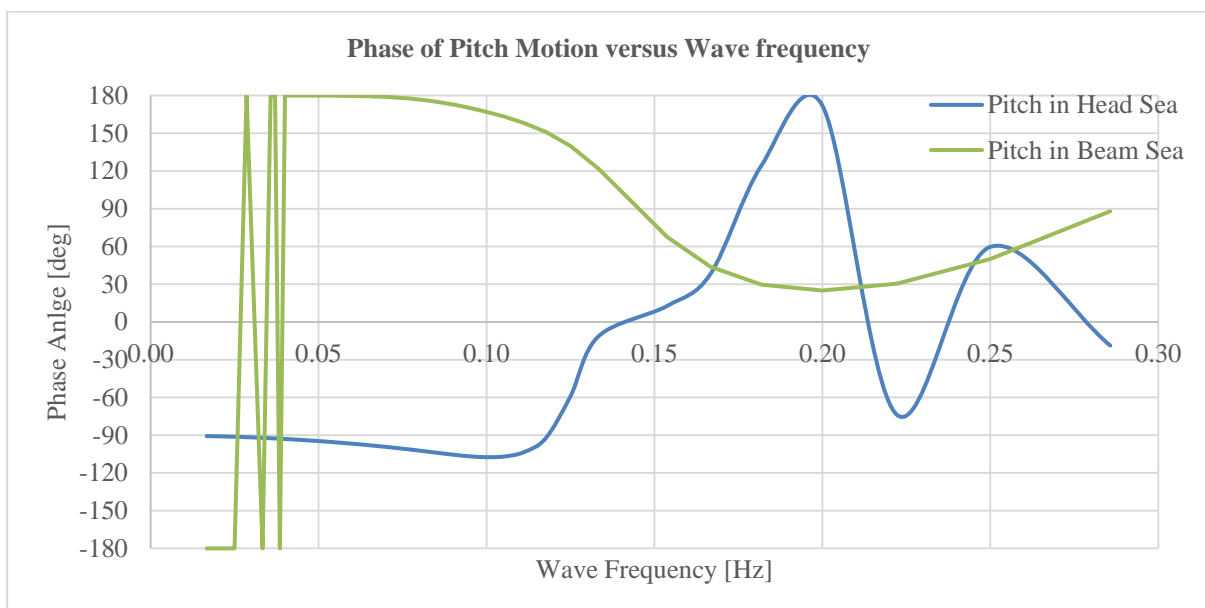


Figure 8-7: Phase angle of Pitch Motion transfer function at COG of vessel

In beam sea, the phase angle between pitch motion and wave motion is varying $180^\circ < \phi_5 < 90^\circ$, when the wave frequency is less than the natural frequency in pitch (0.15 Hz). The phase angle varies $90^\circ < \phi_5 < 30^\circ$ for the wave frequencies higher than the natural frequency in pitch. There are some non-uniform behaviour on the phase taken from RAO for the frequencies less than 0.05 Hz as shown in Figure 8-7. This can be ignored by comparing with the response amplitude which is very small.

For smaller period ($T=7.5$ s which is equal to 0.13 Hz), the maximum pitch rotation in head sea occurs after 0.5 s, the wave elevation reaches its maximum. The phase angle for the wave frequency 0.13 Hz is -11 deg. The phase angle between pitch motion and wave motion for the longer period, $T=20$ s is -95 deg. The harmonic motion of the wave propagation in head sea and pitch motion of the vessel for the wave periods 7.5 s, 12 s, 20s (0.13 Hz, 0.08 Hz, 0.05 Hz respectively) are shown in Figure 8-8 to illustrate the phase difference.

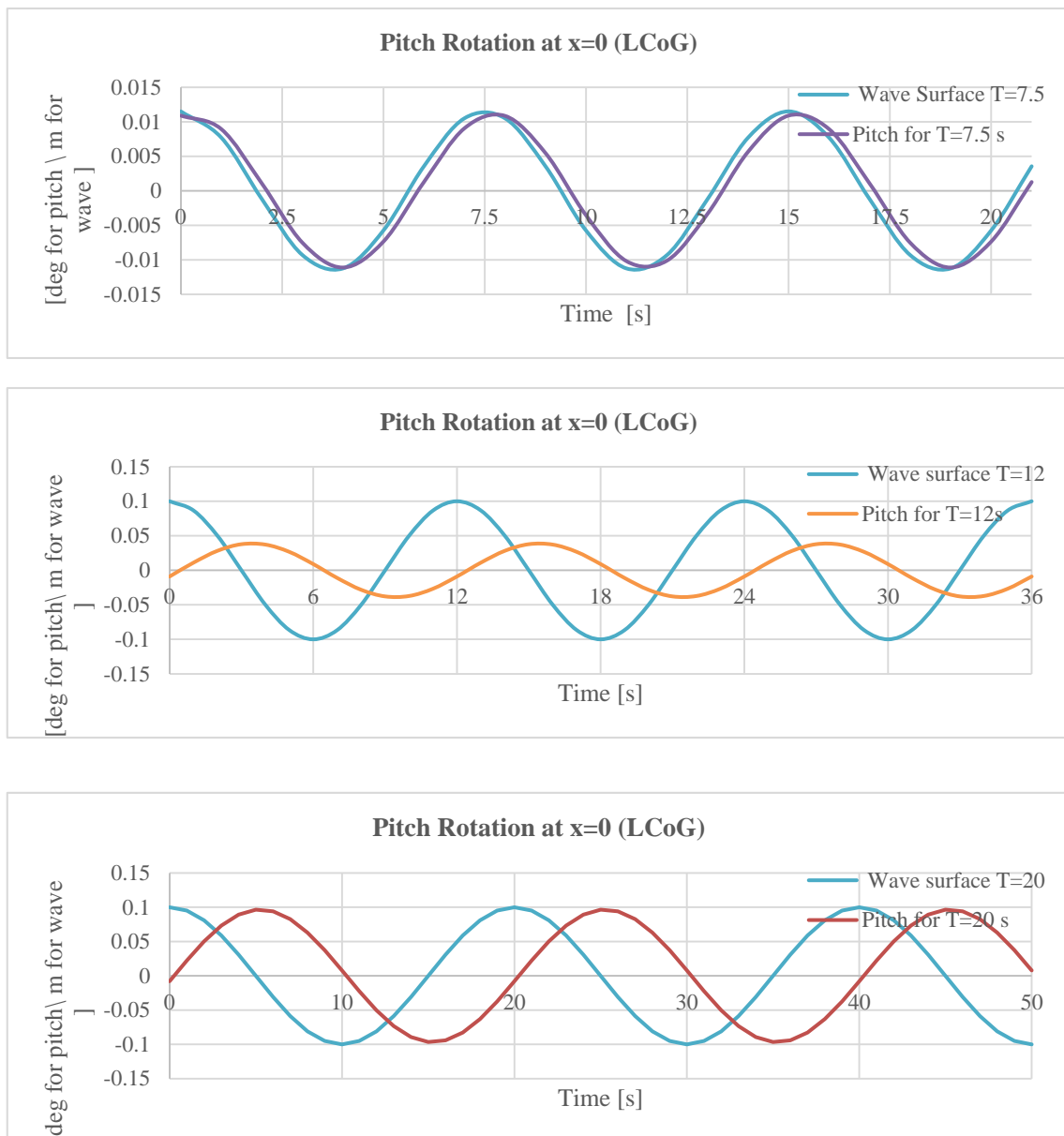


Figure 8-8 Illustrating the phase difference between wave and pitch response for different wave periods in head sea; wave propagation in ‘-’ ve x direction (left side) in the graph

8.2.3. Roll Motion Transfer functions

The roll motion is a non-linear response motion. That means, the roll motion is not directly proportional to the exciting forces. The peak in Figure 8-9 at the frequency 0.07 Hz ($T=14$ s) is due to the natural frequency of ship in roll degree of freedom. The roll motion of the ship is critical when the wave frequency is close to the natural frequency in beam sea. The roll amplitude with the wave propagation direction in head sea is negligible as the roll is caused by the transverse moment due to the excitation forces.

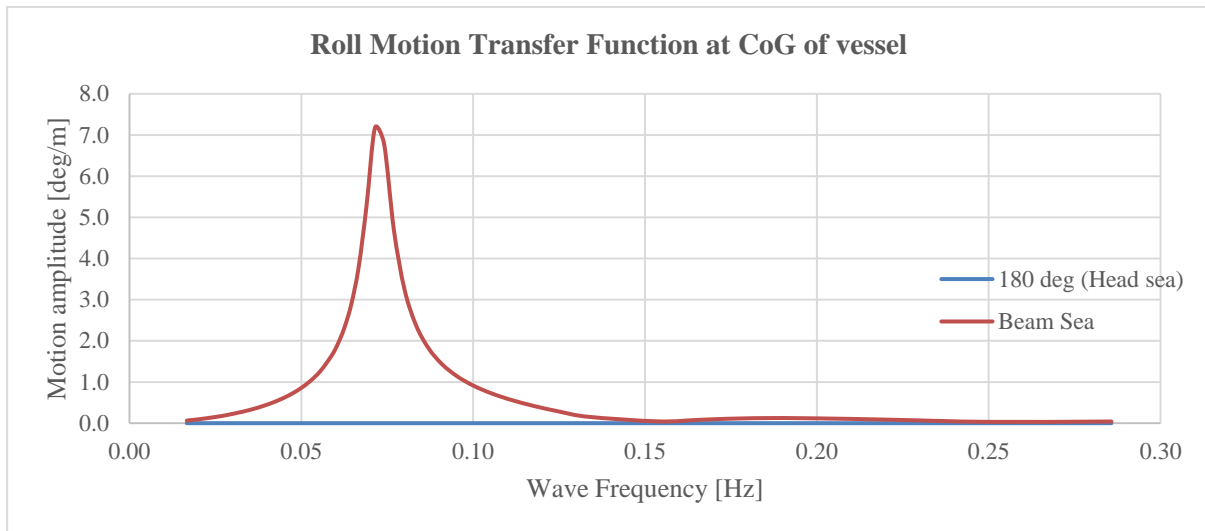


Figure 8-9: Roll Motion transfer function at COG of vessel

The phase angle with wave frequency is plotted for roll motion in Figure 8-10. The phase angle of roll in beam sea varies between $-150^\circ < \phi_4 < -90^\circ$, when the wave frequency is less than the natural frequency of roll of the ship. When the wave frequency is higher than natural frequency, the phase angle varies between $90^\circ < \phi_4 < 150^\circ$. There are some non-uniform behaviour on the phase taken from vessel's RAO for the frequencies higher than 0.13 Hz as shown in Figure 8-10. This can be ignored by comparing with the response amplitude which is very small.

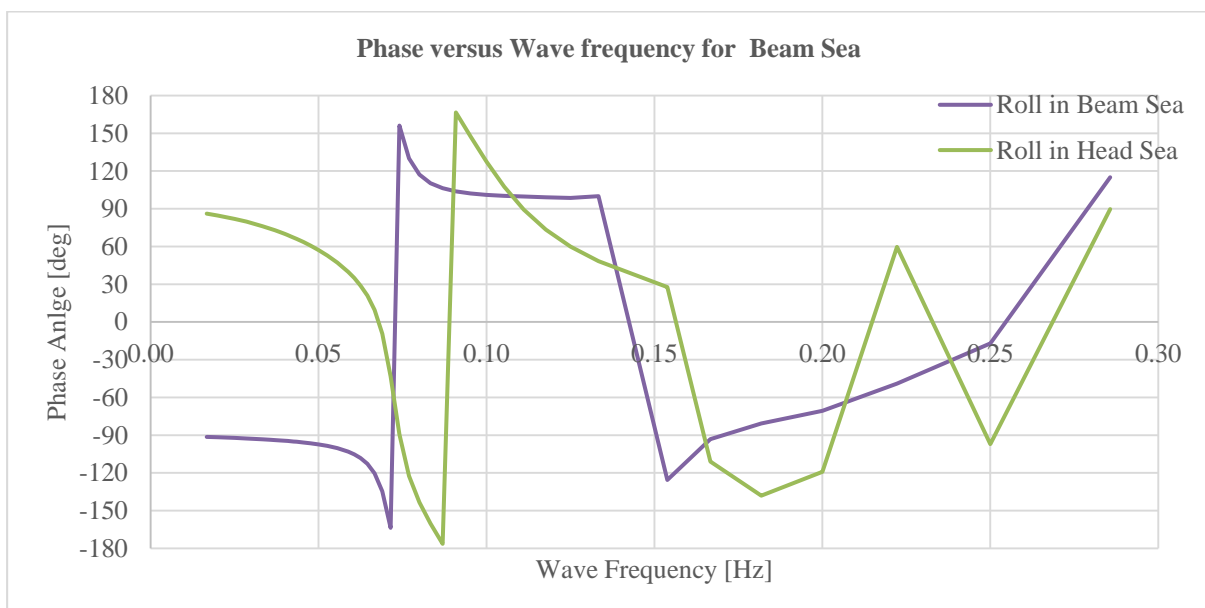


Figure 8-10 Illustrating the phase difference between wave and roll vessel response for varying frequencies

For smaller period ($T=7.5$ s which is equal to 0.13 Hz), the maximum roll rotation in beam sea occurs before the wave elevation reaches its maximum. The phase angle for the wave frequency 0.13 Hz is +100 deg. The phase angle between roll motion and wave motion for the longer period, $T=20$ s is -95 deg. That is the maximum roll amplitude occurs after the maximum wave amplitude as per the phase angle defined in Figure 8-2. The harmonic motion of the wave propagation in beam sea and roll motion of the vessel for the wave periods 7.5 s, 12 s, 20s (0.13 Hz, 0.08 Hz, 0.05 Hz respectively) are shown in Figure 8-11 to illustrate the phase difference.

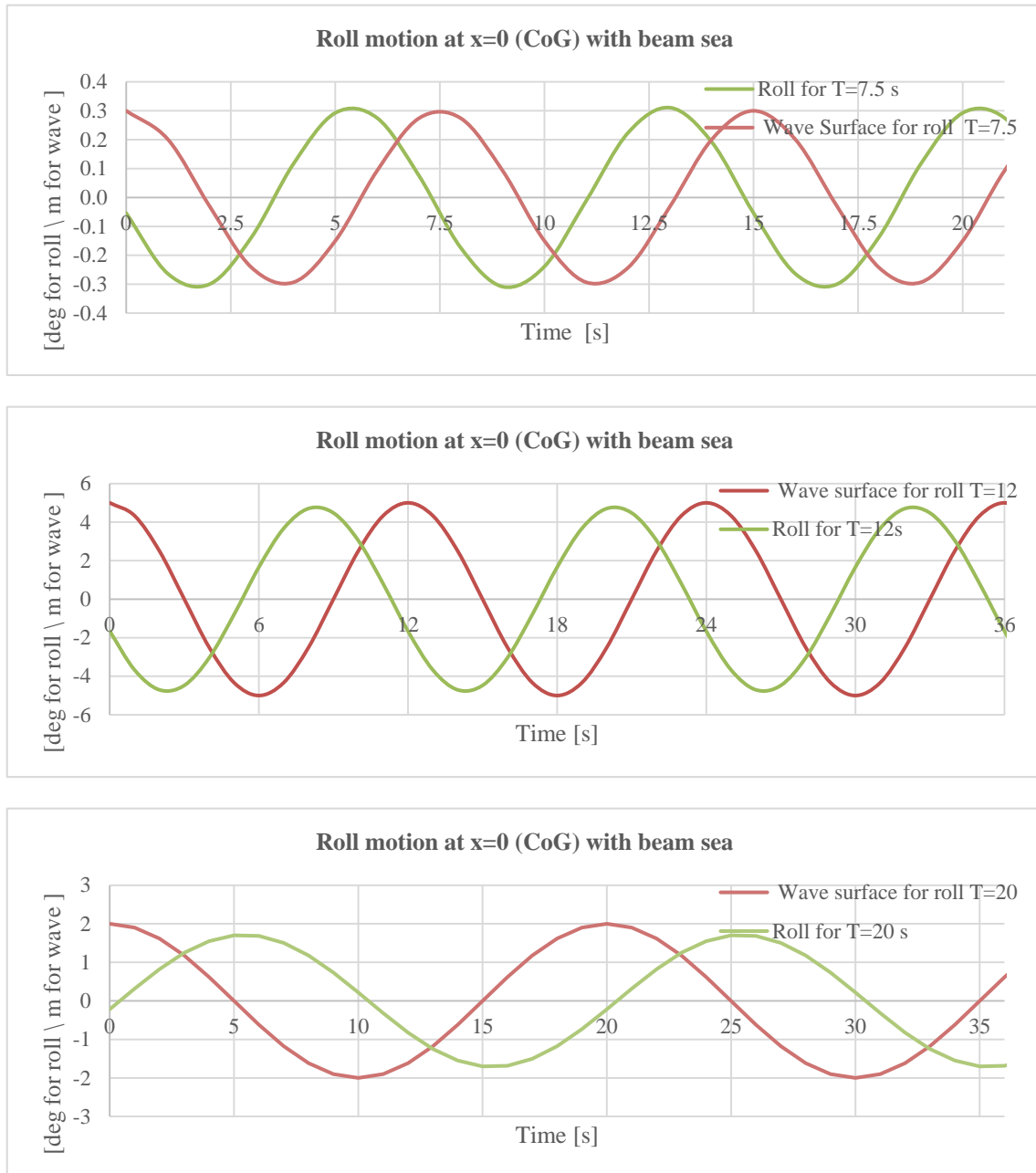


Figure 8-11 Illustrating the phase difference between wave and roll response for different wave periods in beam sea; wave propagation in +ve x direction (right) in the graph

8.2.4. RAO Quality Check

In order to make sure the considered RAO is correct, there are some quality check has been done.

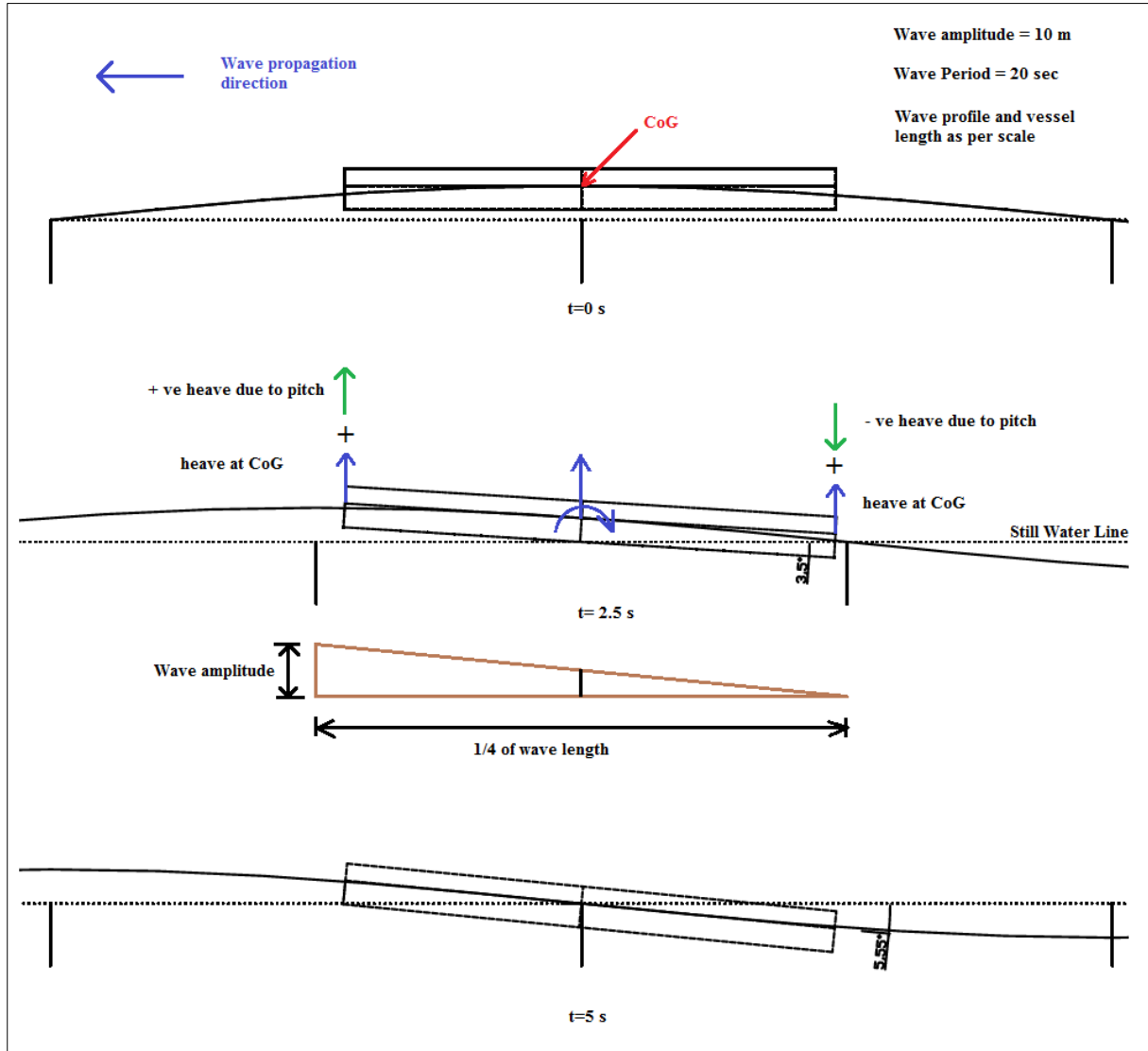


Figure 8-12 RAO quality check for longer wave period (T = 20 sec)

To verify the pitch motion, the longer period wave (T=20 s), vessel dimensions are drawn as per scale in Figure 8-12. The still water line of vessel made parallel to the slope of water surface and then, the pitch angle is measured at different time periods when the wave passed by. The geometrically measured angle from Figure 8-12 is compared with the pitch angle provided in the transfer functions. There are no much difference between them as shown in Table 8-1.

For the plotting of waves in Figure 8-12, the following calculations are made.

$$\text{Length of wave } \lambda = \frac{g}{2\pi} \cdot T^2 = 624.5 \text{ m}$$

$$\text{Wave propagation speed } c = \frac{\lambda}{T} = 31.225 \text{ m/s}$$

In the longer period waves or low frequency waves, the heave amplitude should be equal to the wave amplitude. This can be seen in the heave motion transfer function shown in Figure 8-3. The heave motion measured geometrically at various times for the wave (T=20s), does not match exactly with the

calculated motion from RAO as shown in Table 8-1. But it is expected that, this will match, if the wave period is increased further.

Time	Geometrically Measured motion from the Figure 8-12		Calculated motion from given RAO	
	Heave	Pitch	Heave	Pitch
	[m]	[deg]	[m]	[deg]
0	10	0	9.3	-0.44
2.5	5	3.5	6.6	3.6
5	0	5.55	0	5.5

Table 8-1 Comparison of geometrically measured motion and calculated motion from RAO

By this way, the sign conventions of given RAO is also verified with respect to the co-ordinate system followed in § 8.1 for this study. The aim is to ensure the compatibility between the co-ordinate system in this report and the co-ordinate system followed in the given RAO calculations. For example, in Figure 8-12, the wave propagates in head sea i.e. 180° as per given RAO notation, the heave is expected to be maximum towards upwards at the wave crest. As per the notation in this report, this upwards heave value should be positive. This sign convention is compared with given RAO. They are also positive. If the given RAO is negative, then the sign should be converted according to the co-ordinate system used here. Likewise, the angular displacement such as pitch sign convention also verified by estimating the total heave at bow and stern as shown in Figure 8-12. The total heave at the stern due to components of heave at CoG and the pitch should be higher than the total heave at the bow, if the clockwise pitch rotation is positive.

Roll motion of the vessel in head sea should be very minimum as there are no excitation force to create transverse moment of the vessel. Likewise, the pitch motion in beam sea should be minimum compared to wave propagating on other directions. This has been verified with the RAOs used in this report.

8.3. Motion transfer function of Crane-tip

In general, the motion transfer functions are determined at the CoG of any floating structure by a hydrodynamic software such as WAMIT or tank model test. But, these data cannot be used directly; they needed to be converted to any particular point desired. Motion transfer functions can only exist for linear relationship where motion at a point are linearly transferable to another point. Here, the motion at the CoG of vessel should be converted to motion at crane tip. The crane structure is assumed to be stiff, hence the crane tip motion is calculated based on rigid body motion due the wave excitation forces.

For the installation operation like this, the heave motion of the vessel is significant. The vertical heave motion at crane tip is contributed by the heave, pitch and roll motion of the vessel. The procedure for calculating such a combination of motion is shown below.

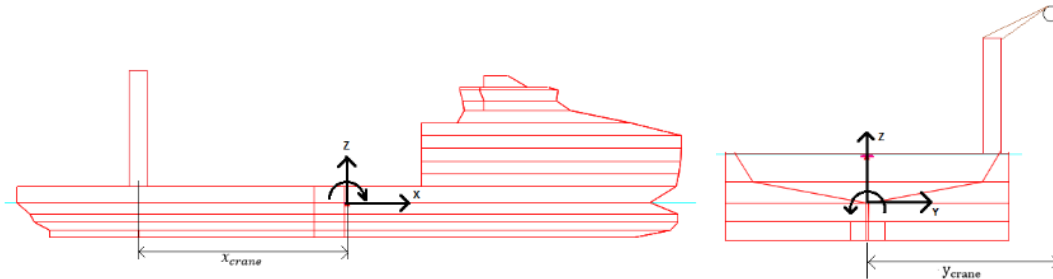


Figure 8-13 Illustrating the combined heave motion

Let us say, the first order motion transfer functions at CoG for heave and pitch are H_3 and H_5 respectively. Then, the combined heave motion transfer function at crane tip (H_{tz}) due to the wave excitation can be calculated by,

$$H_{tz}(\omega) = H_3 - x_{crane} * H_5 \quad \text{-----Eq.8.3.1}$$

x_{crane} – The horizontal distance from CoG to the crane tip in X direction as shown in Figure 8-13; as the crane tip is situated in negative X direction, this distance should be used as negative value.

At $t=2.5$ s, when the wave crest passes the vessel as shown in Figure 8-12, the heave motion at forward most point should be minimum whereas it should be maximum at the aft most side of the vessel. The heave minimum and maximum at any point on the vessel depends on the heave contribution from the pitch and roll motion of the vessel in head sea. In other wave propagation directions, the contribution from the roll component is also to be considered. This is exemplified below by showing the heave values at points which are equal distance from CoG towards forward and aft of the vessel, for the deterministic wave with amplitude =10 m, period = 20 s. It is assumed that, the heave and pitch amplitude occurs simultaneously, i.e. the phase is 0 degree.

$$\text{Heave at forward most point} = \left(0.9138 \frac{m}{m} - 76 m \cdot 0.009677 \frac{rad}{m} \right) \cdot 10 m = 1.8 m$$

$$\text{Heave at aft most point} = \left(0.9138 \frac{m}{m} - (-76 m) \cdot 0.009677 \frac{rad}{m} \right) \cdot 10 m = 16.5 m$$

As expected, the heave value at forward point is minimum than the heave at the aft point. The result based on the equation Eq.8.3.1 shows the sign conventions of RAO and the equations itself are correct.

To compare, how the heave amplitude varies with distance from CoG of the vessel, the heave amplitude is calculated at points equal distance (76 m) from the CoG for the same wave as above.

$$\begin{aligned}
 \text{Heave amplitude at forward most point} &= |H_3(\omega)|e^{i\phi_3} - x_{\text{crane}} |H_5(\omega)|e^{i\phi_5} \\
 &= 0.9138 \cdot e^{i(0.0029)} - 76 \cdot 0.009677 \cdot e^{i(-1.65)} \\
 &= 1.22 \frac{m}{m} \cdot (\text{wave amp} = 10m) = 12.2 m
 \end{aligned}$$

$$\text{Heave amplitude at aft most point} = 1.125 \frac{m}{m} \cdot (\text{wave amp} = 10m) = 11.25 m$$

It can be seen that heave amplitude i.e. maximum heave response at a point, is higher in the forward of the vessel compared to aft side of the vessel for the wave period 20 s (0.05 Hz) in head sea.

The heave amplitude at the above points are calculated for all the wave frequencies in head sea and following sea; and they are plotted in Figure 8-14 & Figure 8-15. It can be noticed that the heave amplitude is always higher at forward side of the vessel than aft side of the vessel, when the wave propagates from head sea.

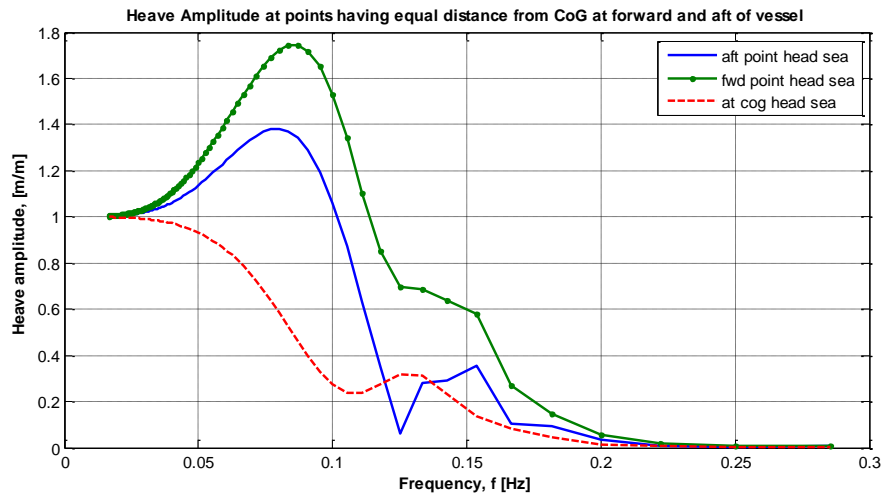


Figure 8-14 Illustrating heave amplitude at points equal distance from CoG with head sea (180 deg sea)

Whereas, in following sea (0 deg) wave propagation, above mentioned is not valid. Between 6 to 10 seconds of wave periods, the heave at aft point is higher than forward as shown in Figure 8-15.

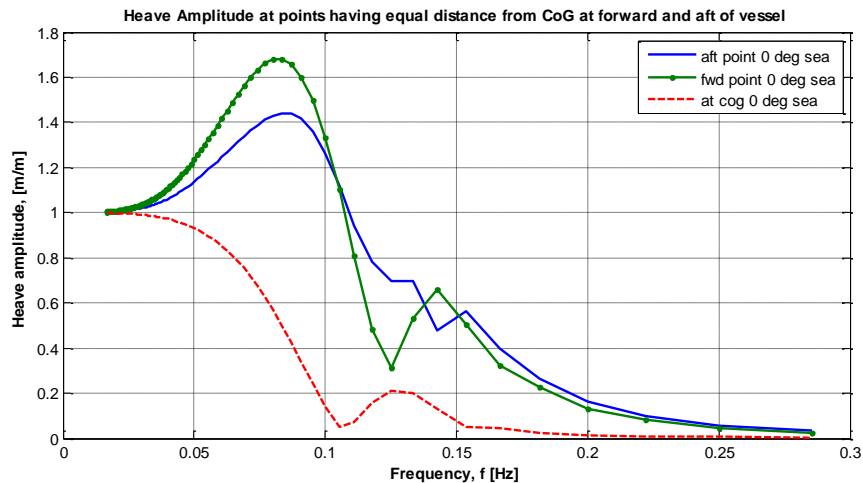


Figure 8-15 Illustrating heave amplitude at points equal distance from CoG with following sea (0 deg sea)

It should be noted that x_{crane} is not an absolute value. The proper sign should be considered based on the co-ordinate system specified. Hence, negative value of x_{crane} is chosen as crane tip is located against the positive x-direction. Likewise, the combined heave motion transfer function at crane tip due to heave, pitch and roll motion of the vessel can be calculated as

$$\begin{aligned} H_{tz}(\omega) &= H_3(\omega) - x_{crane} * H_5(\omega) + y_{crane} * H_4(\omega) \\ &= |H_3(\omega)|e^{i\phi_3} - x_{crane} |H_5(\omega)|e^{i\phi_5} + y_{crane} |H_4(\omega)|e^{i\phi_4} \end{aligned} \quad \text{----- Eq.8.3.2}$$

where, x_{crane} – distance from RAO origin to crane tip in X direction

y_{crane} - distance from RAO origin to crane tip in Y direction

As the heave motion at crane tip is found out by superimposing vertical harmonic motion at crane tip due to the heave, pitch and roll motions of the ship, the combined motion should also be a harmonic motion. Hence, the combined heave motion at crane tip can be defined as,

$$H_{tz}(\omega) = |H_{tz}(\omega)| e^{i\phi_{tz}} \quad \text{----- Eq.8.3.3}$$

where, $|H_{tz}(\omega)|$ – Vertical crane tip motion amplitude

ϕ_{tz} – Phase angle between wave elevation and crane tip motion

By equating the equations Eq.8.3.2 & Eq.8.3.3,

$$\begin{aligned} |H_{tz}(\omega)| &= \sqrt{(|H_{tz}(\omega)| \sin(\phi_{tz}))^2 + (|H_{tz}(\omega)| \cos(\phi_{tz}))^2} \\ \phi_{tz} &= \arctan \left\{ \frac{|H_{tz}(\omega)| \sin(\phi_{tz})}{|H_{tz}(\omega)| \cos(\phi_{tz})} \right\} \end{aligned}$$

The final form of crane tip motion (η_{tz}) will be

$$\begin{aligned} \eta_{tz}(t, \omega) &= |H_{tz}(\omega)| \xi(t) e^{i\phi_{tz}} \quad \text{----- Eq.8.3.4} \\ &= |H_{tz}(\omega)| \xi_0 \cos(\omega t + \phi_{tz}) \quad \text{(taking real part)} \end{aligned}$$

The above theory can be referred from (Journee & Massie, 2001).

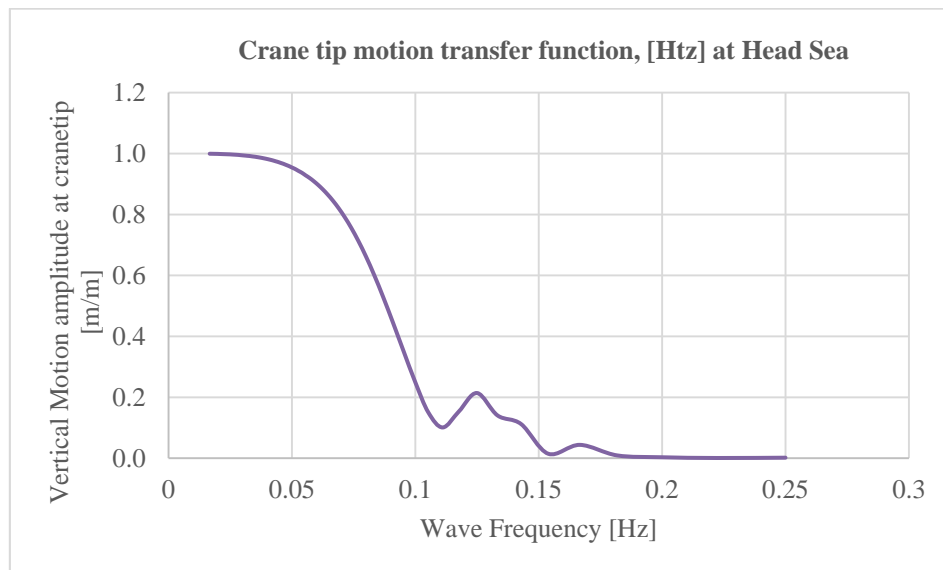


Figure 8-16: Crane tip heave motion transfer function at Head sea (180 deg)

The motion amplitude at crane tip is plotted for head and beams in Figure 8-16 & Figure 8-17. The peak value of crane tip amplitude at wave frequency 0.13 Hz is due to the vessel's natural period in heave. The natural period of the vessel in heave is 7.5 seconds.

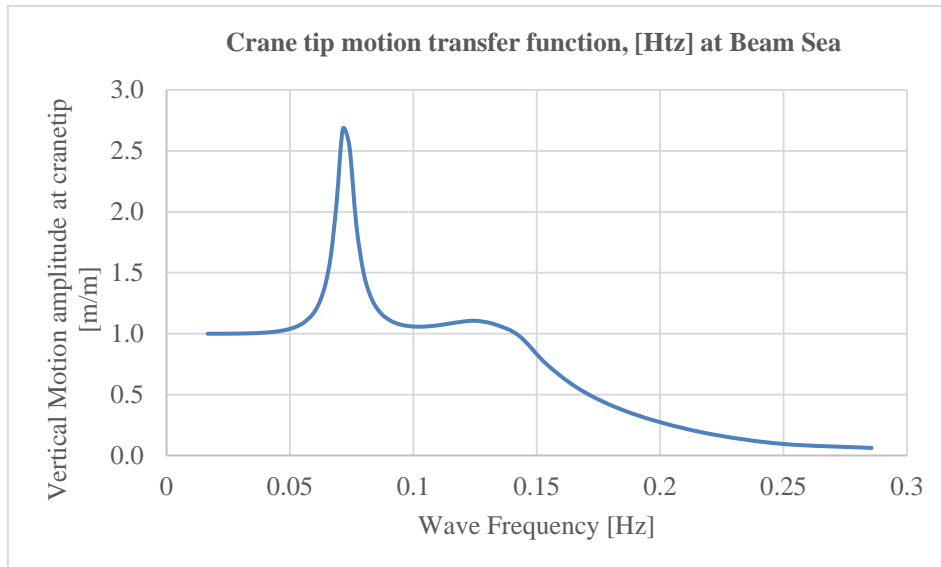


Figure 8-17: Crane tip heave motion transfer function at beam sea (90 deg)

The peak value of crane tip amplitude at wave frequency 0.07 Hz is due to the vessel's natural period in roll. The natural period of the vessel in roll is 14 seconds.

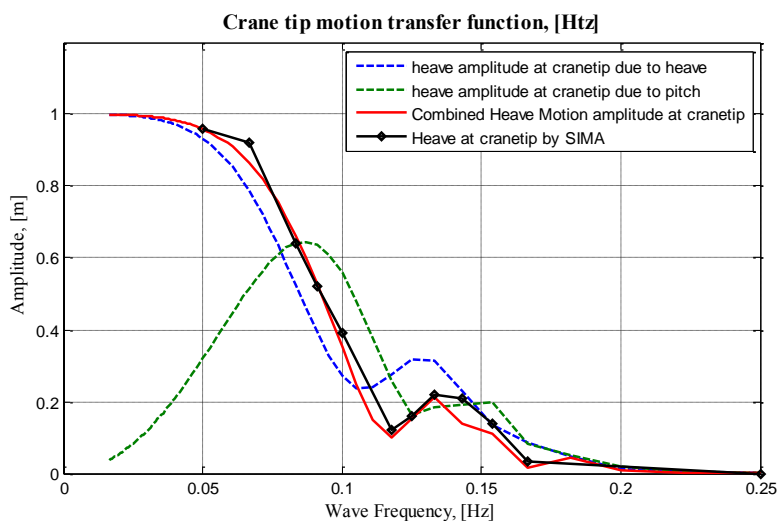


Figure 8-18: Crane tip heave motion transfer function

The effect of heave natural period on the crane tip motion can be seen between the wave frequency 0.1 Hz and 0.15 Hz. The influence of natural period (6.5 s) of pitch on the crane tip motion is very small.

The calculated vertical motion at the crane tip is compared with the motion obtained from SIMO without any hanging object and plotted in Figure 8-18. The results given by SIMO is very close to the calculation shown except in the frequency range of 0.13 to 0.16 Hz (7.5 s to 6 s). This variation is due to the missing RAO data for the 7s wave period. Otherwise, the calculation presented above is a good approximation to find out the crane tip motion transfer function.

The phase angle for crane tip motion in head sea is shown in Figure 8-19. The influence of natural frequency (0.13 Hz) of heave is clearly seen by the change of the phase angle from -125° to $+180^\circ$. Likewise, the influence of natural frequency of pitch (0.15 Hz) is seen due the change of phase angle from $+140^\circ$ to -180° .

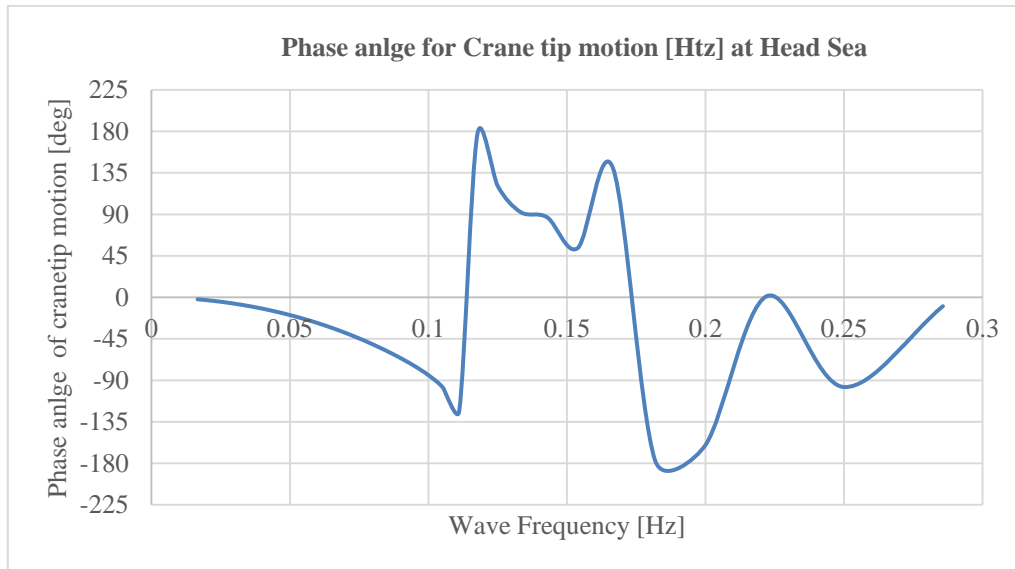


Figure 8-19: Phase angle for Crane tip vertical motion transfer function at Head sea

The influence of natural frequency (0.07 Hz) of roll is clearly seen in the phase angle of crane tip motion for the beam sea which is shown in Figure 8-20, by the change of the phase angle from -150° to $+150^\circ$. The phase angle after the influence of roll natural frequency, it should extend to zero degree for higher wave frequency waves. But the phase angle goes below zero and changed its sign at 0.13 Hz due to the natural frequency of heave.

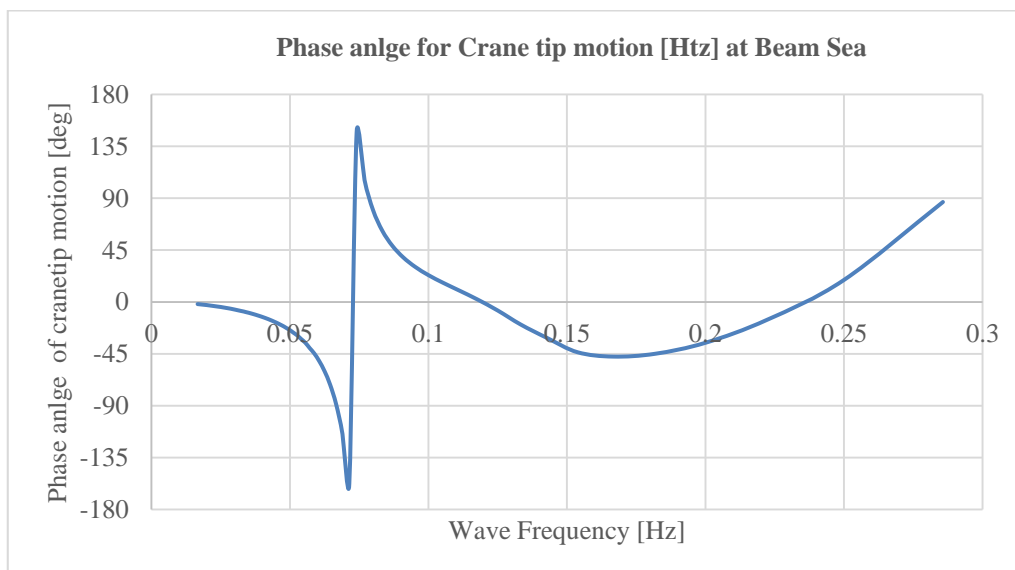


Figure 8-20: Phase angle for Crane tip vertical motion transfer function at Beam sea

8.4. Motion transfer function of Equipment

When the lifting object is hanging from the crane tip, the motion of mass is influenced by the crane tip oscillation. In the same way, the vessel motion can also be influenced by the hanging equipment. But, in this study, it is not considered the influence of hanging mass on the vessel motions i.e. uncoupled motion is considered. The crane wire between crane tip and the mass is assumed as a massless, linear spring with stiffness “k”. Only steady state response is considered here. The transient response due to the initial conditions is not considered. The dynamic model for the cases lifting in air and subsea lowering case are shown in Figure 8-21.

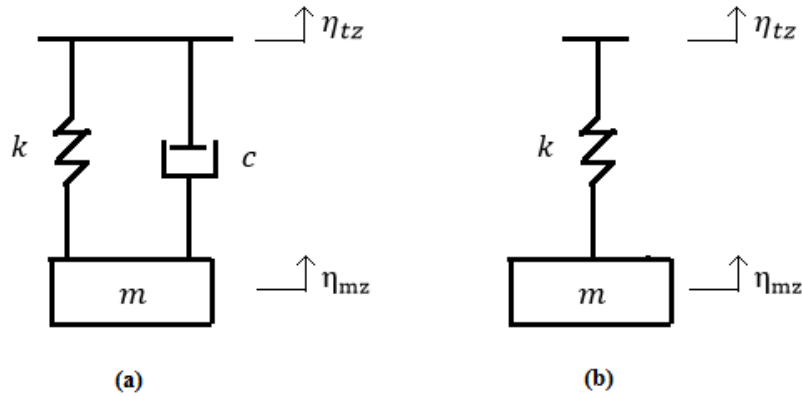


Figure 8-21: Dynamic model for case a) Subsea lowering, case b) Lifting in air

Then, Equation of motion for the vertical displacement of hanging equipment for the case of subsea lowering can be written as,

$$m\ddot{\eta}_{mz}(t) + c\dot{\eta}_{mz}(t) + k\eta_{mz}(t) = k\eta_{tz}(t) + c_2\dot{\eta}_{mz}(t) \quad \text{----- Eq.8.4.1}$$

where, m – mass of the hanging equipment in tonne, should be included the added mass in subsea case,

c – damping value at the mass in kN.s/m

c_2 - damping at crane tip

k – stiffness of wire in kN/m,

η_{mz} – vertical motion of mass in m

η_{tz} – vertical motion of crane tip in m

The right hand side (RHS) of the equation Eq.8.4.1 is the exciting force on the hanging equipment. The excitation force at the equipment is only caused due to the force on the wire. The damping at the crane tip is negligible i.e. $c_2 = 0$.

Hence the equation of motion Eq.8.4.1 for subsea lowering case becomes,

$$m\ddot{\eta}_{mz}(t) + c\dot{\eta}_{mz}(t) + k\eta_{mz}(t) = k\eta_{tz}(t) \quad \text{----- Eq.8.4.2}$$

Natural frequency of the lifting system for the un-damped case,

$$\omega_0 = \sqrt{\frac{k}{m}} \text{ (in rad/s)}$$

$$\omega_0 = \frac{1}{2\pi} \sqrt{\frac{k}{m}} \text{ (in Hz)} \quad \text{----- Eq.8.4.3}$$

$$\omega_0 = \frac{1}{2\pi} \sqrt{\frac{7690 \text{ kN/m}}{2230 \text{ ton}}} = 0.29 \text{ Hz}$$

When the crane tip motion is harmonic, then the motion of the hanging equipment will also be a harmonic motion. Hence, assuming solution as $\eta_{mz} = \eta_{mz0} \cdot e^{i\omega t}$ for Eq.8.4.2, motion transfer function (H_{mz}) for the subsea equipment from the crane tip excitation can be obtained as below. η_{mz0} is the amplitude of vertical motion of mass. It should be noted that the functions are in complex form.

$$H_{mz}(\omega) = \frac{\eta_{mz}}{\eta_{tz}}$$

where, $H_{mz}(\omega)$ is motion transfer function between the displacement of mass and crane tip

$$\begin{aligned} H_{mz}(\omega) &= \frac{k}{-\omega^2 m + i\omega c + k} \\ &= \frac{k e^{i\phi_{mz}}}{[(k - m\omega^2)^2 + c^2\omega^2]^{1/2}} \end{aligned}$$

Using the complex form relation, $x + iy = A e^{i\phi}$, where $A = \sqrt{x^2 + y^2}$ and $\tan \phi = y/x$

$$H_{mz}(\omega) = |H_{mz}(\omega)| e^{i\phi_{mz}}$$

$$|H_{mz}(\omega)| = \frac{k}{[(k - m\omega^2)^2 + c^2\omega^2]^{1/2}}$$

$$\phi_{mz} = \arctan\left(\frac{c\omega}{k - m\omega^2}\right) \quad \text{----- Eq.8.4.4}$$

If the damping is zero ($c=0$), then phase angle between vertical motion of crane tip and equipment will be zero, i.e. in-phase. This is the case, when the equipment is hanging in air.

$$\eta_{mz} = H_{mz}(\omega) \cdot \eta_{tz}$$

By substituting η_{tz} with transfer function between the wave excitation and crane tip motion, the motion at the mass can be obtained directly from wave amplitude elevation as follows,

$$\begin{aligned} \eta_{mz} &= |H_{mz}(\omega)| e^{i\phi_{mz}} |H_{tz}(\omega)| e^{i\phi_{tz}} \xi(t) \\ &= |H_{mz}(\omega)| \cdot |H_{tz}(\omega)| \cdot \xi_0 e^{i(\omega t + \phi_{tz} + \phi_{mz})} \end{aligned}$$

The vertical motion amplitude at the mass is slightly higher than the vertical motion amplitude at the crane tip. It can be seen in Figure 8-22, the motion amplitude of mass is shifted upwards with respect to the motion amplitude of the crane tip. The phase angle between them also zero i.e. in-phase as the phase angle depends on the damping at the mass as per Eq.8.4.4. The increase in the motion amplitude of the mass at higher frequency is due to the natural frequency of the lifting system considered for this study which is equal to 0.29 Hz.

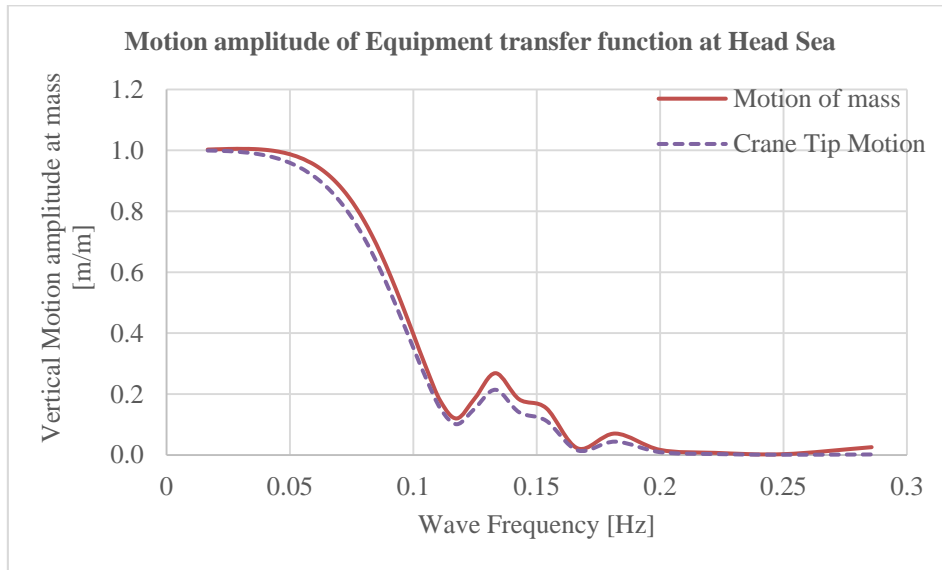


Figure 8-22: Motion amplitude of transfer function at mass for Head sea (180 deg)

8.5. Dynamic tension transfer function of Equipment

Dynamic tension in the cable can be calculated by stress and strain relationship. It leads to the final form as multiplication of relative displacement and linear stiffness “k”. The weight of wire is ignored for simplicity.

$$H_{FD}(\omega) = \frac{F_D}{\xi(t)}$$

where, H_{FD} - Dynamic tension transfer function in complex form, F_D – dynamic tension on the wire

$$\begin{aligned} F_D &= H_{FD}(\omega) \cdot \xi(t) && \text{-----Eq. 8.5.1} \\ &= |H_{FD}(\omega)| e^{i\phi_{FD}} \cdot \xi(t) \\ &= |H_{FD}(\omega)| e^{i\phi_{FD}} \cdot \xi_0 e^{i\omega t} \\ &= |H_{FD}(\omega)| \xi_0 e^{i(\omega t + \phi_{FD})} \end{aligned}$$

where, ϕ_{FD} is the phase difference between the wave motion and dynamic tension variation

As the dynamic tension on the wire is also a harmonic function, it can be written in complex form as,

$$\begin{aligned} F_D &= |F_D| e^{i\phi_{FD}} \\ E &= \frac{\sigma}{\varepsilon} = \frac{F_D}{A \varepsilon} \end{aligned}$$

where, E – Young’s modulus of elasticity, A – cross sectional area of wire, L – length of wire,

$$\begin{aligned} F_D &= (\eta_{tz} - \eta_{mz}) \frac{EA}{L} \\ &= (\eta_{tz} - \eta_{mz}) k \\ &= k [\xi H_{tz}(\omega) - \xi H_{tz}(\omega) H_{mz}(\omega)] \\ &= k \xi H_{tz}(\omega) [1 - H_{mz}(\omega)] && \text{-----Eq. 8.5.2} \end{aligned}$$

By equating Eq. 8.5.1 & Eq. 8.5.2,

$$H_{FD}(\omega) = k \cdot H_{tz}(\omega) [1 - H_{mz}(\omega)]$$

The above equation can be simplified for un-damped situation as $c = 0$. This is the case where the lifting object hang on the air.

The dynamic tension on the wire becomes, for un-damped case with $\omega \ll \omega_0$ (natural frequency of the lifting system)

$$F_D = -\omega^2 m e^{i\omega t} \eta_{tz}$$

This equation shows that, the dynamic tension on the wire does not depend on the stiffness of the system where the wave frequency is much lesser than natural frequency of the system.

The above theory mentioned can be referred from (Nielsen, 2007), (S. Rao, 2005).

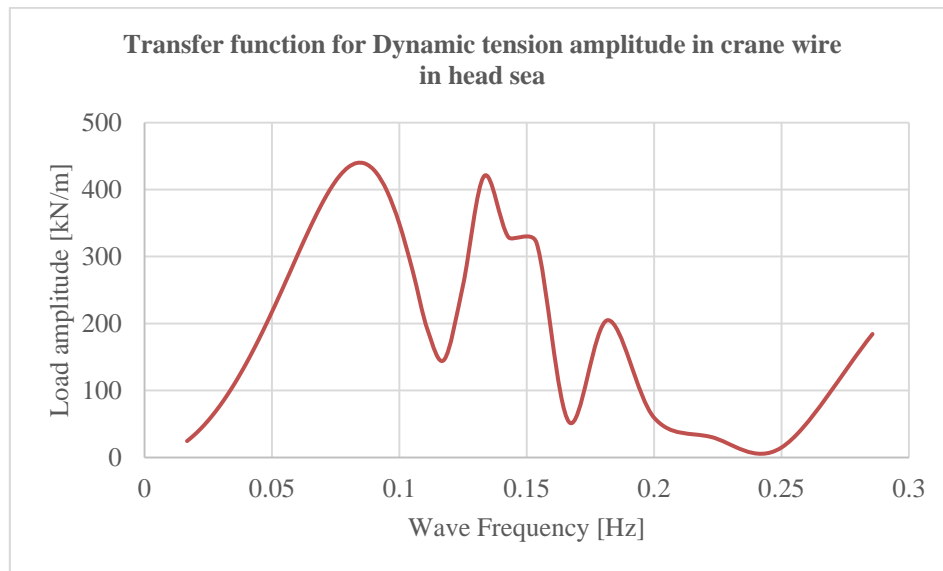


Figure 8-23: Transfer function for dynamic tension amplitude at the structure for Head Sea

The first peak at the dynamic tension amplitude between the wave frequencies 0.05 Hz & 0.1 Hz as shown in Figure 8-23, is due to the pitch motion of the vessel. The second peak between 0.1 Hz and 0.15 Hz is caused by the natural frequency in heave. The third peak at 0.15 Hz is due to the natural frequency in pitch motion. The fourth peak between 0.15 Hz and 0.2 Hz is caused by the combination of pitch and heave motion. At the end of the curve the dynamic tension amplitude increases to 200 kN/m is due to the natural frequency of the lifting system for un-damped case as shown in Eq.8.4.3 which is equal to 0.29 Hz for the lifting system considered for this study.

The dynamic tension amplitude in crane wire is plotted for the wave frequencies in Figure 8-24, when the wave propagates from beam sea. The first peak between 0.05 Hz and 0.1 Hz is caused by the vessel's natural frequency in roll motion. The second peak close to the wave frequency 0.15 Hz is due to the influence of vessel's natural frequency in heave motion. At the end of the curve, the dynamic tension amplitude goes to high peak value due to the resonance between natural frequency of the lifting system (0.29 Hz) and the wave frequency.

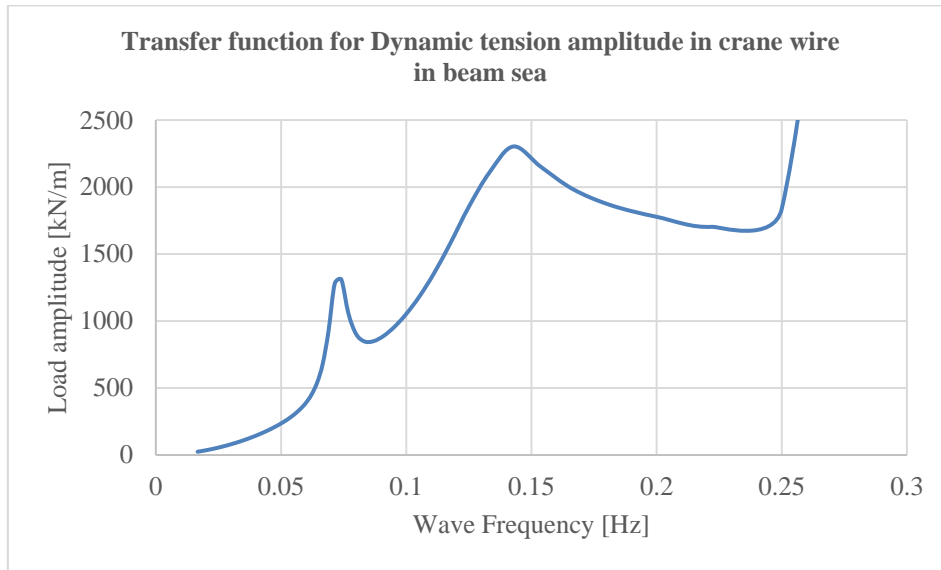


Figure 8-24: Transfer function for dynamic tension amplitude at the structure for Beam Sea

9. Response Spectrum

9.1. Response Spectrum of Total Sea

The response spectrum for the response of specific structural component, here, the dynamic tension in the wire can be obtained by assuming the response is linear to the wave excitation force. The wave spectrum multiplied by square of amplitude of dynamic tension transfer function will lead to the response spectrum for dynamic tension. The response spectrum is also function of wave frequency like wave spectrum. The example response spectrum for $H_s=4\text{m}$, $T_p=10\text{ s}$ is shown in Figure 9-1.

The response spectrum for dynamic tension (S_{FD}) on the crane wire is obtained by,

$$S_{FD}(\omega) = |H_{FD}(\omega)|^2 S_{\Xi\Xi}(\omega)$$

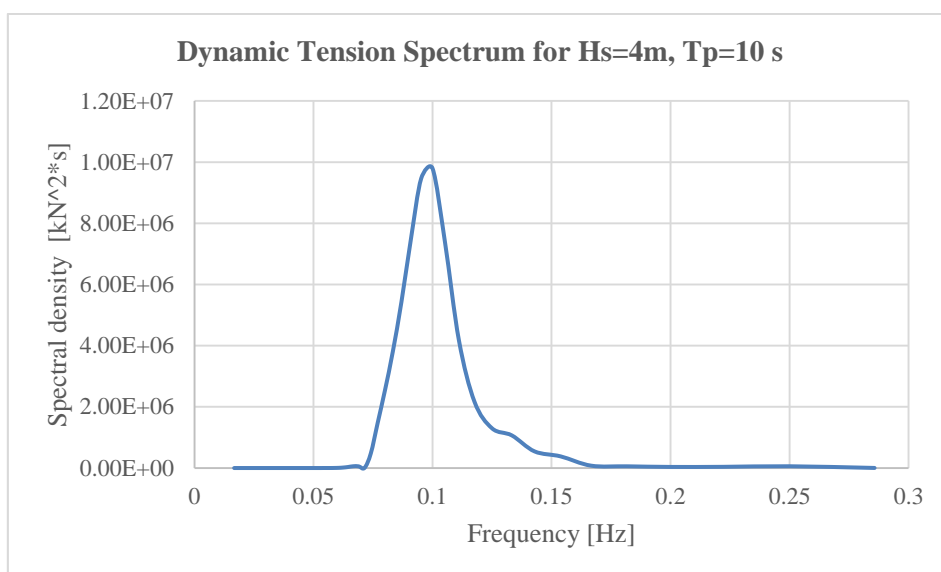


Figure 9-1 Response Spectrum for $H_s = 4\text{m}$, $T_p = 10\text{ s}$, $\Gamma = 2$

If the response spectrum derived based on the linear assumption, the response quantity can be modelled as Gaussian probability distribution. This distribution is function of two parameters which are mean value and standard deviation.

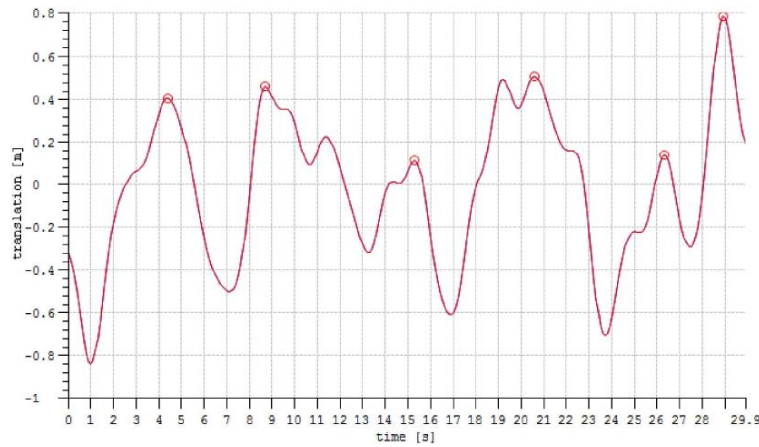


Figure 9-2 Definition of global maxima shown with red circle (Marintek, 2015)

The global maxima is the maximum amplitude of the process between the two consecutive zero-up crossings as shown in Figure 9-2. The global maxima can be modelled as Rayleigh distribution for the stationary Gaussian process with the reasonable adequacy. Rayleigh distribution is a one parameter distribution which is standard deviation.

This theory is referred to (Haver S. , 2014).

9.2. Combined Response Spectrum of Wind and Swell Sea

The response due to the two different wave propagation direction is assumed to be uncoupled. That means, the response of swell sea is not effected by the wind sea from a different direction and vice versa. The response spectrum is calculated for wind sea direction and swell direction, then added together to get the combined response spectrum.

The roll motion of the ship is assumed to be linear which is slightly conservative due to the fact that the damping in rolling increases non-linearly. As they have been assumed linearly, the total response spectrum can be superimposed.

$$\text{Combined Response Spectra } S_{FD_C}(\omega) = |H_{FD_W}(\omega)|^2 S_{\Xi\Xi_W}(\omega) + |H_{FD_S}(\omega)|^2 S_{\Xi\Xi_S}(\omega) \quad \text{-----Eq. 9.2.1}$$

where, $|H_{FD_W}|$ – dynamic tension amplitude due to wind sea

$|H_{FD_S}|$ - dynamic tension amplitude due to swell sea

$S_{\Xi\Xi_W}$ – wave spectrum for pure wind sea

$S_{\Xi\Xi_S}$ – wave spectrum for pure swell sea

The above approach is referred from (Vestbøstad, Haver, Andersen, & Albert, 2002).

The combined response spectra for wind dominated sea and swell dominated sea based on Eq. 9.2.1 are shown in Figure 9-3 & Figure 9-4, when the wind sea propagate in head sea and swell sea propagate in beam sea.

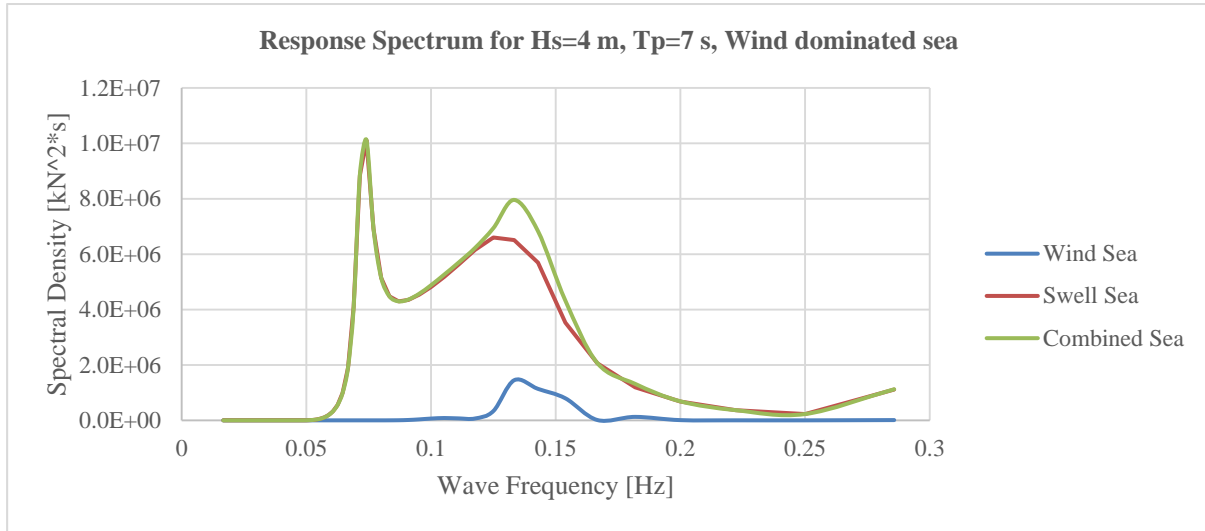


Figure 9-3 Dynamic Tension Response Spectrum for the crossing sea state of $H_s = 4\text{m}$, $T_p = 7\text{ s}$

Even in wind dominated sea shown in Figure 9-3, the response spectral energy due to the swell sea in beam sea direction is much larger. Because the dynamic tension amplitude at beam sea is much higher at the frequencies 0.07 Hz and 0.14 Hz due to natural frequencies as shown in Figure 8-24 than the dynamic tension amplitude at head sea.

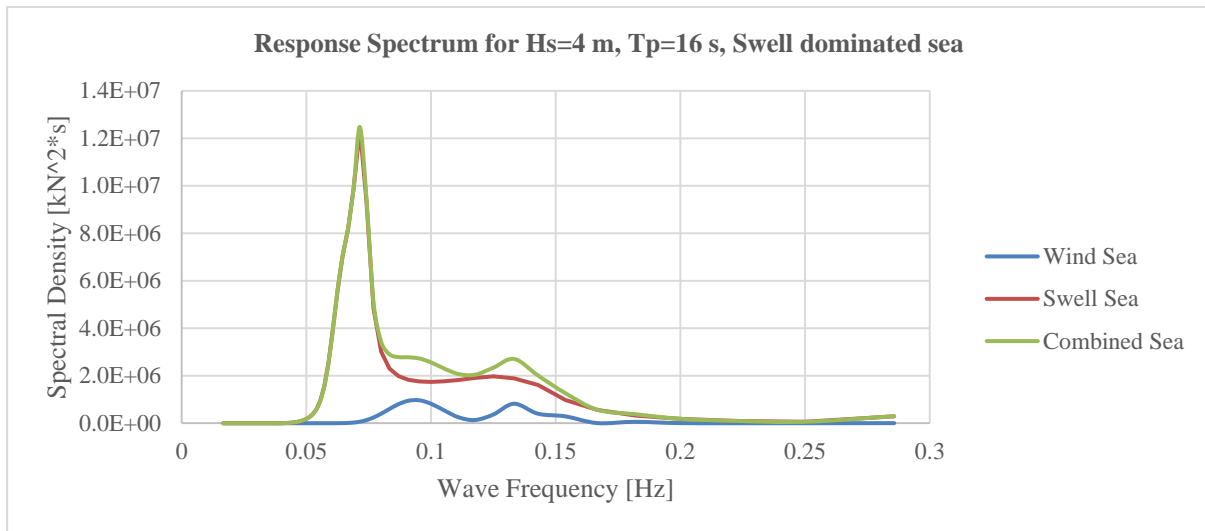


Figure 9-4 Dynamic Tension Response Spectrum for the crossing sea state of $H_s = 4\text{m}$, $T_p = 16\text{ s}$

The response due to swell sea at beam sea is clearly visible in Figure 9-4, as the primary response spectral energy peak is in the low frequency range. The vessel's natural frequency in roll increase the spectral energy further, as that is also in the low frequency range (0.07 Hz).

10. Heave Compensation

The heave compensation is used to reduce the heave motion at different systems. There are different types of heave compensation is used in the industry. They are Passive Heave Compensators (PHC), active heave compensators (AHC) and combined active and passive compensators.

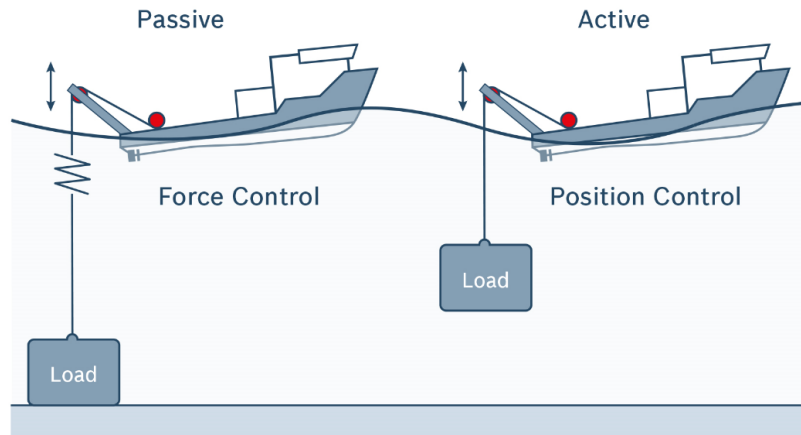


Figure 10-1 Functional Difference between Active and Passive Heave Compensations (Heave Compensation, 2015)

10.1. Passive Heave Compensation

The PHC is used for three different purposes,

- i) to reduce the dynamic tension variation on the crane wire,
- ii) to avoid resonance in deep water lift
- iii) to reduce the landing velocity to the seabed.

In this study, the first case is focused. The passive heave compensators are simply the spring and damper system. The accuracy of a PHC is dependent on the behaviour of gas volume, friction and inertia system. The PHC maintains the tension on the wire rather than the position of the load.

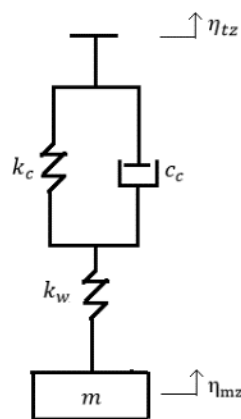


Figure 10-2 Dynamic Model for lifting in air with PHC (left), Photo of PHC during installation (Courtesy: Safelink)

The stiffness of PHC is non-linear which varies with respect to stroke length. Linearized stiffness of PHC is taken for this study. The stiffness and damping characteristics of PHC can be optimized for the need by changing the characteristics of valves, oil level and gas pressure (Cranemaster, 2013). As the

spring of wire and PHC are in series, the equivalent stiffness of the system is estimated by taking inverse of the sum of inverse of each stiffness.

$$\frac{1}{k_{eq}} = \frac{1}{k_w} + \frac{1}{k_c}$$

The stiffness of the crane wire is much higher than the stiffness of PHC. Hence the equivalent stiffness is taken as equal to the stiffness of heave compensator.

$$k_{eq} = k_c$$

The damping characteristics are different for in and out stroke of compensator. It depends the velocity of piston. The average of damping coefficient of in and out stroke is considered for this study.

$$c_c = \frac{1}{2} \left(\frac{F_{d_in}}{V_{in}} + \frac{F_{d_out}}{V_{out}} \right)$$

F_d - Damping force in kN; V – velocity in m/s

By substituting, the equal stiffness of the system and the damping co-efficient of compensator (c_c) in to the equation of transfer function for the motion of equipment in § 8.4,

$$H_{mz_c}(\omega) = \frac{k_c}{-\omega^2 m + i\omega c_c + k_c}$$

The natural frequency of the system with PHC is calculated by,

$$\omega_0 = \sqrt{\frac{k_c}{m}}$$

The above theory mentioned can be referred from (Nielsen, 2007), (S. Rao, 2005).

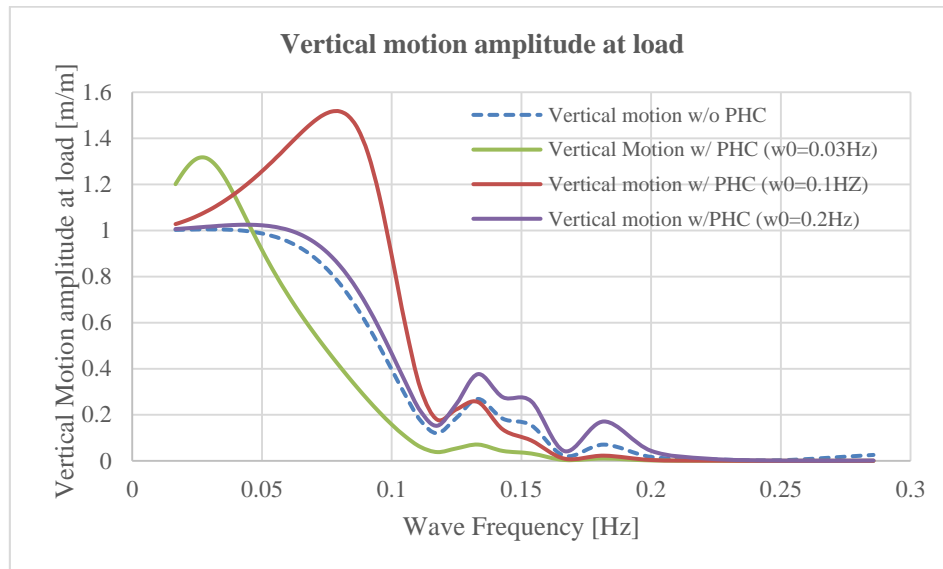


Figure 10-3: The effect of PHC in the motion of load with varying natural period of PHC

The vertical motion amplitude of the suspended mass is lesser compared to the motion without PHC, when the natural frequency of the system with PHC is lower as shown in Figure 10-3. But the PHC system with higher natural frequencies worsens the motion amplitude of the mass than the system without PHC.

The dynamic tension on the crane wire system depends on the relative heave displacement between the crane tip and the hanging equipment and stiffness of the lifting system. The dynamic tension on the wire becomes zero, when the relative displacement is zero. In this case, lifting in air with no PHC, there is no damping. Hence the vertical motion of equipment will be in phase with the vertical crane tip motion. When the PHC is added on the lifting system, due the damping of PHC, there will be a phase angle between them which depends the damping and stiffness of the system as well.

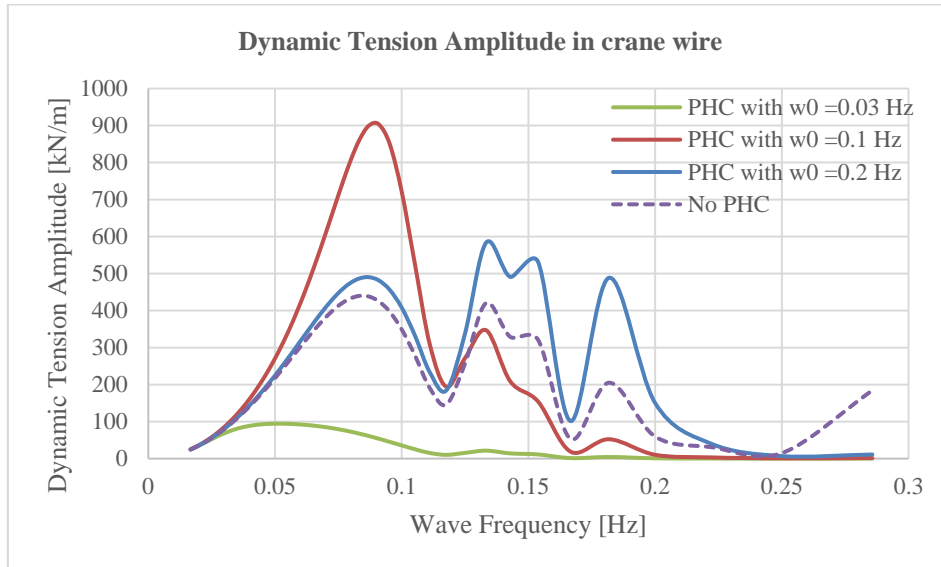


Figure 10-4: The dynamic tension amplitude on crane wire with varying natural period of system with PHC ($c=600$ kN.s/m) in head sea

The dynamic tension amplitude on the crane wire is plotted for various natural period of the system with PHC in Figure 10-4. It can be seen that, the system with lowest natural frequency suppress the dynamic tension in the wire effectively. The system with high natural frequency has no influence on the reduction of dynamic tension. Instead, they increase the dynamic tension due to the effect of natural frequency of the system. So, care should be taken for selecting the stiffness of PHC. As the effectiveness depends on the natural frequency, the system for lifting of heavy weight works better than the light weight lifting.

The efficiency of PHC is assessed by changing the damping characteristics for the PHC with different natural frequencies. By increasing damping, the dynamic tension amplitude can be reduced. This is shown in Figure 10-5 & Figure 10-6. For the natural frequency of the system which is much lower, the amount of damping needed to reduce the dynamic tension is lower, compared to the higher natural frequency of the lifting system with PHC.

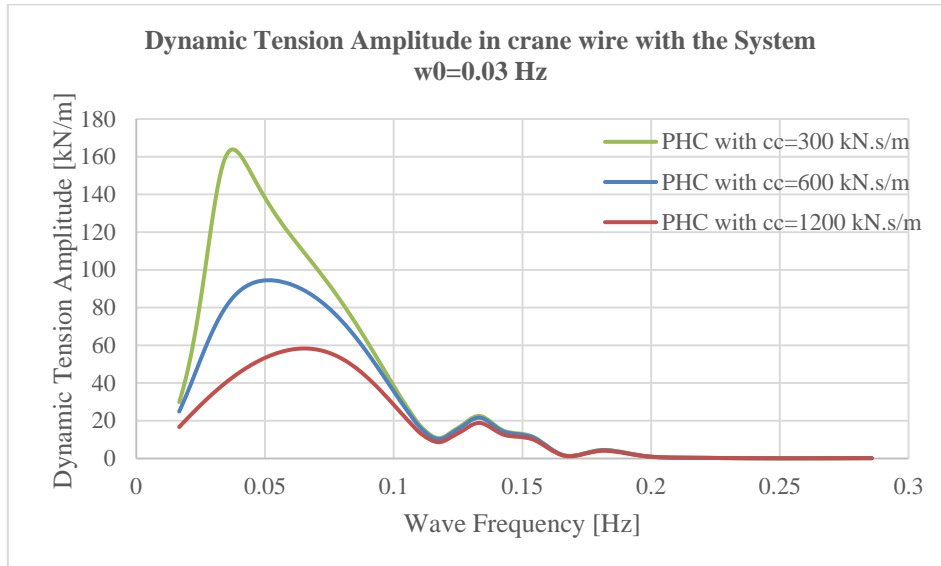


Figure 10-5 The dynamic tension amplitude on crane wire with variation of damping of PHC with the natural period of the system $w_0 = 0.03$ Hz

The peak values of dynamic tension amplitude at 0.03 Hz in Figure 10-5, is due to the natural frequency of the lifting system including PHC:

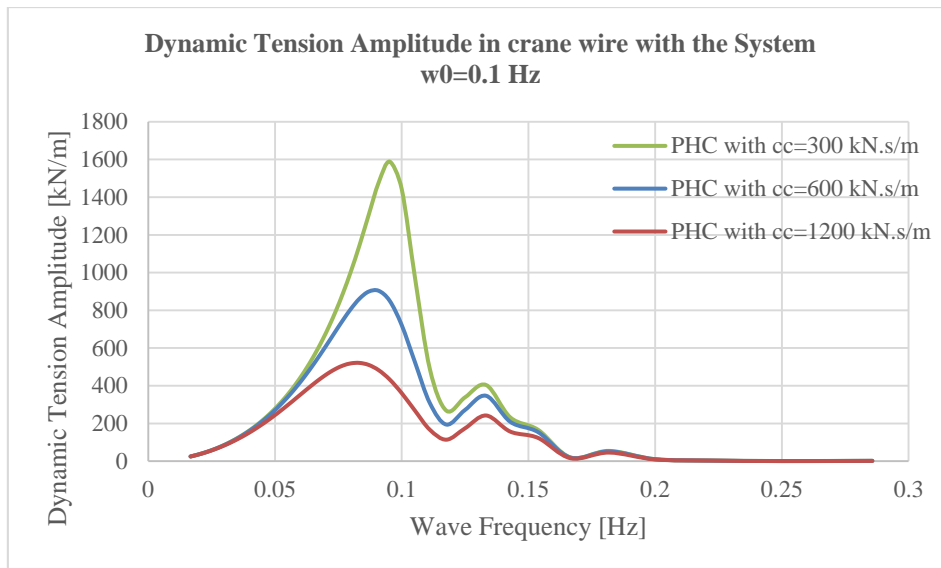


Figure 10-6 The dynamic tension amplitude on crane wire with variation of damping of PHC with the natural period of the system $w_0 = 0.1$ Hz

From Figure 10-6, due to the resonant motion, the dynamic tension amplitude is much higher for the low damping of compensator. So, in order to reduce the dynamic tension amplitude due to the resonance, higher amount of damping is required to decrease the dynamic tension on the wire.

10.2. Active Heave Compensation

The active heave compensators uses actively controlled winches and hydraulic systems. In order to control these active system, they need a reference signals which can be obtained from system such as Motion Reference Unit (MRU) on the vessels. Based on the reference signal, the control system either pay-in or pay out of the winch wire attached to the suspended load to compensate the heave motion of the vessel. If the AHC works perfectly, the heave of the vessel will be completely compensated on the load. But 100% accuracy is not possible with the technology available at the moment. So there will be a residual motion which is not compensated by the AHC.

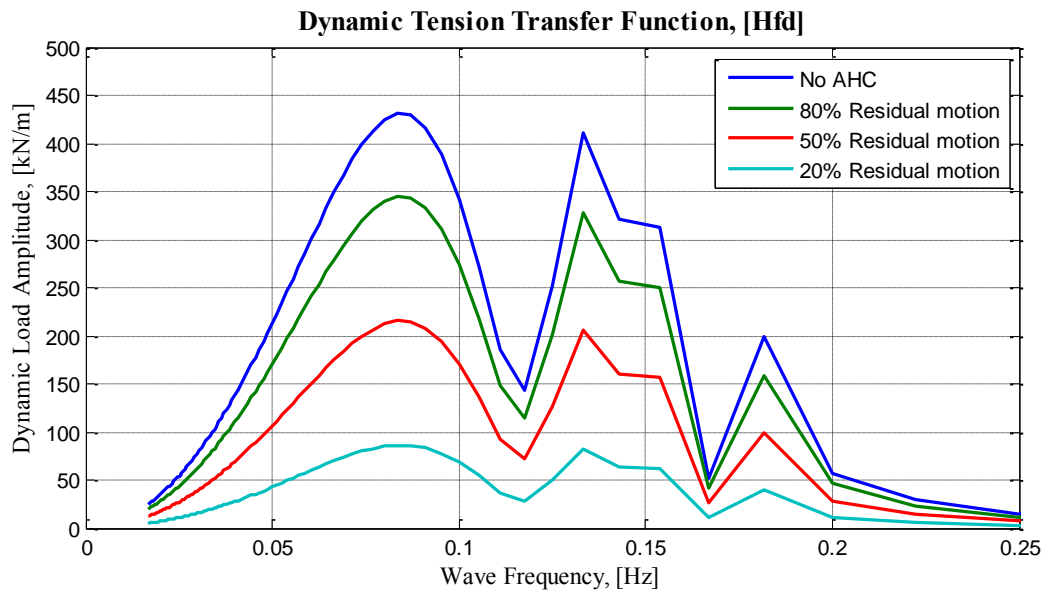


Figure 10-7 Dynamic Tension Variation with the effectiveness of AHC in head sea

In the Active Heave Compensation system, the effectiveness of the system rely on the reference signal and the efficiency of the active control system. The dynamic tension amplitude due to the residual motion left out during compensation are plotted in Figure 10-7. It can be seen that, the residual motion at the mass is lower, the dynamic tension amplitude is also lower.

11. Limiting Sea-state

11.1. Deterministic approach

Deterministic approach is a very simplified method to determine the limiting sea state for the operation. This approach is followed based on DNV recommended practice (DNV-RP-H103, 2014)

In deterministic response calculation, the dynamic tension on the wire is obtained by multiplying the dynamic tension transfer function as shown in Figure 8-23 with the amplitude of a wave. The amplitude of wave is increased until the dynamic tension on the wire reaches up to the allowable dynamic tension on the wire. Then, the maximum allowable individual wave height is the twice the maximum allowable wave amplitude. As the amplitude of dynamic transfer function for the high frequency of waves are very lower, the obtained limiting individual wave heights are much higher as shown in Figure 11-1.

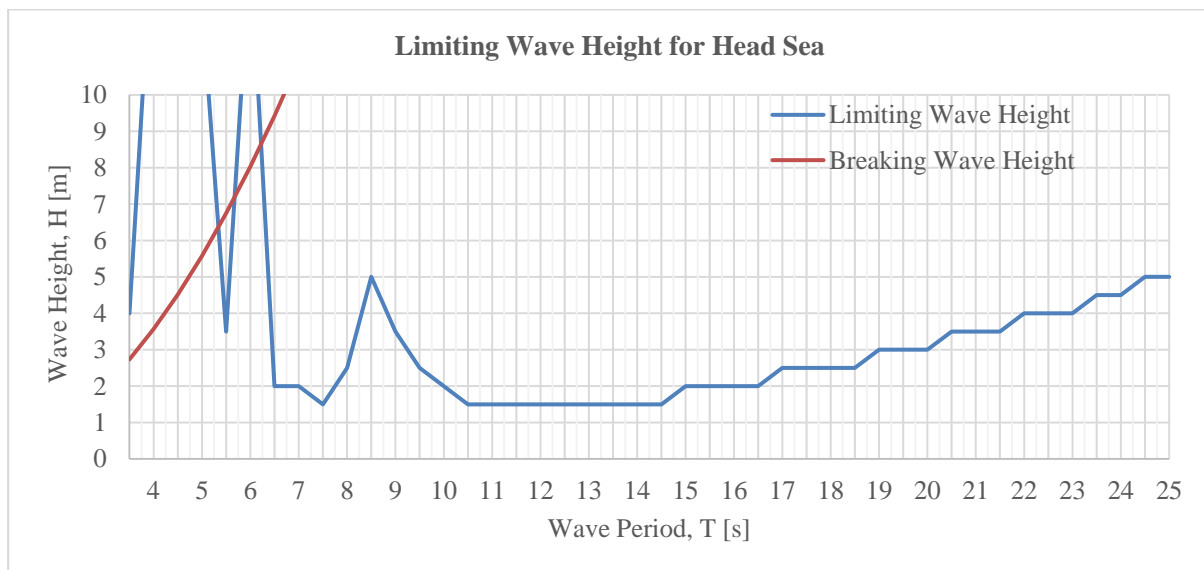


Figure 11-1: Limiting sea state based on dynamic hook capacity (deterministic case) in head sea

There is a question arises, how bigger the wave height can be. The maximum wave height depends upon its breaking. The breaking wave height for the water depth 'd' is based on the maximum steepness of a wave. If the steepness of a wave is higher than this limit, the wave will break and vice versa. The wave breaking criteria is written as

$$\frac{H_b}{\lambda} = 0.142 \tanh \frac{2\pi d}{\lambda}$$

H_b – Breaking wave height

This can be simplified for deep water case based on dispersion relation which gives relation between wave length and time period,

$$\frac{H_b}{\lambda} = \frac{1}{7}$$

Based on this criterion, the obtained wave height higher than breaking wave height is disregarded in Figure 11-1 and considered as limiting sea state.

The peak in the limiting wave height for the wave period $T=8.5$ s is due to the very low dynamic tension amplitude for the wave frequency 0.12 Hz as shown in Figure 8-23.

In order to convert the individual wave height to significant wave height, it is considered that the limiting individual wave height as most probable largest wave height in 3 hours stationary sea state. Hence, the significant wave height is calculated as,

$$H_s = \frac{H_{max}}{1.86}$$

The wave period for the most probable largest wave height is assumed as,

$$T_{Hmax} = 0.9 \cdot T_p$$

$$T_p = \frac{T_{Hmax}}{0.9}$$

From this expression, the spectral peak period is computed from the wave period corresponds to the maximum wave height in 3 hours.

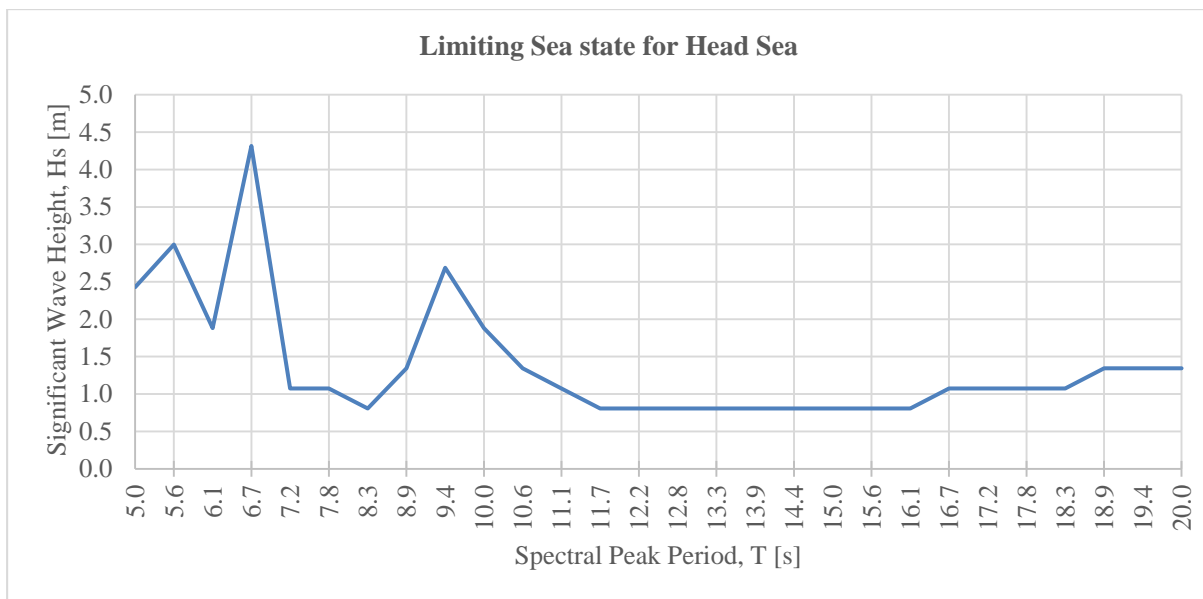


Figure 11-2: Conversion of Limiting Sea state from deterministic to stochastic case in head sea

11.2. Stochastic Approach

Limiting sea-state for this marine operation is computed by considering the dynamic tension on the crane hook as the only limiting parameter. The limiting sea-state is obtained by comparing standard deviation of the critical quantity i.e. allowable dynamic tension, with the standard deviation from the response spectrum. The standard deviation of critical quantity should be higher than the obtained standard deviation from the response spectrum.

The dynamic tension response quantity is a linear response quantity. Hence, this response process can be modelled as a Gaussian distribution. For the Gaussian process, the distribution of global maxima as defined in Figure 9-2 of dynamic tension response random variable (T) follows the Rayleigh distribution and can be written as,

$$F_{T_G}(t) = P(T_G \leq t) = 1 - \exp\left\{-\frac{1}{2} \left(\frac{t}{\sigma_{T_G}}\right)^2\right\}$$

Rayleigh distribution is the one parameter distribution. The only parameter is the standard deviation of the response quantity. σ_{T_G} is the standard deviation of the random variable, dynamic tension.

The distribution of extreme dynamic tension response in 3 hours sea state, can be written as, by assuming the global maximums in 3 hour period as a statistically independent and identically distributed quantity,

$$F_{T_{3h}}(t) = [F_{T_G}(t)]^{n_{3h}} = \left[1 - \exp \left\{ -\frac{1}{2} \left(\frac{t}{\sigma_{T_G}} \right)^2 \right\} \right]^{n_{3h}}$$

$$n_{3h} - \text{number of response cycles in 3 hours} = \frac{10800}{T_z}$$

$$T_z - \text{Average zero cross-up period} = 2\pi \sqrt{\frac{M_0}{M_2}}, \text{ This expression is valid, if } \omega \text{ is in rad/s.}$$

The acceptance criteria is the probability of exceedance (q_{3h}) of the critical response quantity. The probability of exceedance is the measurement of the risk taken for the installation. Risk is defined as the product of probability of failure and consequences of failure. It is obvious that, choosing the low probability of exceedance (failure probability) for an operation will give low risk and vice versa. For this study, the probability of exceedance of allowable dynamic tension (F_{D_all}) on the crane wire is considered as 0.01.

$$P(T_G > F_{D_all}) \leq q_{3h}$$

$$1 - P(T_G \leq F_{D_all}) \leq q_{3h}$$

$$1 - \left[1 - \exp \left\{ -\frac{1}{2} \left(\frac{F_{D_all}}{\sigma_{T_G}} \right)^2 \right\} \right]^{n_{3h}} \leq q_{3h}$$

$$\sigma_{T_G} \leq \frac{F_{D_all}}{\sqrt{-2 \ln \left[1 - (1 - q_{3h})^{\frac{1}{n_{3h}}} \right]}}$$

The limiting standard deviation of the response quantity ($\sigma_{C,FD}$),

$$\sigma_{C,FD}(T_p) = \frac{F_{D_all}}{\sqrt{-2 \ln \left[1 - (1 - q_{3h})^{\frac{1}{n_{3h}}} \right]}}$$

The standard deviation of the dynamic tension response,

$$\sigma_{T_G} = \sigma_{FD}(H_s, T_p) = \sqrt{\sum_{i=1}^N |H_{FD}(\omega)|^2 \cdot S_{\Xi\Xi}(\omega, H_s, T_p) \cdot \Delta\omega}$$

For each spectral peak period, the significant wave height has to be increased to find out the limit until the condition below is valid.

$$\sigma_{FD}(H_s, T_p) \leq \sigma_{C,FD}(T_p)$$

From the above procedure, the limiting sea state in head sea is calculated and plotted in Figure 11-3.

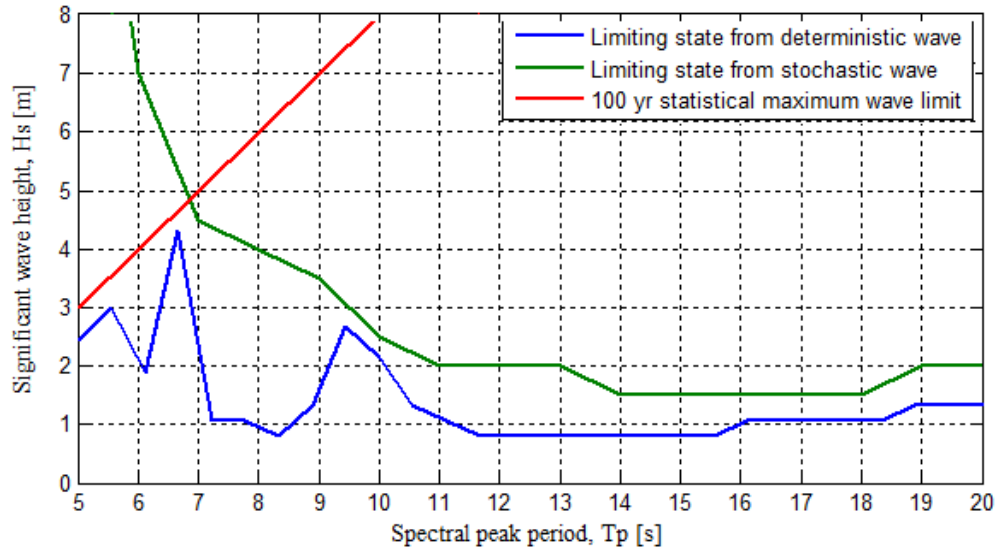


Figure 11-3: Limiting Sea state from Deterministic and Stochastic method for head sea

100 year statistical wave limit is the wave limit which has the probability of exceedance as 0.01 annually. This has been plotted in Figure 11-3 in order to consider the most probable sea states in this study. The obtained limiting sea states beyond this limit are not important based on their probability of occurrence.

Two approaches have been followed to obtain the limiting sea state for this operation. The approach based on stochastic waves gives higher sea state than deterministic approach. This can be understood from the Figure 11-3. The difference is almost 1 m significant wave height for many spectral periods. So, it is very essential to follow the stochastic approach where the cost efficient installation is required.

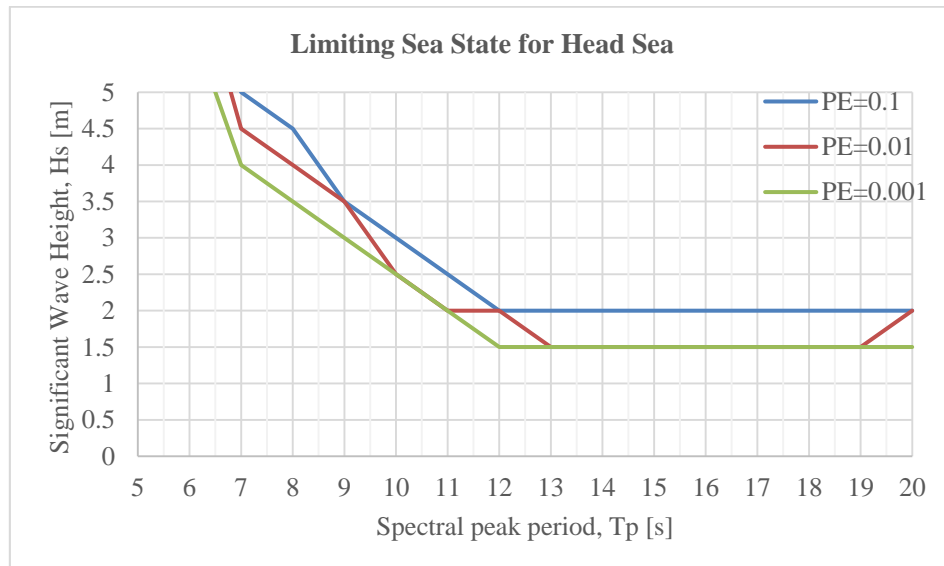


Figure 11-4: Limiting Sea state for head sea with various probability of exceedance (PE) of allowable dynamic tension

The sensitivity of probability of exceedance of allowable dynamic tension with respect to limiting sea state is plotted for head sea and beam sea in Figure 11-4 & Figure 11-5. In general, the probability of exceedance is higher, the limiting sea state will also be higher. When the probability of exceedance of critical quantity is decreased, the limiting sea state will also be lowered. In Figure 11-4, for the

spectral peak periods higher than 12 s, the lowering of probability of exceedance below 0.01 do not have any influence on the limiting sea-state.

Whereas limiting sea state in beam sea as shown in Figure 11-5, the influence of the probability of exceedance of the critical quantity is nothing for the spectral peak periods less than 16 s.

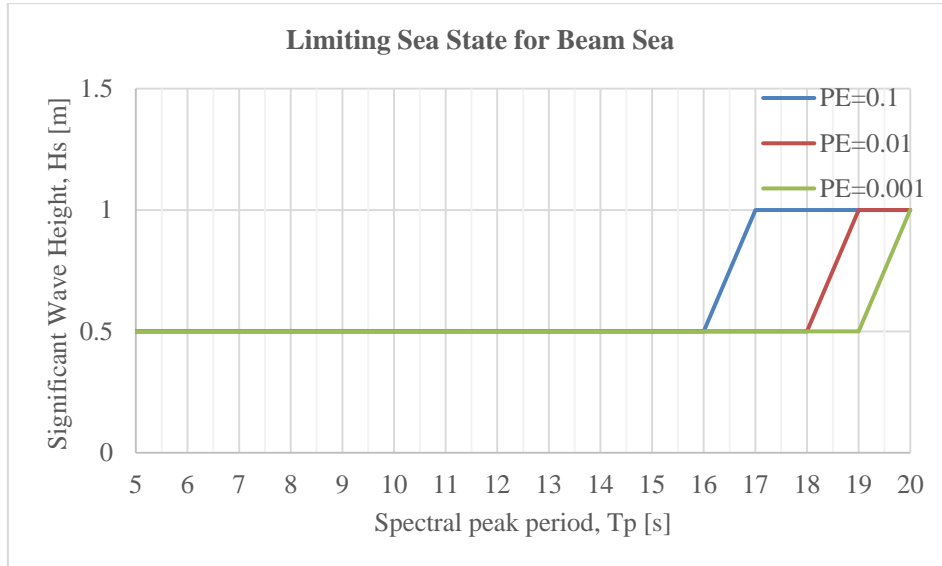


Figure 11-5: Limiting Sea state for beam sea with various probability of exceedance (PE) of allowable dynamic tension

The limiting sea state for the crossing sea where the wind sea and swell sea coming from different directions. It is considered that the vessel heads towards the wind sea as head sea. Then, the limiting sea states shown in Figure 11-6 are obtained by varying the swell direction between head and beam seas. The stochastic approach described above in this section, has been followed to obtain this limiting sea state for combined sea.

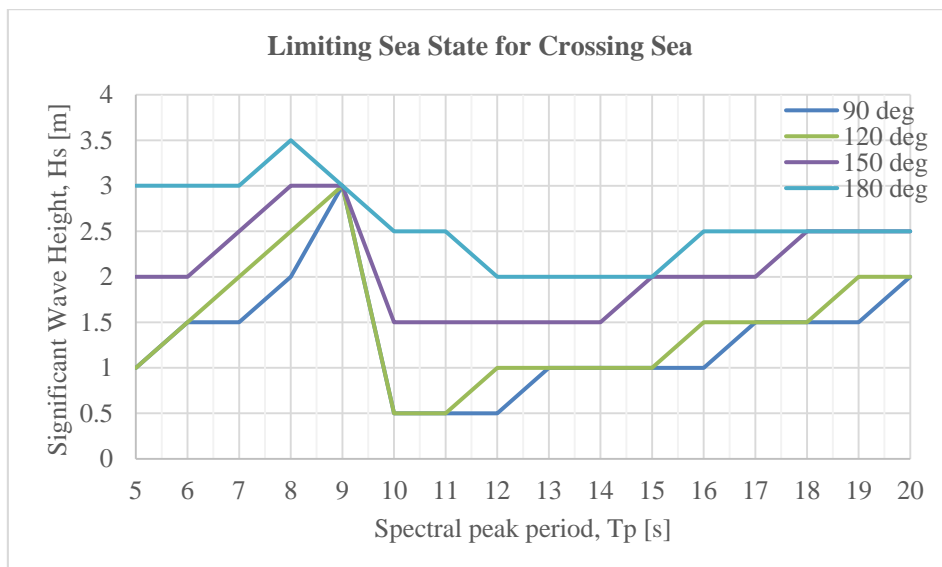


Figure 11-6: Limiting Sea state based on dynamic hook capacity for crossing sea with Wind Sea in head sea, Swell sea in different wave direction

The swell on the side of the vessel reduces the limiting sea state for the installation. When the swell propagates in beam sea direction of the vessel, the limiting sea state is as low as 0.5 m. The

limiting sea states obtained using combined wave spectrum when wind and swell seas propagate in head sea together, are mostly higher than single peak Jonswap spectrum.

There is a convergence for the $T_p = 9$ s in limiting sea state regardless of swell sea direction. This is because the combined wave spectrum becomes single peak spectrum for this spectral period. When $T_p = T_{pf}$ as shown in Appendix -1: Crossing Sea Spectral Parameters, the sea state is called as locally fully developed sea state. In this situation, there is no swell spectrum. So the response spectrum will also be a single peak spectrum in wind sea direction.

12.Planning of Marine Operations

After getting the limiting sea state based on limiting criteria, the planning of marine operation has to be done. For this study of planning a marine operation, the hindcast data, WAM10 from Haltenbanken area (Latitude: 65.29, Longitude: 7.32) in Norwegian continent shelf is used from year 1957 until 2014. The hindcast data consists of Date with the interval of 3 hours as the sea state considered for 3 hours, Wind Speed in m/s and its direction, significant wave height, spectral peak period and direction for Total Sea, Wind Sea and swell sea. The excerpts from the hindcast file is shown in Figure 12-1.

WAM WIND AND WAVES																
LATITUDE: 65.29, LONGITUDE: 7.32																
				WIND		TOTAL SEA					WIND SEA			SWELL		
YEAR	M	D	H	WSP	DIR	HS	TP	TM	DIRP	DIRM	HS	TP	DIRP	HS	TP	DIRP
1957	9	1	6	7.0	33.	1.1	5.2	4.3	36.	26.	0.7	5.2	36.	0.8	5.2	351.
1957	9	1	9	7.9	21.	1.1	5.2	4.2	21.	27.	0.9	5.2	21.	0.6	6.3	66.
1957	9	1	12	8.4	26.	1.2	5.7	4.3	21.	26.	1.1	5.2	21.	0.6	6.9	351.

Figure 12-1: Excerpt of Hindcast data file

The wave propagating from North direction is considered as 0 degree, whereas 180 degree from south as shown in Figure 12-2. The significant wave height of the total sea is obtained by taking square root of sum of square of significant wave heights of wind sea and swell.

$$H_{S_{total}} = \sqrt{H_{S_{wind}}^2 + H_{S_{swell}}^2}$$

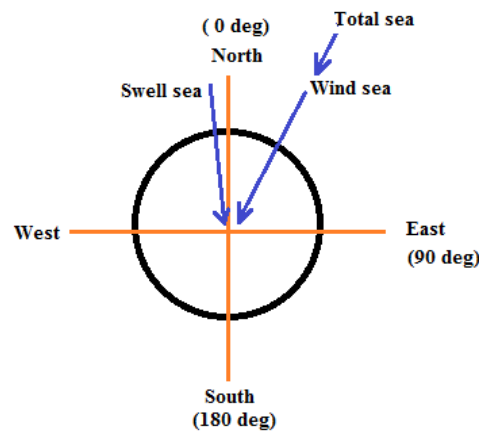


Figure 12-2: Wave directions in hindcast data for (1-9-1957) 6th hour

12.1. Wind Speed Correction

According to (Nygaard, Einar, 2015) & (Haver S. K., 2015), there has been study conducted to compare the wind speed in hindcast data with measured wind speed at offshore platforms. The comparison study revealed that the extreme wind speed from hindcast analysis was slightly low side. Assuming the measured wind speed is correct, the wind speed from hindcast data is corrected for the speed more than 15 m/s by increase of 20% of difference speed above 15 m/s.

$$W_{hc_corr} = W_{hc} + 0.2 (W_{hc} - 15)$$

W_{hc} – Wind speed from hindcast analysis in m/s; W_{hc_corr} – corrected wind speed in m/s.

The above correction is based on the belief that measured wind speed at the platforms are the correct data. The measured wind speed may be influenced by the geometry of platform. In order to investigate that, CFD (Computational Fluid Dynamic) analysis has been conducted. The results show that the influence of platform geometry increases the wind speed. But the result could not give the exact difference of influence. The measured wind speed at offshore wind mast, where the wind speed is not disturbed by the structure, is almost similar to the hindcast data. The research is ongoing about this correction procedure. At this juncture, it is recommended to correct the wind speed from hindcast data as mentioned above. (Nygaard, Einar, 2015)

During the phase of lifting the equipment in air, the wind speed is significant parameter due to the pendulum motion of the equipment hanging from crane. Therefore, the correction of this wind speed is necessary to calculate extreme pendulum motion of the mass and plan the operation accordingly.

12.2. Randomizing spectral peak periods

The WAM10 hindcast data are plotted for the scatter of spectral peak period with significant wave height for total sea as shown in Figure 12-3. It can be understood from the scatter plot, the spectral peak periods are discrete values. In total, there are 24 discrete values. The distribution of spectral peak periods are not uniform between the intervals. For example, there are 3 discrete values between T_p of 3 s and 4s, and nothing between 15 & 16 s. This is because, the spectral peak period values are converted from the natural logarithmic of T_p where the spacing between the values are constant. When the T_p values are converted from $\ln(T_p)$, the spacing is not constant. That is why, the spectral periods non-uniformly distributed.

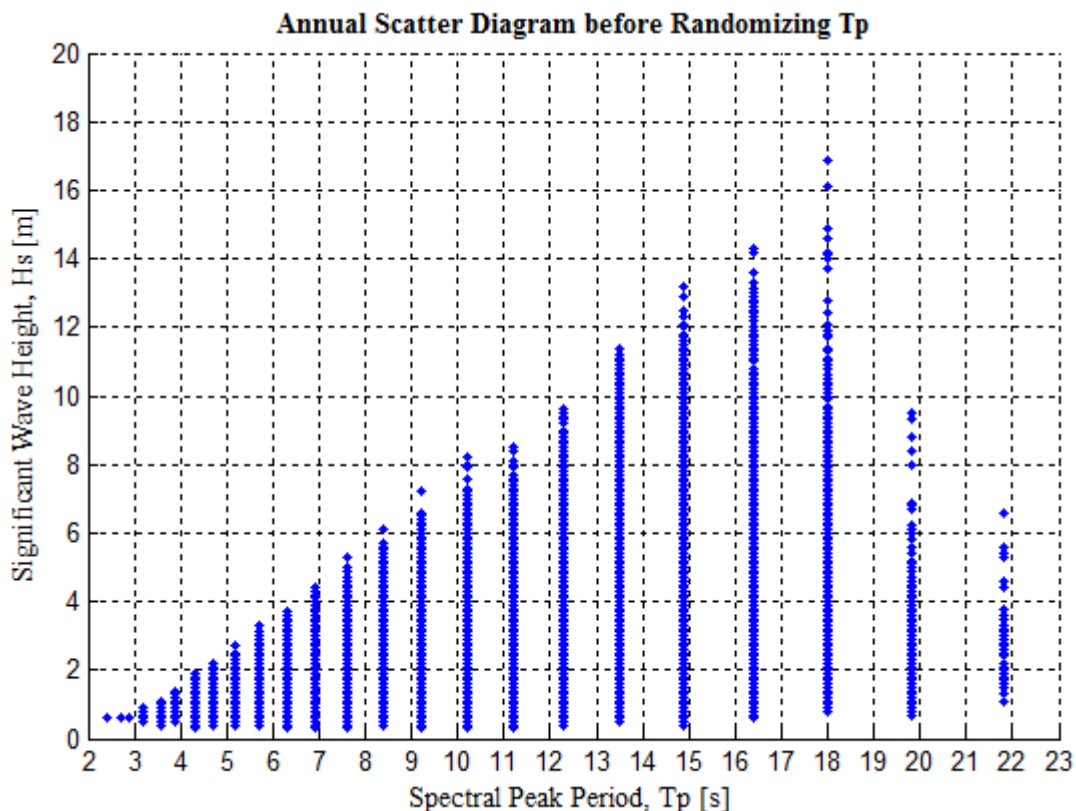


Figure 12-3: Annual Scatter Diagram before randomizing Spectral Peak Period for Total sea (Haltenbanken area)

Due to the discrete values of spectral peak period, the fatigue in a mooring study is increased significantly compared to the scatter diagrams produced based on smooth Log-normal (LoNoWe) model (Statoil, 2009). Hence, the data between the intervals are to be uniformly distributed i.e. non-discretized.

The discrete spectral peak period values in the WAM10 hindcast data are described based on the rounding off to the one decimal of actual T_p and the natural logarithmic spacing,

$$T_p = 3.244 \cdot e^{0.09525 (i-1)} \text{ where, peak period number } i = 1, 2, \dots$$

The obtained values from the above expression are matching with the hindcast data. The peak period number is written as, from the above expression

$$i = \text{round} \left[1 + \frac{\ln\left(\frac{T_{p_hindcast}}{3.244}\right)}{0.09525} \right]$$

The peak period number for the spectral peak period in the WAM10 hindcast data are calculated based on above expression. Then, the discrete values of T_p are randomized by,

$$T_{p_rand} = 3.244 \cdot e^{0.09525 (i-0.5- rand)}$$

‘rand’ is a function which uniformly distribute random numbers between 0 and 1.

The randomized spectral peak period is plotted with respect to the significant wave height in Figure 12-4. The T_p are distributed evenly, and they are not anymore discrete values. This approach is verified with LoNoWe model and measured data. The randomized spectral periods are close to the properties of LoNoWe model and the measured data. (Statoil, 2009)

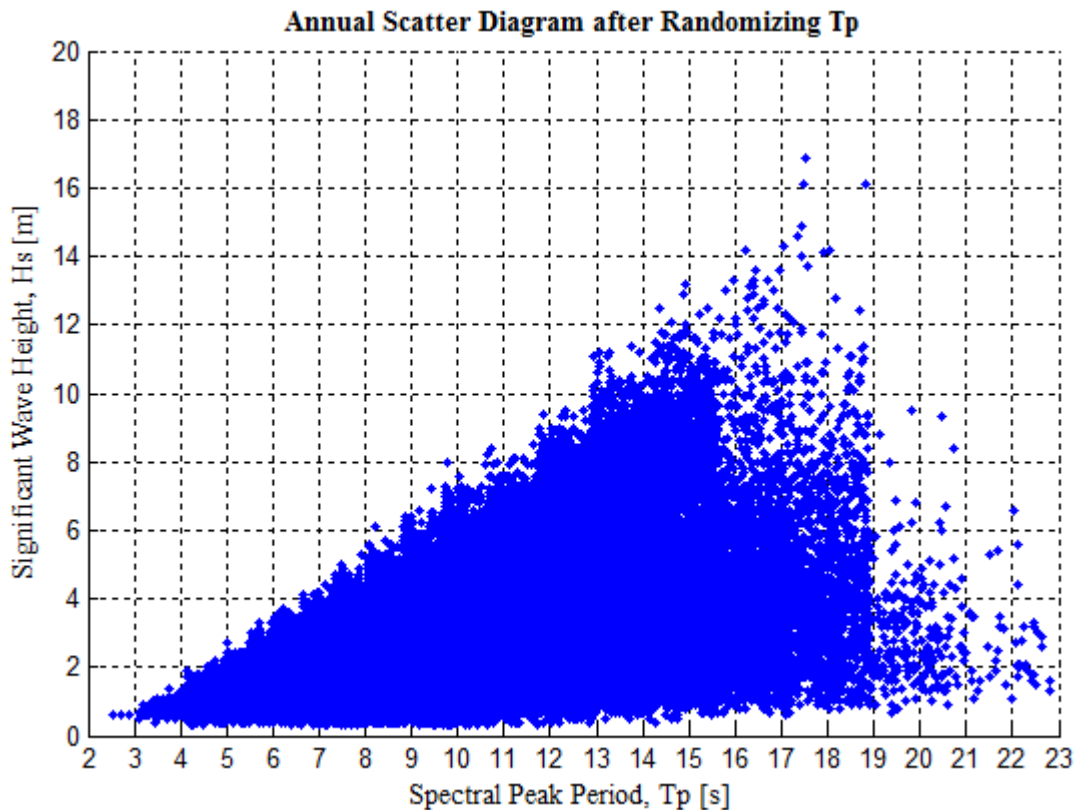


Figure 12-4: Annual Scatter Diagram after randomizing Spectral Peak Period for Total sea (Haltenbanken area)

Likewise, the components of Total sea, wind sea and swell sea are also plotted with randomised spectral peak period as shown in Figure 12-5 & Figure 12-6

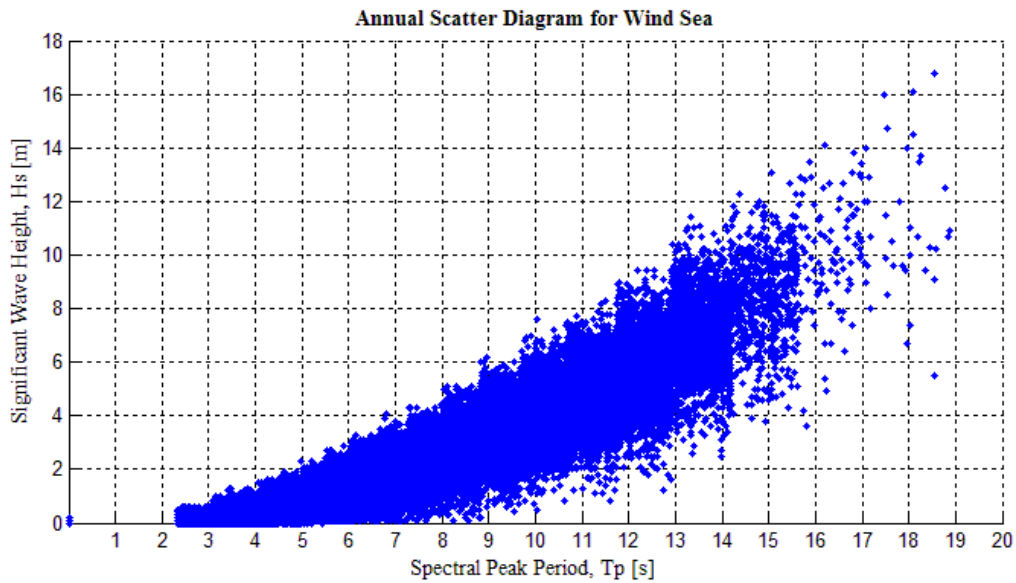


Figure 12-5: Annual Scatter Plot for wind sea for the period 1957-2014 (Haltenbanken area)

The wind sea grows when the wind speed increases; after a time the energy of wind is dissipated, then no more energy to create wind sea. But the remaining propagating waves after the wind energy becomes zero, considered as swell sea; This can be clearly seen on Figure 12-5. For example, the wind sea for 15 s has the minimum wave height around 4 m; there are no wind seas less than 4 m as they are considered as swell sea due to dissipation of wind energy.

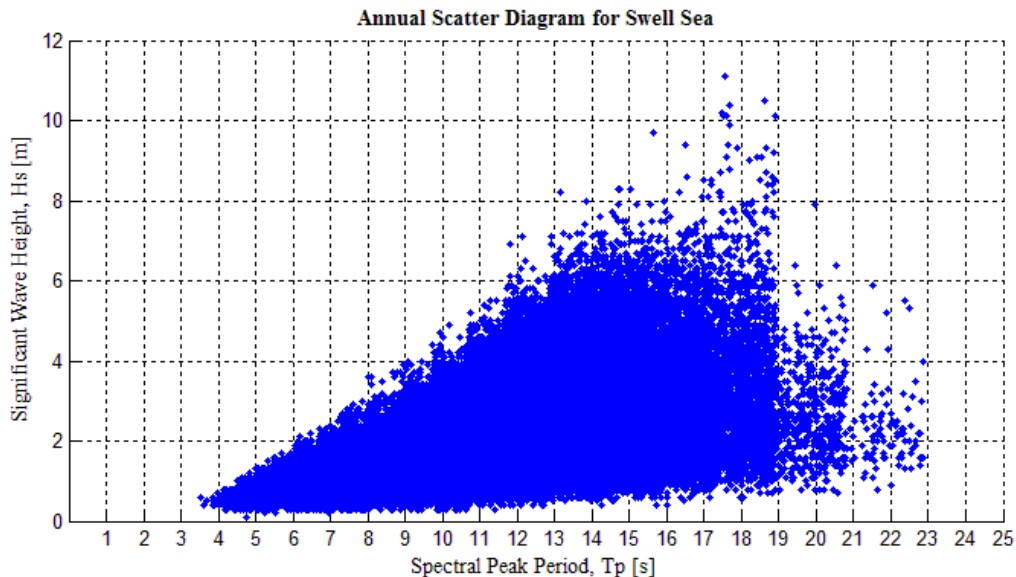


Figure 12-6: Annual Scatter Plot for Swell sea for the period 1957-2014 (Haltenbanken area)

Also, the monthly scatter plots are presented Figure 12-7 & Figure 12-8 with randomised spectral peak periods. It can be seen that, the sea state is decreasing from January to July; then it is increasing after July until December.

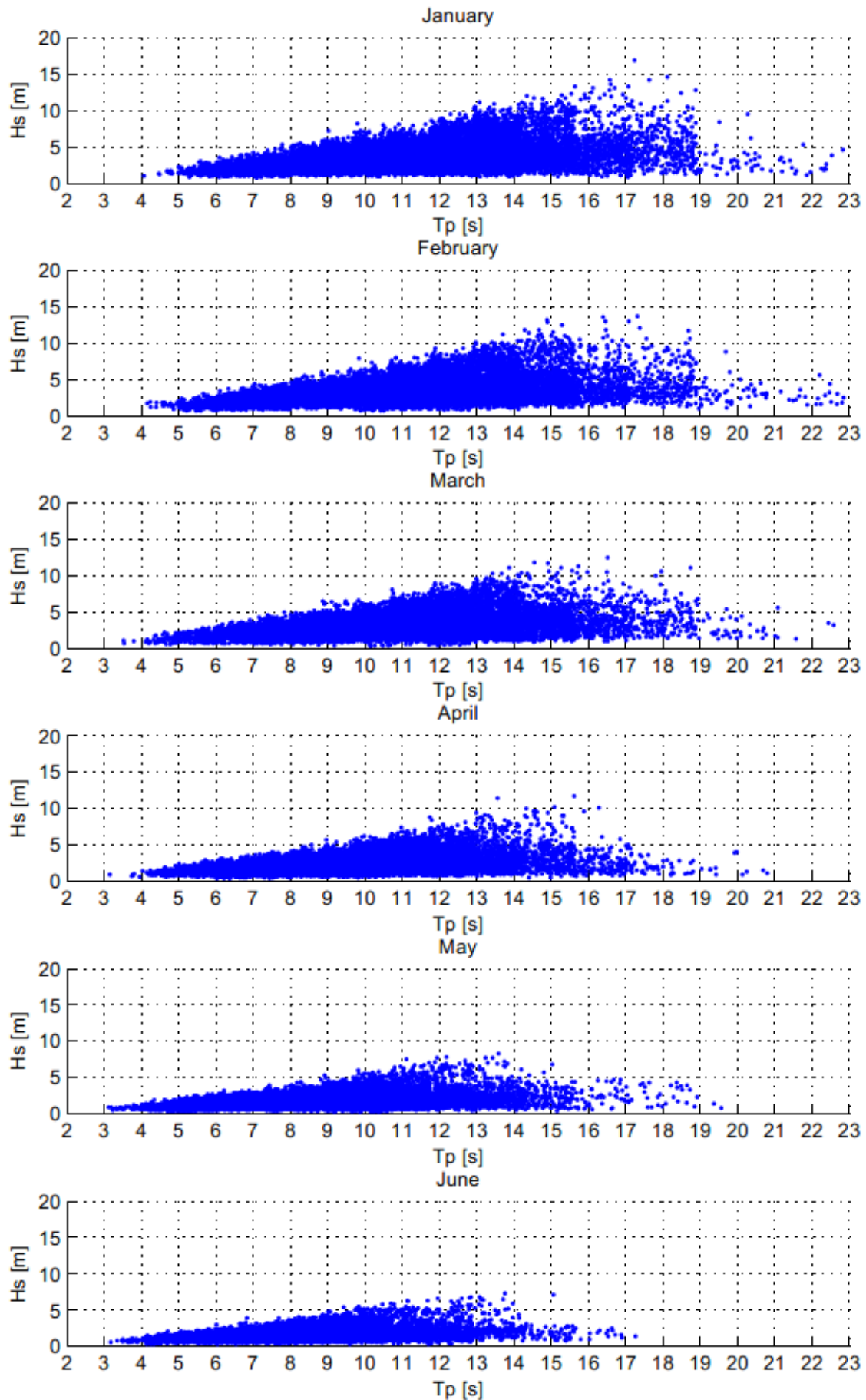


Figure 12-7: Monthly Scatter Diagram from January to June (Haltenbanken area)

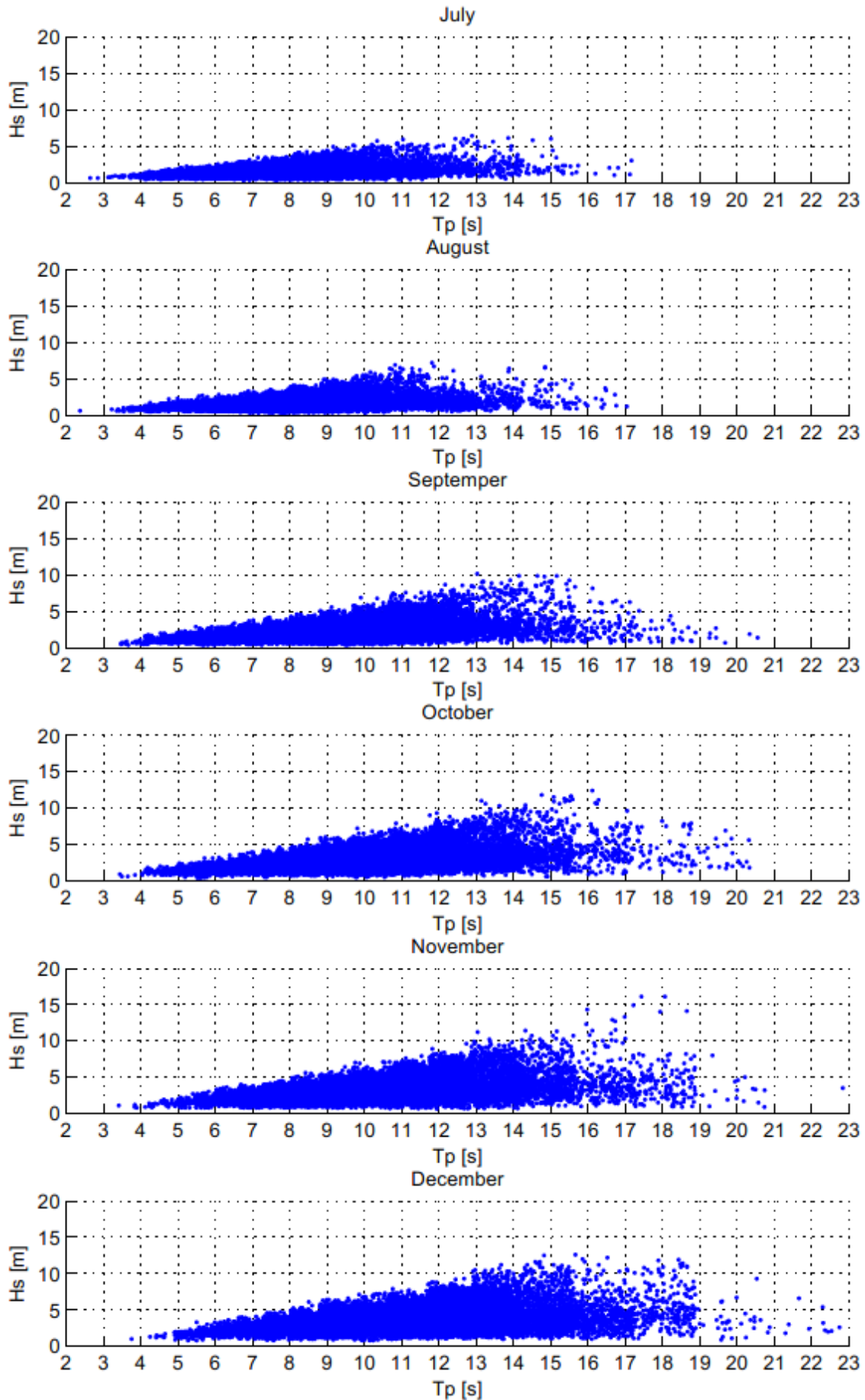


Figure 12-8: Monthly Scatter Diagram from July to December (Haltenbanken area)

12.3. Annual and Monthly Scatter Table

When the duration of a marine operation is exceeding the duration of reliable weather forecast, that operation is classified as an un-restricted operation. The weather conditions for un-restricted operations will be defined based on the available weather statistics from the past years. From the weather statistics i.e. hindcast data, the scatter tables have to be produced for this purpose.

After randomising the spectral peak periods in the WAM10 hindcast file, the scatter table with Significant wave height and Spectral peak period is produced by counting the number of 3 hrs sea state within the intervals of them. The annual scatter table is shown in Table 12-1. Also, the produced scatter tables in month wise are also presented in Appendix -2: Monthly Scatter .

The percentage of times the possibility of operations during a year can be find out from this scatter table as shown below. It is assumed here, the spectral peak period is not a limiting quantity for sea state.

$$\begin{aligned} & \text{Percentage of times the possibility of a operation} \\ & = \frac{\text{Total number of Seastate less than the limiting seastate (i.e.cumulative)}}{\text{Total number of seastate}} \end{aligned}$$

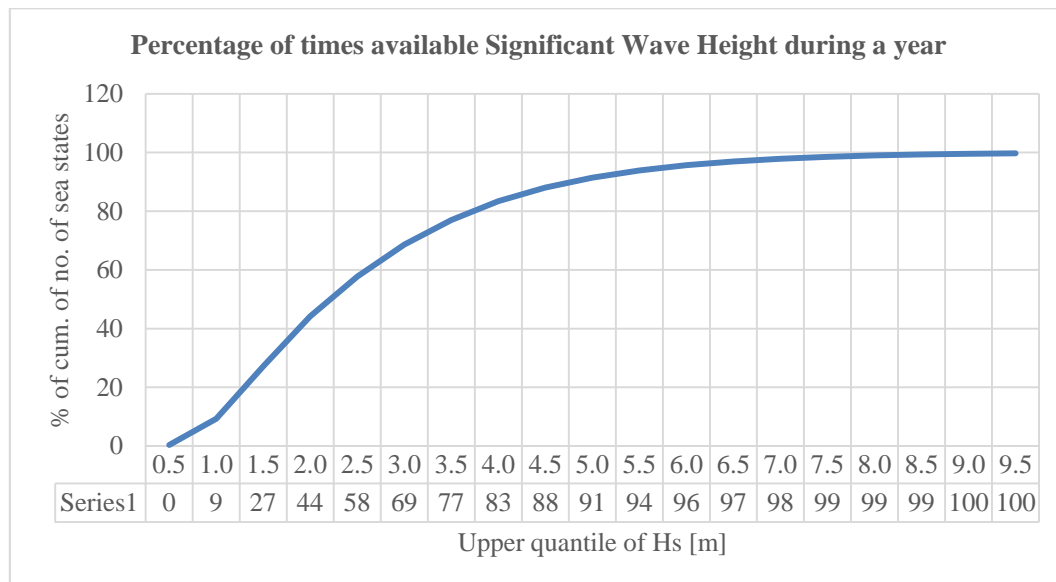


Figure 12-9: Percentage of times available Significant Wave Height during a year from the sample between year 1957-2014

The operation limited by sea state with $H_s = 2$ m, will have the possibility of success during a year is 44 %. Or, the percentage of an unsuccessful operation in a year is $100 - 44 = 56\%$. Likewise, this percentages can be found from Figure 12-9 for the other limiting sea state. In general sense, this shows that higher the limiting sea state leads to higher possibility of a successful operation. The same approach can be used to find the percentage with significant wave height and spectral peak period.

The drawback of the scatter table is the unavailability of duration statistics of a window. Hence the subsequent chapters are focusing on the statistics including the duration of windows. This would be very handy for planning of an operation.

The percentage of sea states for a spectral peak period of total sea in the year between 1957-2014 is plotted in Figure 12-10.

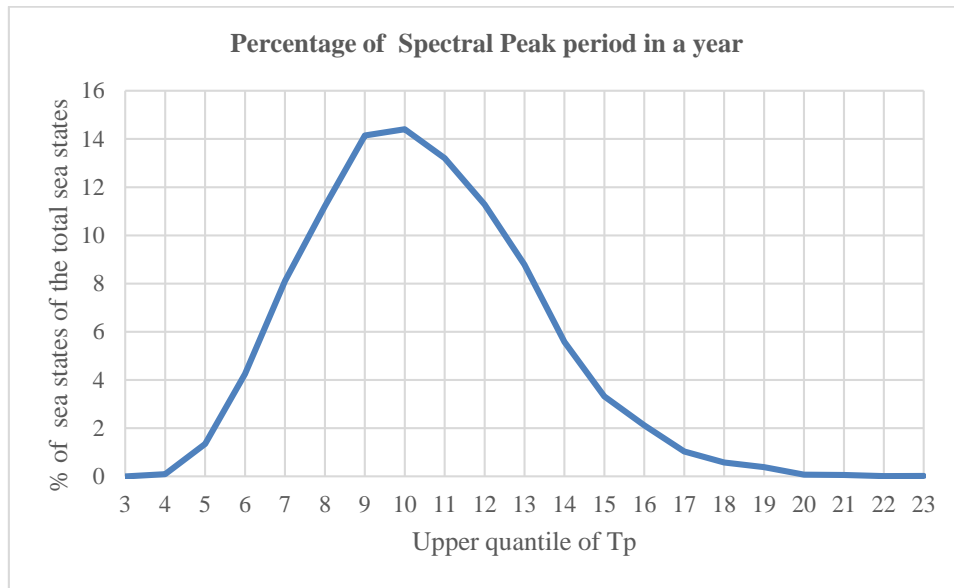


Figure 12-10: Percentage of times available Spectral Peak Period during a year from the sample between year 1957-2014

The maximum number of spectral period values are between 7 s to 13 s as shown in Figure 12-10. So, these values can be used in preliminary stage of time consuming numerical simulation of a marine operations with irregular sea state.

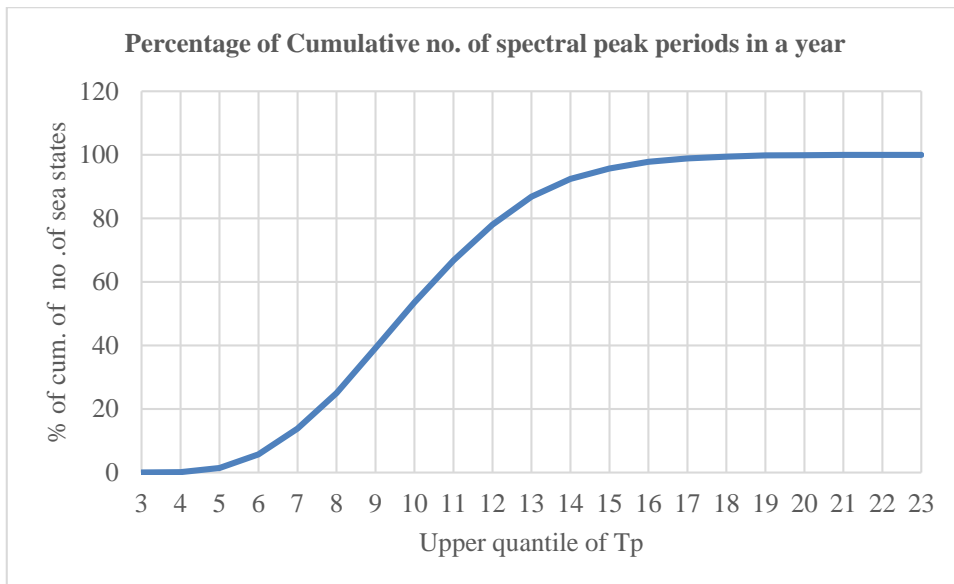


Figure 12-11: Percentage of Cumulative of Spectral Peak Period during a year from the sample between year 1957-2014

In same way, the percentage of cumulative number of sea states for a spectral peak period of total sea in the year between 1957-2014 is plotted in Figure 12-11. It can be seen that 87 % of sea state in a year is with spectral peak period which is less than 13 s. So, the spectral peak period between 7 s to 13 s is a good start for the simulations as mentioned above.

12.4. Percentage of times non-exceedance of sea-state

It is assumed that, the sea-state is driven by the significant wave height; not by spectral peak periods. The percentage of times not exceeding a significant wave height in a particular duration is calculated as follows.

$$\text{Percentage of times non exceedance of seastate} = \frac{\text{Number of hours not exceeding } H_s}{\text{Total duration in hours}} \times 100$$

The hindcast data are screened for each month. Number of hours less than particular H_s in a particular month is filtered for the year from 1957 to 2014. Then, the calculated number of hours are averaged with respect to the total number of a particular month in the database. There by, the percentage of times not exceeding a particular significant wave height are obtained from 1957 to 2014 and tabled in Table 12-2. The average percentage of not exceeding an H_s in a year is calculated by taking the percentage of number of hours less than H_s in the period between the years from 1957 to 2014.

		Month												Year
		Jan	Feb	Mar	Apr	May	Jun	Jul	Aug	Sep	Oct	Nov	Dec	
Significant Wave Height, H_s [m]	< 0.5	0.00	0.00	0.09	0.11	1.06	0.61	1.02	0.94	0.34	0.11	0.00	0.00	0.36
	< 1.0	0.42	1.01	2.28	6.16	17.44	20.70	26.60	23.55	8.97	2.79	1.56	0.30	9.32
	< 1.5	4.63	6.48	10.63	24.37	46.70	55.15	62.30	57.71	29.93	13.94	8.85	4.55	27.10
	< 2.0	14.40	17.49	24.56	45.89	70.49	78.05	81.86	78.85	50.99	30.98	22.26	14.46	44.19
	< 2.5	27.41	31.08	40.01	63.69	83.96	89.25	91.06	88.77	66.24	46.45	36.83	27.79	57.71
	< 3.0	41.00	44.74	54.02	76.29	91.24	94.04	95.73	93.88	77.61	60.56	51.83	42.10	68.59
	< 3.5	53.69	57.41	65.05	84.54	95.08	96.72	97.98	96.68	85.50	71.68	64.54	54.82	76.97
	< 4.0	64.52	67.61	74.43	89.96	97.19	98.16	99.11	98.39	90.46	80.50	75.15	65.22	83.39
	< 4.5	72.82	75.40	81.97	93.49	98.28	98.90	99.50	99.17	93.66	86.88	82.51	73.97	88.05
	< 5.0	79.55	81.80	87.13	95.91	98.88	99.51	99.81	99.52	95.77	91.07	87.44	80.91	91.44
	< 5.5	84.96	86.29	90.66	97.46	99.36	99.80	99.92	99.82	97.27	93.85	90.91	86.25	93.88
	< 6.0	88.71	89.95	93.77	98.46	99.61	99.88	99.99	99.91	98.24	95.88	93.61	89.95	95.66
	< 6.5	91.43	92.79	95.97	98.98	99.82	99.94	100.00	99.97	98.79	96.96	95.55	92.86	96.92
	< 7.0	93.63	94.78	97.32	99.36	99.94	99.99	100.00	99.99	99.18	97.91	97.01	95.11	97.85
	< 7.5	95.40	96.27	98.32	99.61	99.96	100.00	100.00	100.00	99.49	98.75	97.97	96.72	98.54
	< 8.0	96.72	97.31	98.90	99.74	99.99	100.00	100.00	100.00	99.70	99.23	98.76	97.75	99.01
	< 9	98.54	98.77	99.65	99.90	100.00	100.00	100.00	100.00	99.92	99.69	99.47	98.90	99.57
< 10	99.34	99.65	99.87	99.97	100.00	100.00	100.00	100.00	99.99	99.87	99.80	99.50	99.83	
< 11	99.76	99.87	99.95	99.99	100.00	100.00	100.00	100.00	100.00	99.94	99.89	99.86	99.94	
< 12	99.87	99.94	99.99	100.00	100.00	100.00	100.00	100.00	100.00	99.99	99.93	99.98	99.98	
< 13	99.94	99.98	100.00	100.00	100.00	100.00	100.00	100.00	100.00	100.00	99.95	100.00	99.99	
< 14	99.97	100.00	100.00	100.00	100.00	100.00	100.00	100.00	100.00	100.00	99.96	100.00	99.99	
< 15	99.99	100.00	100.00	100.00	100.00	100.00	100.00	100.00	100.00	100.00	99.99	100.00	100.00	

Table 12-2: Percentage of times not exceeding the Significant Wave Height (Month wise and annually) in the year between 1957 to 2014

It can be seen from the table, the significant wave height is less than 15 m annually, 100 percentage of times. Where as in the month of July, the significant wave height is less than 6.5 m, 100% of times. For an operation required sea state of $H_s \leq 2$ m, 82 % times the sea state is less than 2 m in July month or 82% times the probability of success of an operation in July month. Likewise, for the same sea state, annually, 44% times the sea state is less than 2m. The lowest percentage of sea state less than 2 m can be seen in the months of December and January as 14%. In the months of Jan, Feb, Mar, Nov, Dec of some years, there are no sea state less than 2m as shown in Figure 12-12.

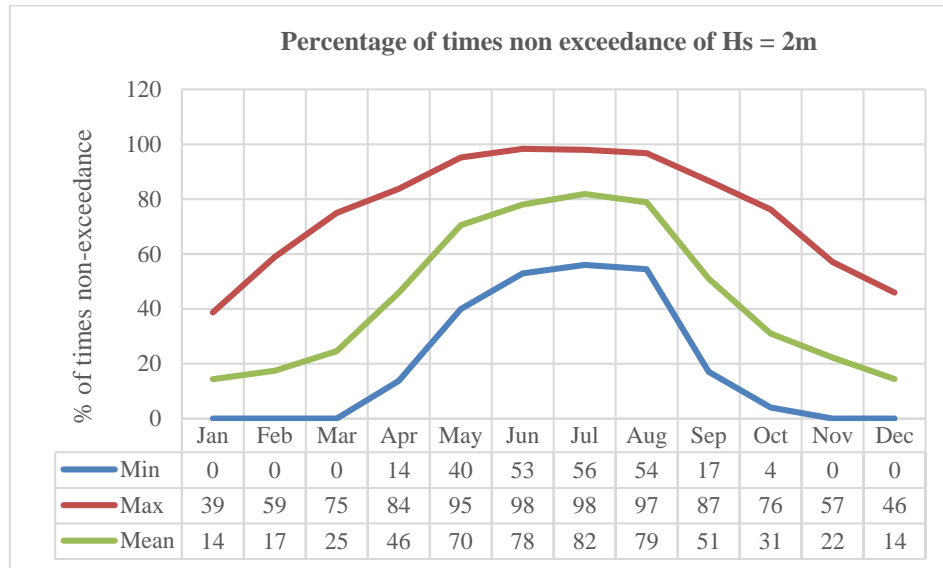


Figure 12-12: Minimum and Maximum Percentage of times not exceeding the Significant Wave Height in a month, in the year between 1957 to 2014

12.5. Average duration of a sea state

As the scatter table did not give the info about the duration of a sea state, the average duration of a window has been estimated for $H_s \leq 1$ m, 2 m & 3m in a month by screening through the duration of sea states for total sea in the hind cast data for the Haltenbanken area.

The mean duration of a continuous window with the sea state less than particular significant wave height (H_s) is higher in the mid months (May to Aug) of a year. The mean duration in the beginning and end months (Sep to Apr) of a year is lesser in general sense. This trend can be seen in Figure 12-13 to Figure 12-15.

If the limiting operational sea-state is lower, then the expected duration of sea state window for the continuous operation is also lower and vice versa. It can be seen from the Figure 12-13, the operation with 72 hours duration, $H_s \leq 1$ m has very less probability of success, even during the summer months of a year. In the month of July, it has the maximum average duration of 35 hours; Whereas, for the sea state $H_s \leq 2$ m, the maximum average duration of window is 136 hours in the month of July. For $H_s \leq 3$ m, the maximum average duration of window is 593 hours in the month of July. It should be noted that these are the average values. For the sea state $H_s \leq 2$ m, most of the duration varies from 8 hours to 22 hours in December month, 58 hours to 136 hours in July month.

These durations give the results that, the July month of a year is the best period of the year to do an operation which is weather sensitive and needs longer installation duration. The worst period of the year is in month of December and January. Even in the worst part of the year, the installation operations ($H_s \leq 2$ m) are possible with the durations equal to ~24 hours. But the probability of success is to be considered. This aspects are discussed in chapter § 12.8.

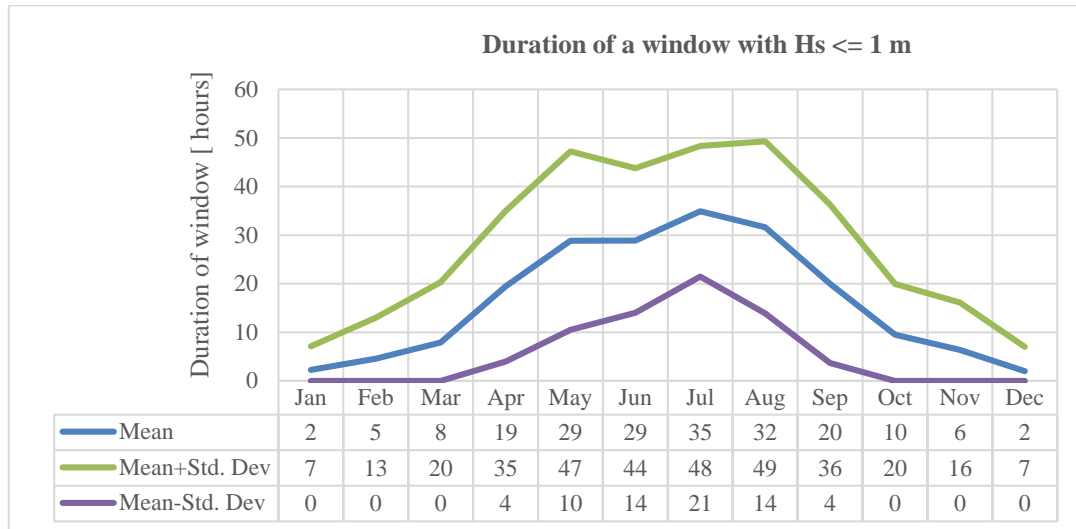


Figure 12-13: Duration of a window for the significant wave height ($H_s \leq 1$ m) from year 1958 to 2013 in month wise

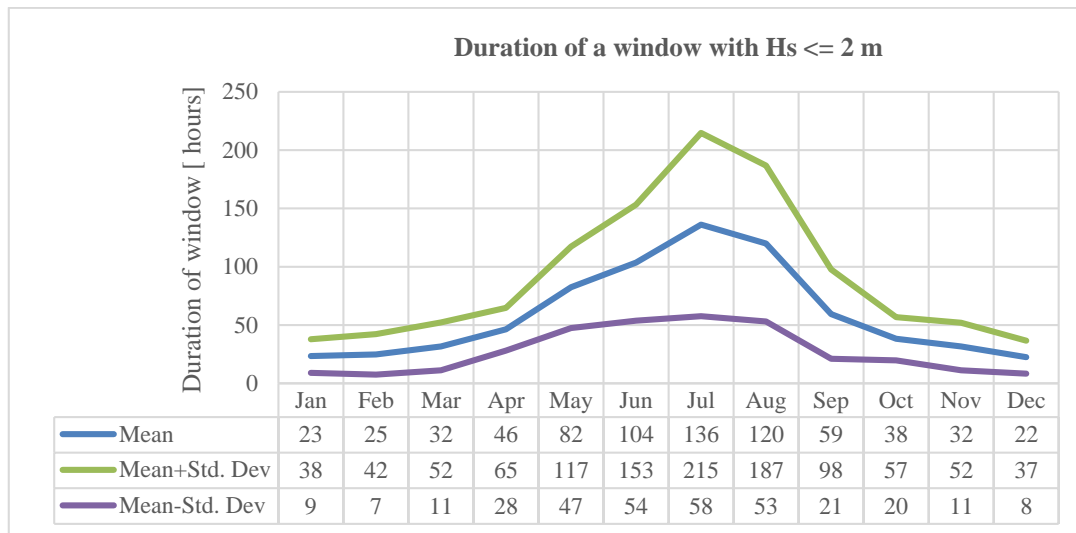


Figure 12-14: Duration of a window for the significant wave height ($H_s \leq 2$ m) from year 1958 to 2013 in month wise

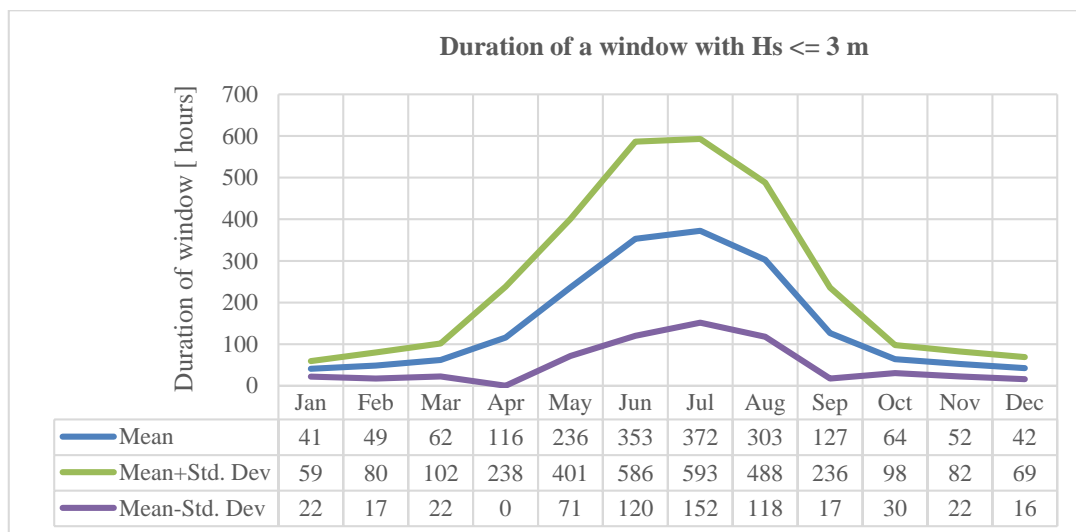


Figure 12-15: Duration of a window for the significant wave height ($H_s \leq 3$ m) from year 1958 to 2013 in month wise

12.6. Number of possible Weather Window

As the average duration table and scatter table did not give the number of possible windows for the particular duration, the no. of windows for 12 hours of operation with various sea state $H_s \leq 1$ m, 1.5 m, 2 m & 2.5 m are counted from the weather statistics. The number of possible weather window with particular duration of operation with a significant wave height gives an overview of planning an operation in a year. The spectral peak period is not considered here.

The hindcast data are screened through for each year and taken the episodes in which the sea states are less than a significant wave height. Then, each episode is checked for how many number of windows with the duration of operation are available. Then, the total number of windows in a year as shown in Table 12-3, is calculated by summing up the available number of windows in each episodes.

It can be seen that, the number of windows in a year increase with the higher sea state. An operation with the lesser sea state will have the lesser number of windows in a year. So it is advisable to choose the method and installation aids to have the higher sea state, thereby increase the possibility of installation in a year with high probability.

The number of windows in a month for $H_s \leq 2$ m with durations 6 hours to 72 hours are calculated between the start of the month until the end of the month as shown in Figure 12-16 to Figure 12-20. The window crossing between the ends of month to the beginning of next month is not considered for counting of windows. However, the results shown will not be influenced as they are less than couple of windows.

For a operation required a sea state of $H_s \leq 2$ m with 12 hours duration, the average number of windows available is 49 in the month of July as a maximum as shown in Figure 12-17. In July, the number of windows are mostly between 42 to 49 windows. In the worst month of December, the number of windows varying from 0 to 14 mostly. So, this operation is mostly unsuccessful in December month.

The average number of windows with various operational durations are plotted and discussed in subsequent chapters. In average sense, if the operational durations are longer, the average number of windows are lesser and vice versa. The highest number of windows for any duration is available in the month of July. The lowest number of windows are in the month of December and January.

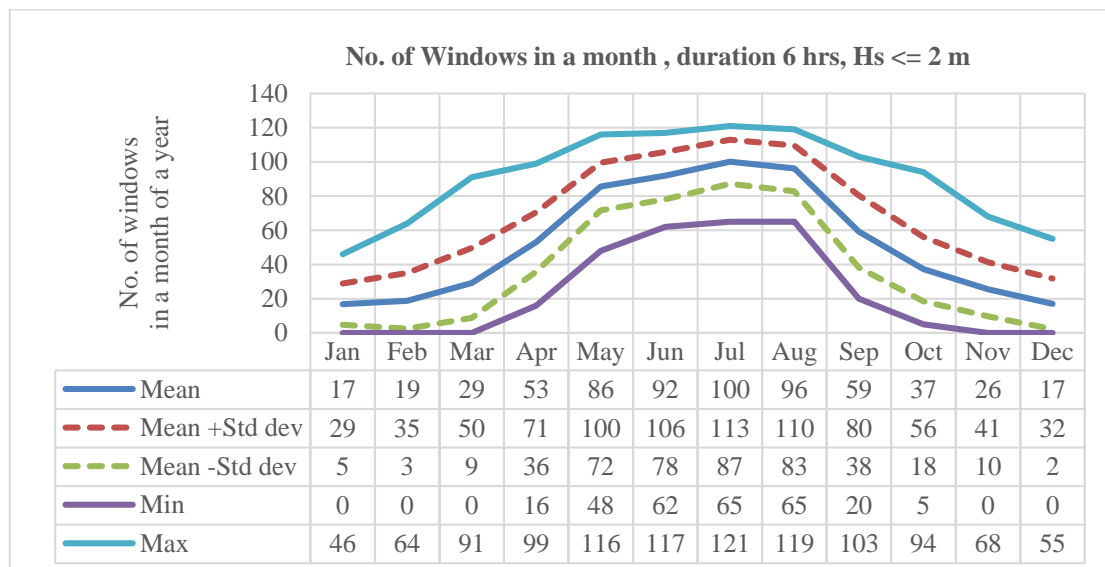


Figure 12-16: No. of windows in a month for duration 6 hours, $H_s \leq 2.0$ m, from year 1958 to 2013

Year	Total No. of windows in year wise, window duration = 12 hours			
	Hs <= 2.5	Hs <= 2	Hs <= 1.5	Hs <= 1
1958	461	368	236	89
1959	382	277	154	51
1960	478	383	255	98
1961	389	304	171	45
1962	409	314	170	50
1963	422	303	193	46
1964	396	280	169	52
1965	445	323	176	62
1966	454	351	218	68
1967	382	289	182	71
1968	444	361	254	98
1969	441	347	216	78
1970	453	338	178	60
1971	369	271	176	64
1972	402	299	184	66
1973	357	263	162	56
1974	423	332	217	75
1975	342	244	142	50
1976	404	302	168	49
1977	444	329	199	65
1978	421	323	198	77
1979	441	314	167	45
1980	431	340	217	77
1981	413	311	178	51
1982	325	234	135	49
1983	363	272	139	39
1984	437	330	193	64
1985	422	315	166	39
1986	405	313	189	54
1987	425	317	174	50
1988	385	295	185	51
1989	334	236	115	35
1990	344	275	177	53
1991	375	276	159	42
1992	364	284	187	57
1993	386	308	194	63
1994	376	290	165	52
1995	343	246	126	39
1996	437	330	188	62
1997	382	294	191	70
1998	423	329	202	68
1999	397	301	180	70
2000	392	285	170	63
2001	436	331	171	43
2002	427	333	194	68
2003	374	305	215	83
2004	375	287	168	50
2005	344	251	141	38
2006	388	283	174	46
2007	310	231	130	38
2008	373	277	173	49
2009	369	254	133	48
2010	462	340	187	36
2011	323	238	131	44
2012	405	301	182	55
2013	382	277	160	42
Minimum	310	231	115	35
Mean	398	300	178	57
Max	478	383	255	98

Table 12-3: Total number of windows available for the significant wave height from year 1958 to 2013

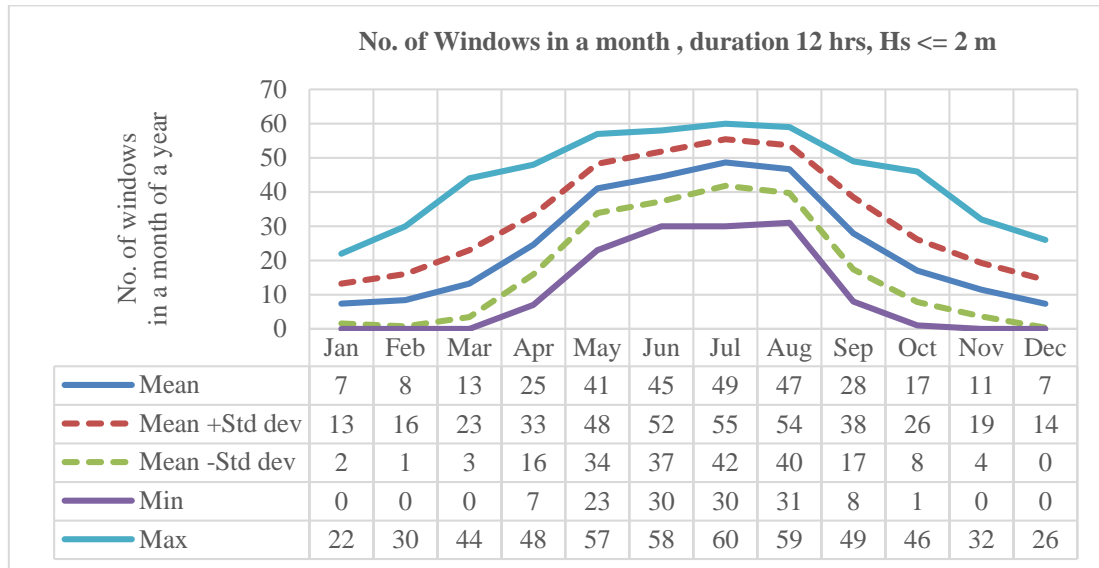


Figure 12-17: No. of windows in a month for duration 12 hours, Hs<=2.0 m, from year 1958 to 2013

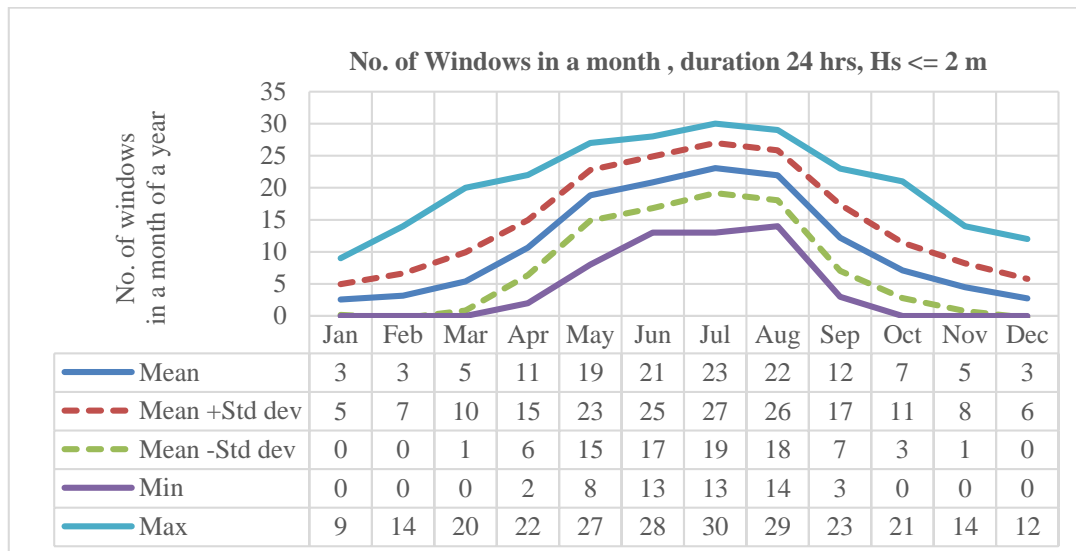


Figure 12-18: No.of windows in a month for duration 24 hours, Hs<=2.0 m, from year 1958 to 2013

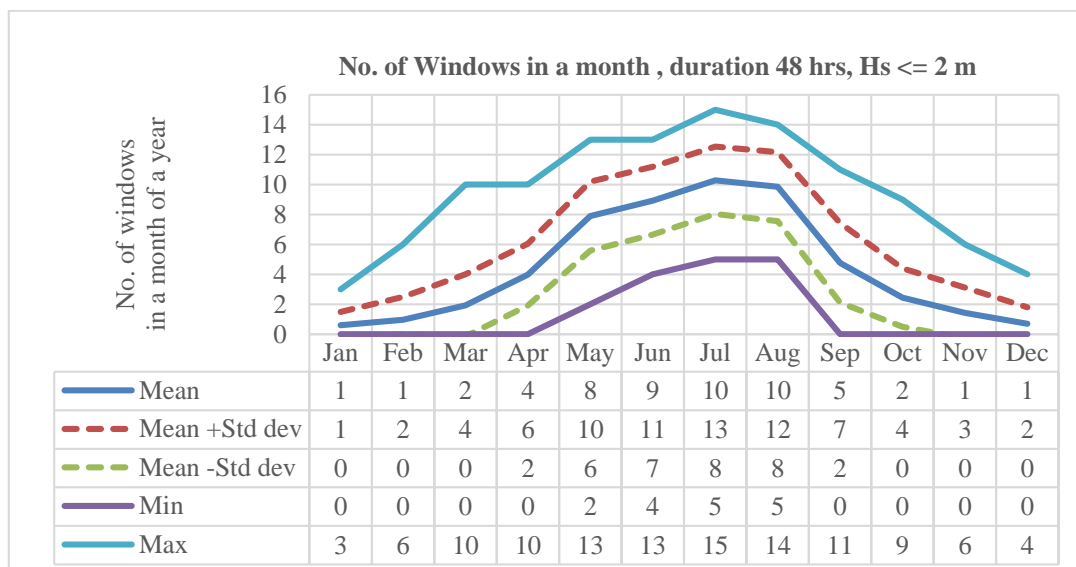


Figure 12-19: No. of windows in a month for duration 48 hours, Hs<=2.0 m, from year 1958 to 2013

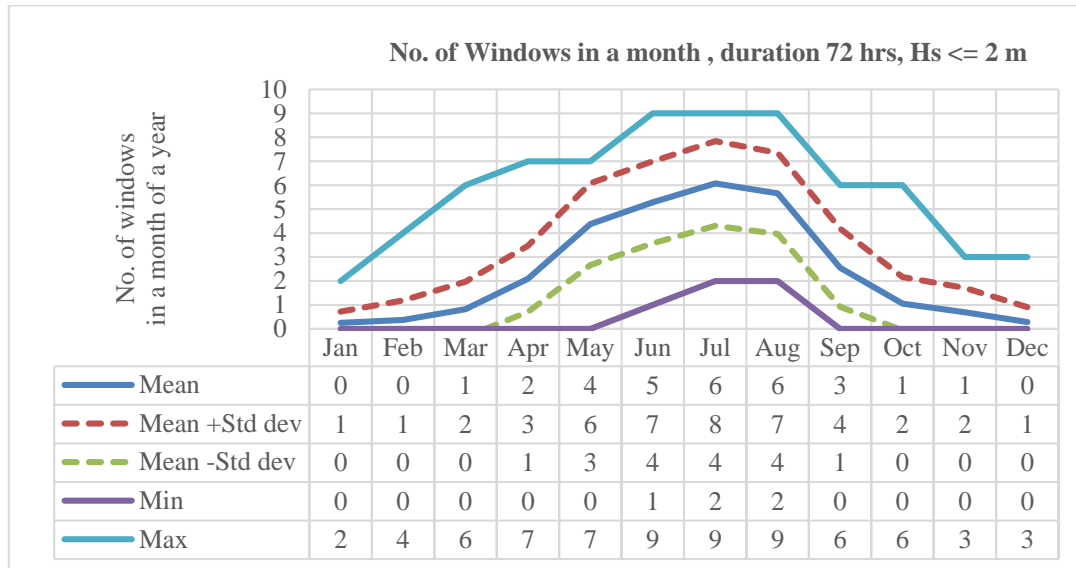


Figure 12-20: No. of windows in a month for duration 72 hours, Hs<=2.0 m, from year 1958 to 2013

12.7. Sensitivity of weather window with respect to duration

The number of windows for the duration 6, 12, 24, 48 & 72 hours has been established and presented in Appendix -3: Total No. of Windows in Month wise. It can be seen from the results, the number of window for 6 hours are little more than twice as number of windows for 12 hours. Whereas, the number of windows for 24 hours is halved as the number of windows for 12 hours. But the durations of operations go to 72 hours, some of the months, there are no windows at all. Hence, the duration of operations is lesser, the possibility of weather window for installation is higher and vice versa. For an operation required a sea state of $H_s \leq 2$ m with 12 hours duration, the average number of windows decreases, if the operation planned in a month before or after July. In the month of December, there are 7 average number of windows as shown in Figure 12-21. These windows have to be look along with the probability of success.

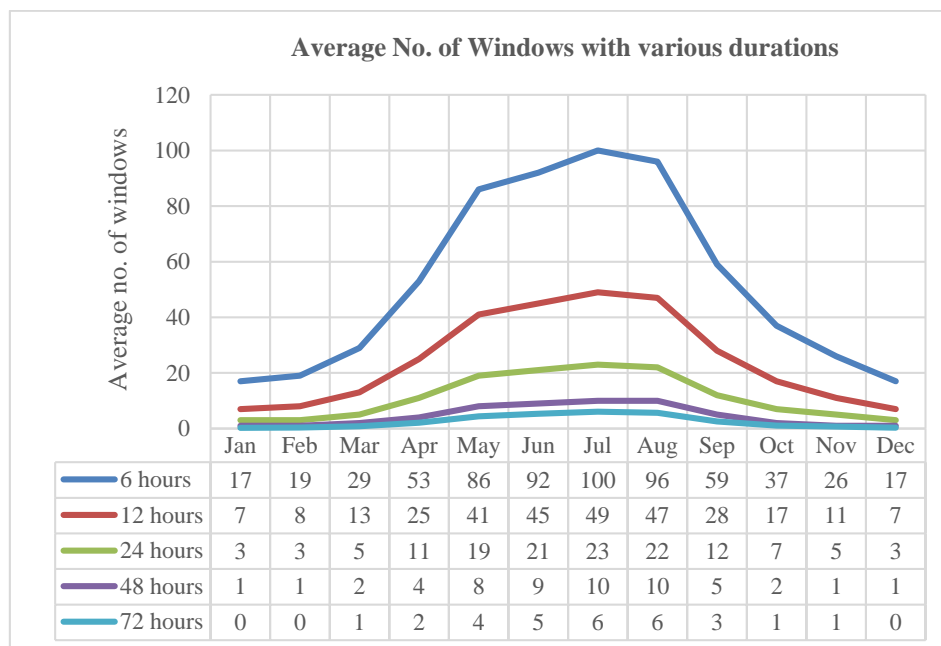


Figure 12-21: Average number of windows available for the significant wave height (Hs<=2m) from year 1958 to 2013 for different durations

12.8. Benefits of dividing the operation into phases

The operation which requires 72 hours weather window with the sea state of $H_s = 2$ m is taken. The total duration required to complete this operation in one go, is calculated, if the operation starts on the first day of every month.

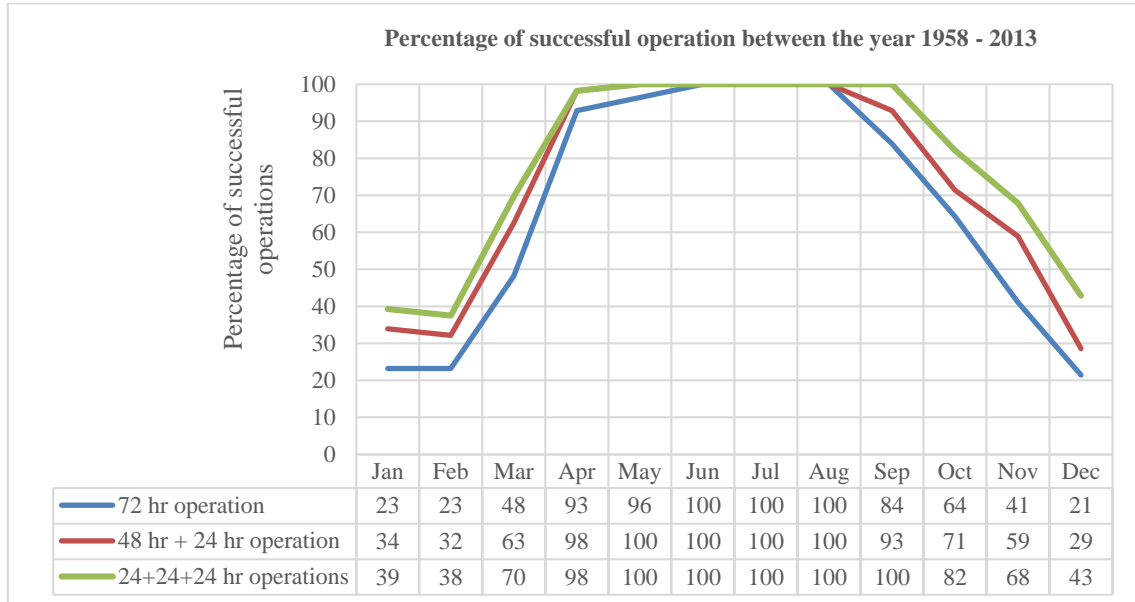


Figure 12-22: Percentage of successful operation in a month, $H_s \leq 2.0$ m, from year 1958 to 2013

When the 72 hours operation is split to 48 +24 hours operation, the probability of successful installation is increased up to maximum of 20%, minimum of 10% in the months from September to April as shown in Figure 12-22. Likewise, the operation is split by 24+24+24 hours from 72 hours operation, the percentage of successful installation is increased up to maximum of 30% and minimum of 20% in the months of September to March. This increase in percentage is due to the number of new possible windows compared to un-split 72 hours continuous operation.

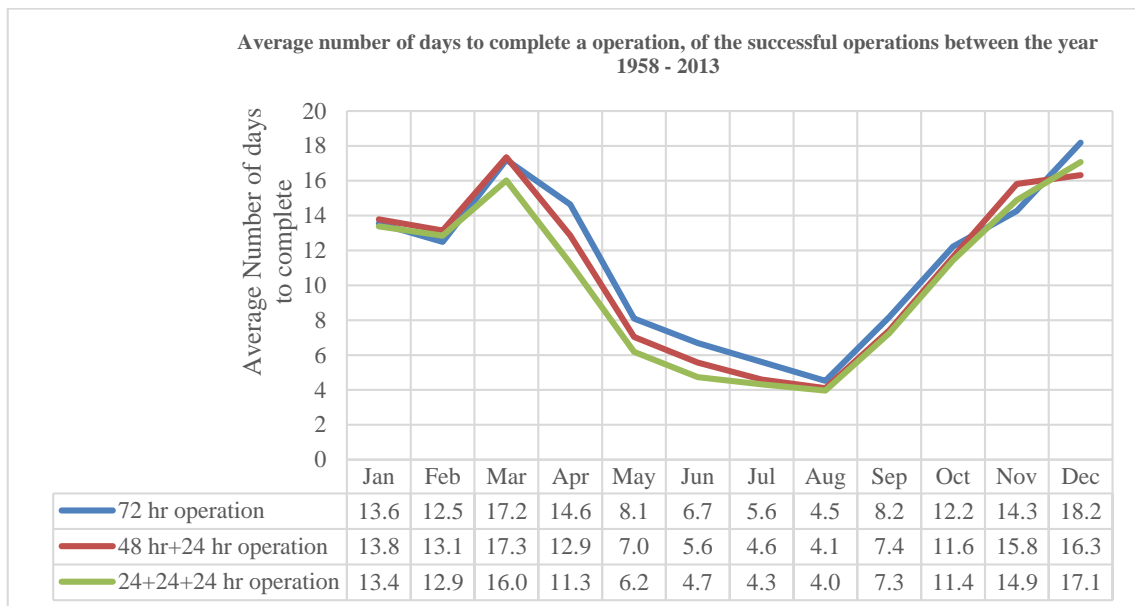


Figure 12-23: Average number of days to complete an operation in a month, $H_s \leq 2.0$ m, from year 1958 to 2013

The average number of days to complete the operation with 48+24 hours, 24+24+24 hours split is lower than the 72 hours continuous operation from the month of March to October as shown in Figure 12-23. There are two reasons for this. One, the window with continuous 72 hours has the earlier windows with 48 hours, 24 hours. So, the number of days to complete the split hours of operation is reduced compared to the days needed for 72 hrs continuous operation. Especially, this is the only reason of decreasing average number of days for the months which have 100% success for 72 hours continuous operation. Second, there are new possible windows in the months April, May, Sep & October where 72 hours of operation is not at all possible. The average days to complete the operation with this new possible windows are lesser than the average days to complete the 72 hour continuous operation.

In the month of November, the percentage of successful operation for 48+24 hours is increased by 20% as a maximum compared to 72 hours continuous operation. The percentage is increased as there are new possible windows. The average number of days to complete 48+24 hrs operations is also increased compared to 72 hours operation. Because, the average number of days to complete this operation with new possible windows due to split where 72 hours operation is not possible, is higher than the average number of days to complete the 72 hours operation in that month. This can be seen from the spreading of data shown in Figure 12-24, Figure 12-25 & Figure 12-26. This is same for 24+24+24 hours operation as well.

It is also noticed that, the number of days to complete the operation with the new possible windows, due to 48+24 hrs split in the month from November to February where 72 hours operation is not possible, are longer than in the month of April to October. This is same for 24+24+24 hours operation as well.

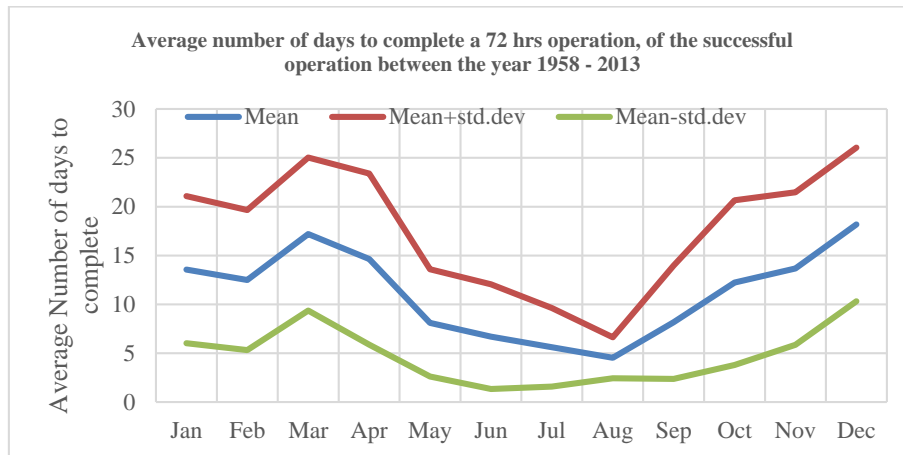


Figure 12-24: Average number of days to complete a 72 hrs operation in a month, $H_s \leq 2.0$ m, of the successful operations from year 1958 to 2013

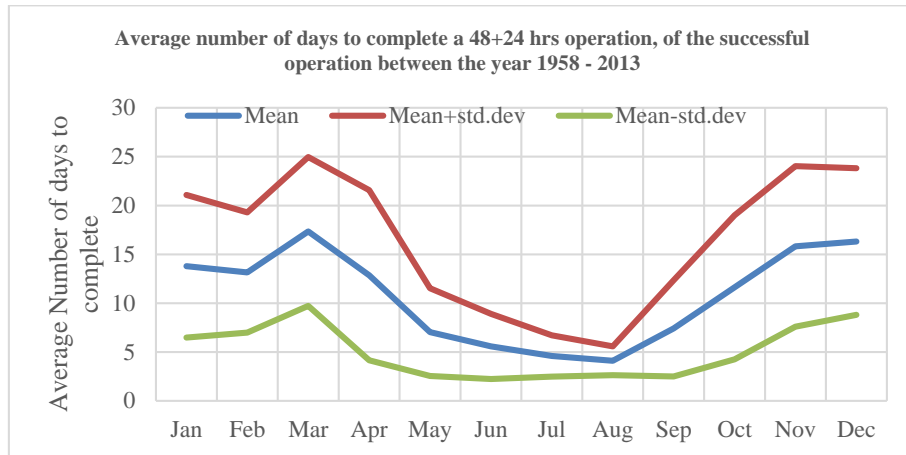


Figure 12-25: Average number of days to complete a 48+24 hrs operation in a month, $H_s \leq 2.0$ m, of the successful operations from year 1958 to 2013

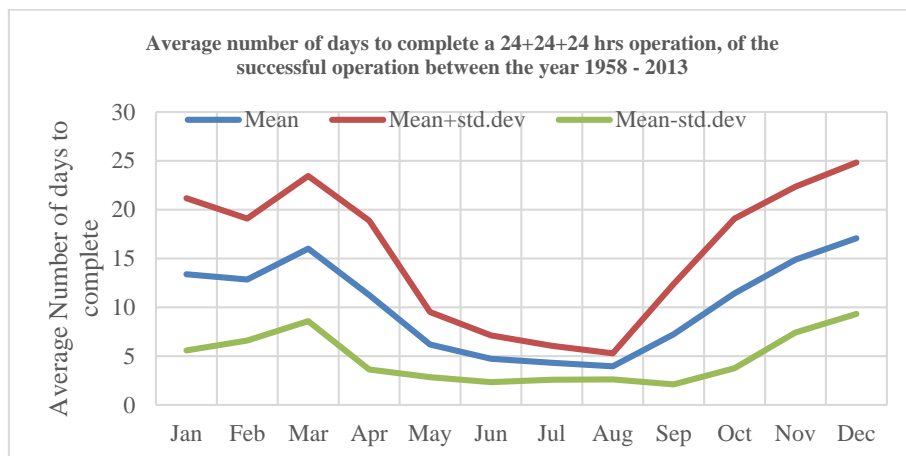


Figure 12-26: Average number of days to complete a 24+24+24 hrs operation in a month, $H_s \leq 2.0$ m, of the successful operations from year 1958 to 2013

So, based on the above results, splitting a continuous operation into phases is not effective in the months from April to August. Because, in these months, 100 percentage of successful operation with longer weather window is possible. Also, splitting the operation into phases gives less variation of average number of days to complete the operation.

Between months from September to March, the splitting the operations into phases increase the probability of successful operation up to 30%. When the operation is split into 48+24hours, getting the 48 hours window takes longer time. Still, it is better than 72 hours continuous operations. If there is a possibility to split the 48+24 hours to 24+24+24 hours for the operation planned to happen between September to March, it is a good decision to do so as there is a higher probability of success of installation with bit longer time to complete.

13. Conclusion

Installing a subsea equipment in harsh environment with a floating crane vessel is challenging. This study focused on different aspects of limiting sea state calculation and planning of that marine operations. The above mentioned are the two key tasks to be performed before executing that operation.

Limiting sea state is mainly depending on the vessel motion and lifting arrangement. The summary of study about the vessel motions and lifting system described below.

Heave, Pitch and Roll motions of the vessel are the significant motions for the installation of any equipment. Those motions are briefly described with respect to the variation of wave frequencies. Each motion is amplified largely, when the wave frequency matches with the natural frequency of the vessel for that particular motion. The variation of phase angles are shown against the wave frequencies and discussed about the phase angles before and after natural frequency of that degree of freedom.

The transfer function of the vessel taken for this study is qualitatively verified for heave, pitch and roll motions. Based on this check, the co-ordinate system used for this study is also ensured that they are compatible.

To introduce the dynamics on the lifting system, the excitation at the crane tip is derived from the transfer function of the vessel at CoG. The same derivation can be used for calculating motion at any point on the vessel.

Based on the derivation for calculating motion at any point, Heave amplitude is calculated at two points both are same distance away from CoG longitudinally. The results shown that, heave amplitude is higher in the forward side of the vessel's CoG than the aft side of the vessel for head sea. This is not the case, when the wave propagate in following sea where heave at aft side of the vessel is higher at certain wave frequencies.

The crane tip motion transfer function is plotted for head sea and beam sea. In the lower frequencies of wave, the heave amplitude is equal to wave amplitude for head sea and beam sea. The heave amplitude in beam sea is 2.7 times the wave amplitude at the resonance with the natural frequency of the roll.

The dynamics on the lifting system arrangement are derived based on the single degree of freedom system with the base excitation and damped case. Since the lifting in air is an un-damped case, the damping coefficient replaced as zero. But, for the case with Passive Heave Compensation, the damping coefficient is replaced with the respective value.

Dynamic tension on the crane wire is dependent on the relative displacement and stiffness of the lifting system. The transfer function for dynamic tension amplitude is derived and plotted for head sea and beam sea. These amplitudes are greatly influenced by the vessel's natural frequencies in heave, pitch and roll motions.

Estimating limiting sea state based on deterministic approach is simple. The wave amplitude is increased until to reach the dynamic tension on the wire is reached up to allowable limit. The obtained deterministic wave height and wave period is converted to significant wave height and spectral peak period. The result is compared with the stochastic approach followed. It is found that, the deterministic approach is more conservative than stochastic approach.

In the stochastic approach, two type of wave spectra are used. One is single peak Jonswap spectrum for total sea and the second one is double peak wave spectrum by superimposing Jonswap spectrum for wind and swell sea.

Based on the single peak wave spectrum, the response spectrum is obtained for total sea in head sea and beam sea direction. The results shown that, the limiting sea state for head sea is higher than the beam sea of the vessel. The limiting sea state in head sea is almost three times the limiting sea state in beam sea for this operation. It shows that, heading the vessel towards head sea is the best method to install a equipment, if there are no swells.

A sensitivity study has been carried out by varying the probability of exceedance of the critical limiting quantity i.e. allowable dynamic tension. As expected, the limiting sea state is higher for the high probability of exceedance and vice versa. By increasing the probability of exceedance from 0.001 to 0.1 gives 0.5 m higher limiting sea state in average sense.

As mentioned above, the combined spectrum for wind and swell sea are obtained by superimposing the Jonswap spectrum of them. Then, by keeping the wind sea in head sea direction, and varying the swell sea direction from beam sea to head sea, the limiting sea states are obtained. It gives better sea state than the single peaked spectrum of total sea. The lowest sea state is occurred when the swell sea in beam sea direction.

To improve the limiting sea state, the lifting arrangement with the heave compensations has been studied. It is found that, Passive Heave Compensation can be used to reduce the dynamic tension on the crane wire and motion of the mass, with careful selection of natural frequency of the system. The lowest natural frequency suppress the dynamic tension and motion of the mass effectively compared to higher natural frequency of the system, when the equipment suspended in air. The results are also shown that increasing the damping co-efficient of PHC, reduces the dynamic tension on the lifting system.

Active Heave Compensation (AHC) system in the lifting arrangement works based on the reference signal and active equipment. The heave motion on the lifting system with AHC is caused by the residual motion. It is shown that the lesser the residual motion leads to lesser dynamic tension on the crane wire.

After getting the limiting sea state based on limiting conditions, the study of planning of operation is carried out using long term weather statistics. For this purpose, 60 years of hindcast data from Haltenbanken area in North sea is used. The hindcast data is corrected for the wind speed based on the measurements available at the offshore platforms. Then, discrete values of spectral peak period is randomised and uniformly distributed.

From the corrected hindcast data, annual and monthly scatter tables and plots are produced. The percentage of success of operation in a year is checked with the produced annual scatter table. The probability of successful operation is increased, if the limiting sea state is increased. The operation with the limiting sea state $H_s \leq 2$ m, has the 45 % of success rate in a year. Likewise, 87 % of the year, the spectral peak period is less than 13 s. This has been estimated from the scatter table.

The percentage of times not exceeding a sea state in month wise produced from the monthly scatter table. It has been seen that, for $H_s \leq 2$ m, the percentage of not exceeding this sea state is maximum of 82 % in July month and minimum of 14% in December and January month.

As the scatter table did not give the info about the duration of a sea state, the average duration of a window has been estimated for $H_s \leq 1$ m, 2 m & 3m. The minimum and maximum of average duration for the particular sea state is shown below.

	Maximum	Month	Minimum	Month
	[hours]		[hours]	
$H_s \leq 1$ m	35	July	2	Dec & Jan
$H_s \leq 2$ m	136	July	22	Dec
$H_s \leq 3$ m	372	July	41	Jan

As the average duration table and scatter table did not give the number of possible windows for the particular duration, the no. of windows for 12 hours of operation with various sea state $H_s \leq 1$ m, 1.5 m, 2 m & 2.5 m are counted from the weather statistics. The number of windows are higher for the high limiting sea state. The summary of the no. of windows annually are shown below.

Year	Total No. of windows in year wise, window duration = 12 hours			
	$H_s \leq 2.5$	$H_s \leq 2$	$H_s \leq 1.5$	$H_s \leq 1$
Minimum	310	231	115	35
Mean	398	300	178	57
Max	478	383	255	98

The number of windows for sea state $H_s \leq 2$ m, is established for various durations of operations from 6 hours to 72 hours. When the duration of operation increases, the availability of operational window decreases as shown below in the table. The highest number of windows for any duration is available in the month of July. The lowest number of windows are in the month of December and January.

Duration	Jan	Feb	Mar	Apr	May	Jun	Jul	Aug	Sep	Oct	Nov	Dec
6	17	19	29	53	86	92	100	96	59	37	26	17
12	7	8	13	25	41	45	49	47	28	17	11	7
24	3	3	5	11	19	21	23	22	12	7	5	3
48	1	1	2	4	8	9	10	10	5	2	1	1
72	0	0	1	2	4	5	6	6	3	1	1	0

Dividing a longer operation in to smaller phases gives higher probability of successful operation in the months from September to April. Whereas, in the months from May to August, there is no increase in percentage of success due to the split of duration of operation, as there is 100% success for these months for 72 hours.

Average number of days to complete the operation, if the operation is started on first day of every month, are decreased in the months from March to October. The number of days increased for rest of the months, due to the new possible windows where the operations are not possible at all.

14. References

- Cranemaster. (2013). *Technical Product Sheet for CM3-250T-2500-A*. Langesund, Norway.
- DNV-OS-H101. (2011). *Marine Operations, General*. Oslo: Det Norske Veritas AS.
- DNV-RP-C205. (2010). *Environmental Conditions and Environmental Loads*. Det Norske Veritas.
- DNV-RP-H103. (2014). *Modelling And Analysis of Marine Operations*. Oslo: Det Norske Veritas AS.
- Faltinsen, O. (1990). *Sea Loads on Ships and Offshore Structures*. Cambridge: Cambridge University Press.
- Gudmestad, O. T. (2014). *Marine Technology & Operations - Lecture Notes*. Stavanger: University of Stavanger.
- Haver, S. (2014). *Description of Metocean Characteristics for planning of marine operations - Lecture Notes*. Stavanger: University of Stavanger.
- Haver, S. K. (2015). *Private communications*. Stavanger.
- Heave Compensation*. (2015, 04 18). Retrieved from Bosch Rexroth:
<http://www.boschrexroth.com/en/xc/industries/machinery-applications-and-engineering/offshore/products-and-solutions/heave-compensation/index>
- Journee, J., & Adegeest, L. (2003). *Theoretical Manual of Strip Theory Program "SEAWAY for Windows"*. Delft University of Technology.
- Journee, J., & Massie, W. (2001). *Offshore Hydrodynamics*. Delft University of Technology.
- Kenneth, Aarset; Sarkar, Arunjyoti; Karunakaran, Daniel;. (2011, January 1). Lessons Learnt from Lifting Operations and Towing of Heavy Structures in North Sea. Offshore Technology Conference. doi:10.4043/21680-MS
- Marintek. (2015). *SIMA Help documents*.
- Nielsen, F. G. (2007). *Lectures Notes in Marine Operations*. Trondheim: Norwegian University of Science and Technology.
- Nygaard, Einar. (2015). *Wam10 data archive - Use of wind and wave data*. Statoil.
- Orcaflex Help Manual. (2014, 11 01). Retrieved from
<http://www.orchina.com/SoftwareProducts/OrcaFlex/Documentation/Help/>
- Risoey, T., Mork, H., Johnsgard, & Gramnaes, J. (2007, January 1). The Pencil Buoy Method-A Subsurface Transportation and Installation Method. Offshore Technology Conference. doi:10.4043/19040-MS
- S. Rao, S. (2005). *Mechanical Vibrations*. Singapore: Prentice Hall.
- Statoil. (2009). *Memo: The peak period in the WAM10 hindcast archive*.
- Torsethaugen, K., & Haver, S. (2004). Simplified double peak spectral model for ocean waves. Toulon, France: International Society of Offshore and Polar Engineers.
- Vessel Info. (2015, 06 11). Retrieved from DNVGL:
<https://exchange.dnv.com/Exchange/main.aspx?extool=vessel&subview=dimensions&vesselid=32787>
- Vestbøstad, T. M., Haver, S., Andersen, O. J., & Albert, A. (2002). Prediction of Extreme Roll Motions on an FPSO using Long Term Statistics. *OMAE*. Oslo: ASME.

Appendix -1: Crossing Sea Spectral Parameters

Spectral Parameters for Wind dominated sea $T_p \leq T_{pf}$

$$T_{pf} = a_f H_s^{1/3}$$

$$a_f = 6.6 \text{ sm}^{-1/3} \text{ for the fetch length 370 km}$$

1) Primary peak

(i) Significant wave height

$$H_{w1} = R_w H_s; \quad R_w = (1 - a_{10})e^{-\left(\frac{\varepsilon_l}{a_1}\right)^2} + a_{10}$$

$$a_{10} = 0.7; a_1 = 0.5; a_e = 2$$

$$\varepsilon_l = \frac{(T_{pf} - T_p)}{(T_{pf} - T_l)}; \quad T_l = a_e H_s^{1/2}$$

For values of T_p less than T_l , ε_l value set to 1.

(ii) Spectral peak period

$$T_{pw1} = T_p;$$

(iii) Peak enhancement factor

$$\gamma = k_g s_p^{6/7}; s_p = \left(\frac{2\pi}{g}\right) H_{w1}/T_{pw1}^2$$

$$k_g = 35; g - \text{acceleration due to gravity}$$

2) Secondary peak

(i) Significant wave height

$$H_{w2} = (1 - R_w^2)^{1/2} H_s;$$

(ii) Spectral peak period

$$T_{pw2} = T_{pf} + b_1; \quad b_1 = 2;$$

(iii) Peak enhancement factor

$$\gamma = 1$$

Spectral Parameters for Swell dominated sea $T_p > T_{pf}$

1) Primary peak

(i) Significant wave height

$$H_{s1} = R_s H_s; \quad R_s = (1 - a_{20})e^{-\left(\frac{\varepsilon_u}{a_2}\right)^2} + a_{20}$$

$$a_{20} = 0.6; a_2 = 0.3; a_u = 25; a_3 = 6;$$

$$\varepsilon_u = \frac{(T_p - T_{pf})}{(T_u - T_{pf})}; \quad T_u = a_u$$

For values of T_p above than T_u , ε_u value set to 1.

(ii) Spectral peak period

$$T_{ps1} = T_p;$$

(iii) Peak enhancement factor

$$\gamma = \gamma_f (1 + a_3 \varepsilon_u)$$

$$\gamma_f = k_g s_f^{6/7}; s_f = \left(\frac{2\pi}{g}\right) H_s / T_{pf}^2$$

$$k_g = 35; g - \text{acceleration due to gravity}$$

2) Secondary peak

(i) Significant wave height

$$H_{s2} = (1 - R_s^2)^{1/2} H_s;$$

(ii) Spectral peak period

$$T_{ps2} = a_f H_{s2}^{1/3};$$

(iii) Peak enhancement factor

$$\gamma = 1$$

Appendix -2: Monthly Scatter Tables

Lower	Spectral Peak Period, Tp [s]																							Cum. Sum
	Upper	< 3	3 4	4 5	5 6	6 7	7 8	8 9	9 10	10 11	11 12	12 13	13 14	14 15	15 16	16 17	17 18	18 19	19 20	20 21	21 22	22 23		
0.0	0.5	0	0	0	0	0	0	0	0	0	0	0	0	0	0	0	0	0	0	0	0	0	0	
0.5	1.0	0	0	1	21	24	22	3	6	20	15	14	3	0	0	0	0	0	0	1	0	0	0	
1.0	1.5	0	0	11	68	84	103	95	85	66	69	55	33	17	3	3	4	4	2	1	1	0	0	
1.5	2.0	0	0	13	71	147	124	190	199	156	138	131	112	54	35	14	13	10	5	2	2	3	0	
2.0	2.5	0	0	0	27	140	124	192	259	249	204	184	135	89	70	40	13	10	6	4	3	1	0	
2.5	3.0	0	0	0	5	92	163	186	219	236	241	228	143	91	74	35	20	15	5	4	2	1	0	
3.0	3.5	0	0	0	0	23	131	177	178	226	239	222	140	119	78	52	15	22	4	3	1	1	0	
3.5	4.0	0	0	0	0	8	46	121	181	206	209	192	130	69	63	38	20	24	1	5	0	1	0	
4.0	4.5	0	0	0	0	2	13	80	129	179	171	151	104	71	52	26	14	8	3	0	1	0	0	
4.5	5.0	0	0	0	0	0	0	35	87	150	160	121	95	87	56	12	12	7	2	0	0	0	0	
5.0	5.5	0	0	0	0	0	0	6	41	98	129	117	55	54	31	25	11	10	1	0	0	0	0	
5.5	6.0	0	0	0	0	0	0	0	14	55	114	114	60	53	29	17	10	4	0	1	0	1	0	
6.0	6.5	0	0	0	0	0	0	0	5	44	70	98	61	37	22	19	6	3	0	0	0	0	0	
6.5	7.0	0	0	0	0	0	0	0	0	9	51	87	49	24	16	13	4	4	0	0	0	0	0	
7.0	7.5	0	0	0	0	0	0	0	0	4	30	59	39	27	11	6	9	7	0	0	0	0	0	
7.5	8.0	0	0	0	0	0	0	0	0	4	14	27	47	19	13	3	3	3	0	0	0	0	0	
8.0	8.5	0	0	0	0	0	0	0	0	5	21	39	25	6	4	6	3	0	0	0	0	0	0	
8.5	9.0	0	0	0	0	0	0	0	0	0	5	30	19	15	4	3	2	1	0	0	0	0	0	
9.0	9.5	0	0	0	0	0	0	0	0	0	2	23	24	10	7	4	1	0	0	0	0	0	0	
9.5	10.0	0	0	0	0	0	0	0	0	0	2	11	12	11	5	1	1	1	0	0	0	0	0	
10.0	10.5	0	0	0	0	0	0	0	0	0	0	2	8	5	3	0	0	0	0	0	0	0	0	
10.5	11.0	0	0	0	0	0	0	0	0	0	0	0	0	3	3	2	1	1	0	0	0	0	0	
11.0	11.5	0	0	0	0	0	0	0	0	0	0	1	3	1	1	0	0	0	0	0	0	0	0	
11.5	12.0	0	0	0	0	0	0	0	0	0	0	0	0	0	3	0	1	0	0	0	0	0	0	
12.0	12.5	0	0	0	0	0	0	0	0	0	0	0	0	1	0	0	0	1	0	0	0	0	0	
12.5	13.0	0	0	0	0	0	0	0	0	0	0	0	0	0	1	2	0	0	0	0	0	0	0	
13.0	13.5	0	0	0	0	0	0	0	0	0	0	0	0	1	0	0	0	0	0	0	0	0	0	
13.5	14.0	0	0	0	0	0	0	0	0	0	0	0	0	0	0	1	0	1	0	0	0	0	0	
14.0	14.5	0	0	0	0	0	0	0	0	0	0	0	0	0	0	0	0	0	0	0	0	0	0	
14.5	15.0	0	0	0	0	0	0	0	0	0	0	0	0	0	0	0	0	0	0	0	0	0	0	
15.0	15.5	0	0	0	0	0	0	0	0	0	0	0	0	0	0	0	0	0	0	0	0	0	0	
15.5	16.0	0	0	0	0	0	0	0	0	0	0	0	0	0	0	0	0	0	0	0	0	0	0	
16.0	16.5	0	0	0	0	0	0	0	0	0	0	0	0	0	0	0	0	0	0	0	0	0	0	
16.5	17.0	0	0	0	0	0	0	0	0	0	0	0	0	0	0	0	0	0	0	0	0	0	0	
		0	0	25	192	520	726	1085	1403	1702	1859	1830	1312	907	608	331	170	141	31	20	10	8	Sum	
		0	0	25	217	737	1463	2548	3951	5653	7512	9342	10654	11561	12169	12500	12670	12811	12842	12862	12872	12880	Cum. Sum	

Table 0-2: Monthly Scatter Table after Tp randomization for the samples from year 1957-2014 (February)

Lower Upper	Spectral Peak Period, Tp [s]																							Cum. Sum
	< 3	3 4	4 5	5 6	6 7	7 8	8 9	9 10	10 11	11 12	12 13	13 14	14 15	15 16	16 17	17 18	18 19	19 20	20 21	21 22	22 23	Sum		
0.0	0	1	19	41		9	15	22	14	20	3	3	1	2	0	0	0	0	0	0	0	0	150	
0.5	0	33	170	349	456	342	280	308	308	171	100	48	27	12	11	2	6	0	1	0	0	2316		
1.0	0	4	152	458	549	817	723	512	424	269	135	51	25	9	4	2	1	1	0	0	0	4136		
1.5	0	0	21	306	457	534	561	533	408	275	178	53	16	13	5	2	0	0	0	0	0	3362		
2.0	0	0	0	50	227	285	292	330	297	170	126	68	34	17	3	4	1	1	0	0	0	1905		
2.5	0	0	0	3	63	195	186	168	162	100	80	46	9	12	1	2	1	0	0	0	0	1028		
3.0	0	0	0	0	3	31	135	129	88	58	52	22	11	7	5	0	2	0	0	0	0	543		
3.5	0	0	0	0	0	4	40	75	74	37	24	19	15	4	1	1	5	0	0	0	0	299		
4.0	0	0	0	0	0	0	9	31	42	28	12	14	9	2	4	2	1	0	0	0	0	154		
4.5	0	0	0	0	0	0	1	6	28	26	10	10	0	2	1	0	0	0	0	0	0	84		
5.0	0	0	0	0	0	0	0	5	20	24	15	3	1	0	0	0	0	0	0	0	0	68		
5.5	0	0	0	0	0	0	0	1	8	12	13	1	1	0	0	0	0	0	0	0	0	36		
6.0	0	0	0	0	0	0	0	0	2	9	13	4	1	0	0	0	0	0	0	0	0	29		
6.5	0	0	0	0	0	0	0	0	2	2	9	3	1	0	0	0	0	0	0	0	0	17		
7.0	0	0	0	0	0	0	0	0	0	1	2	0	1	0	0	0	0	0	0	0	0	4		
7.5	0	0	0	0	0	0	0	0	0	0	3	1	0	0	0	0	0	0	0	0	0	4		
8.0	0	0	0	0	0	0	0	0	0	0	0	1	0	0	0	0	0	0	0	0	0	1		
8.5	0	0	0	0	0	0	0	0	0	0	0	0	0	0	0	0	0	0	0	0	0	0		
9.0	0	0	0	0	0	0	0	0	0	0	0	0	0	0	0	0	0	0	0	0	0	0		
9.5	0	0	0	0	0	0	0	0	0	0	0	0	0	0	0	0	0	0	0	0	0	0		
10.0	0	0	0	0	0	0	0	0	0	0	0	0	0	0	0	0	0	0	0	0	0	0		
10.5	0	0	0	0	0	0	0	0	0	0	0	0	0	0	0	0	0	0	0	0	0	0		
11.0	0	0	0	0	0	0	0	0	0	0	0	0	0	0	0	0	0	0	0	0	0	0		
11.5	0	0	0	0	0	0	0	0	0	0	0	0	0	0	0	0	0	0	0	0	0	0		
12.0	0	0	0	0	0	0	0	0	0	0	0	0	0	0	0	0	0	0	0	0	0	0		
12.5	0	0	0	0	0	0	0	0	0	0	0	0	0	0	0	0	0	0	0	0	0	0		
13.0	0	0	0	0	0	0	0	0	0	0	0	0	0	0	0	0	0	0	0	0	0	0		
13.5	0	0	0	0	0	0	0	0	0	0	0	0	0	0	0	0	0	0	0	0	0	0		
14.0	0	0	0	0	0	0	0	0	0	0	0	0	0	0	0	0	0	0	0	0	0	0		
14.5	0	0	0	0	0	0	0	0	0	0	0	0	0	0	0	0	0	0	0	0	0	0		
15.0	0	0	0	0	0	0	0	0	0	0	0	0	0	0	0	0	0	0	0	0	0	0		
15.5	0	0	0	0	0	0	0	0	0	0	0	0	0	0	0	0	0	0	0	0	0	0		
16.0	0	0	0	0	0	0	0	0	0	0	0	0	0	0	0	0	0	0	0	0	0	0		
16.5	0	0	0	0	0	0	0	0	0	0	0	0	0	0	0	0	0	0	0	0	0	0		
17.0	0	0	0	0	0	0	0	0	0	0	0	0	0	0	0	0	0	0	0	0	0	0		
	38	362	1207	1764	2223	2249	2112	1746	1114	723	324	138	77	26	19	11	2	1	0	0	0	14136		
	0	38	400	1607	3371	5594	7843	9955	11701	12815	15538	13862	14000	14077	14103	14122	14133	14135	14136	14136	14136	14136		

Table 0-5: Monthly Scatter Table after Tp randomization for the samples from year 1957-2014 (May)

Installation Analyses of A Subsea Structure

Spectral Peak Period, Tp [s]

Lower	Spectral Peak Period, Tp [s]																					Cum. Sum		
	< 3	3	4	5	6	7	8	9	10	11	12	13	14	15	16	17	18	19	20	21	22		23	
Upper																								
0.0	0	0	16	15	19	15	19	5	2	3	3	5	0	0	0	0	0	0	0	0	0	83	83	
0.5	0	24	141	434	567	504	461	341	161	71	28	5	4	4	7	1	0	0	0	0	0	2749	2832	
1.0	0	3	181	530	753	926	878	672	415	234	80	19	17	17	1	2	1	0	0	0	0	4712	7544	
1.5	0	0	17	229	483	603	569	495	336	209	120	39	18	10	3	2	0	0	0	0	0	3133	10677	
2.0	0	0	1	17	198	345	292	228	169	119	85	54	12	8	4	0	0	0	0	0	0	1532	12209	
2.5	0	0	0	1	24	133	181	132	80	50	31	11	10	2	0	0	0	0	0	0	0	655	12864	
3.0	0	0	0	0	2	30	108	103	68	21	23	10	2	0	0	0	0	0	0	0	0	367	13231	
3.5	0	0	0	0	1	2	33	78	43	16	17	5	1	0	0	0	0	0	0	0	0	196	13427	
4.0	0	0	0	0	0	0	8	41	27	15	7	3	0	0	0	0	0	0	0	0	0	101	13528	
4.5	0	0	0	0	0	0	0	19	31	17	13	4	0	0	0	0	0	0	0	0	0	84	13612	
5.0	0	0	0	0	0	0	0	3	10	17	7	2	1	0	0	0	0	0	0	0	0	40	13652	
5.5	0	0	0	0	0	0	0	1	1	1	4	3	1	0	0	0	0	0	0	0	0	11	13663	
6.0	0	0	0	0	0	0	0	0	0	0	4	3	1	0	0	0	0	0	0	0	0	8	13671	
6.5	0	0	0	0	0	0	0	0	0	0	4	2	0	0	0	0	0	0	0	0	0	6	13677	
7.0	0	0	0	0	0	0	0	0	0	0	0	1	0	1	1	0	0	0	0	0	0	2	13679	
7.5	0	0	0	0	0	0	0	0	0	0	0	0	0	0	0	0	0	0	0	0	0	0	0	13679
8.0	0	0	0	0	0	0	0	0	0	0	0	0	0	0	0	0	0	0	0	0	0	0	0	13679
8.5	0	0	0	0	0	0	0	0	0	0	0	0	0	0	0	0	0	0	0	0	0	0	0	13679
9.0	0	0	0	0	0	0	0	0	0	0	0	0	0	0	0	0	0	0	0	0	0	0	0	13679
9.5	0	0	0	0	0	0	0	0	0	0	0	0	0	0	0	0	0	0	0	0	0	0	0	13679
10.0	0	0	0	0	0	0	0	0	0	0	0	0	0	0	0	0	0	0	0	0	0	0	0	13679
10.5	0	0	0	0	0	0	0	0	0	0	0	0	0	0	0	0	0	0	0	0	0	0	0	13679
11.0	0	0	0	0	0	0	0	0	0	0	0	0	0	0	0	0	0	0	0	0	0	0	0	13679
11.5	0	0	0	0	0	0	0	0	0	0	0	0	0	0	0	0	0	0	0	0	0	0	0	13679
12.0	0	0	0	0	0	0	0	0	0	0	0	0	0	0	0	0	0	0	0	0	0	0	0	13679
12.5	0	0	0	0	0	0	0	0	0	0	0	0	0	0	0	0	0	0	0	0	0	0	0	13679
13.0	0	0	0	0	0	0	0	0	0	0	0	0	0	0	0	0	0	0	0	0	0	0	0	13679
13.5	0	0	0	0	0	0	0	0	0	0	0	0	0	0	0	0	0	0	0	0	0	0	0	13679
14.0	0	0	0	0	0	0	0	0	0	0	0	0	0	0	0	0	0	0	0	0	0	0	0	13679
14.5	0	0	0	0	0	0	0	0	0	0	0	0	0	0	0	0	0	0	0	0	0	0	0	13679
15.0	0	0	0	0	0	0	0	0	0	0	0	0	0	0	0	0	0	0	0	0	0	0	0	13679
15.5	0	0	0	0	0	0	0	0	0	0	0	0	0	0	0	0	0	0	0	0	0	0	0	13679
16.0	0	0	0	0	0	0	0	0	0	0	0	0	0	0	0	0	0	0	0	0	0	0	0	13679
16.5	0	0	0	0	0	0	0	0	0	0	0	0	0	0	0	0	0	0	0	0	0	0	0	13679
17.0	0	0	0	0	0	0	0	0	0	0	0	0	0	0	0	0	0	0	0	0	0	0	0	13679
	27	356	383	1226	2043	2562	2535	2115	1344	777	427	159	66	29	10	3	0	0	0	0	0	0	0	Sum
	0	27	383	1609	3652	6214	8749	10864	12208	12985	13412	13571	13637	13666	13676	13679	13679	13679	13679	13679	13679	13679	13679	13679

Table 0-6: Monthly Scatter Table after Tp randomization for the samples from year 1957-2014 (June)

		Spectral Peak Period, Tp [s]																								
Lower	Upper	<	3	4	5	6	7	8	9	10	11	12	13	14	15	16	17	18	19	20	21	22	23	Cum. Sum		
		3	4	5	6	7	8	9	10	11	12	13	14	15	16	17	18	19	20	21	22	23	Sum			
0.0	0.5	0	0	24	17	15	29	31	14	7	4	0	1	0	0	0	0	0	0	0	0	0	0	142	142	
0.5	1.0	2	26	216	408	829	896	607	362	135	45	14	9	2	0	1	0	0	0	0	0	0	0	3552	3694	
1.0	1.5	0	2	196	519	794	1014	1162	735	328	136	34	20	8	7	3	0	0	0	0	0	0	0	4958	8652	
1.5	2.0	0	0	12	154	455	547	559	427	293	170	65	20	8	7	0	0	0	0	0	0	0	0	2717	11369	
2.0	2.5	0	0	0	13	186	296	322	208	122	70	30	20	7	3	0	1	0	0	0	0	0	0	1278	12647	
2.5	3.0	0	0	0	0	22	131	229	130	62	37	18	15	3	0	1	0	0	0	0	0	0	0	648	13295	
3.0	3.5	0	0	0	0	2	20	100	90	44	19	24	12	1	1	1	0	0	0	0	0	0	0	313	13608	
3.5	4.0	0	0	0	0	0	0	42	68	26	11	5	3	0	1	0	0	0	0	0	0	0	0	156	13764	
4.0	4.5	0	0	0	0	0	0	8	16	16	10	1	2	1	0	0	0	0	0	0	0	0	0	54	13818	
4.5	5.0	0	0	0	0	0	0	7	22	8	4	1	2	0	0	0	0	0	0	0	0	0	0	44	13862	
5.0	5.5	0	0	0	0	0	0	0	4	6	4	1	0	0	0	0	0	0	0	0	0	0	0	15	13877	
5.5	6.0	0	0	0	0	0	0	0	1	0	3	2	1	1	1	1	0	0	0	0	0	0	0	9	13886	
6.0	6.5	0	0	0	0	0	0	0	0	0	0	2	0	0	0	0	0	0	0	0	0	0	0	2	13888	
6.5	7.0	0	0	0	0	0	0	0	0	0	0	0	0	0	0	0	0	0	0	0	0	0	0	0	0	13888
7.0	7.5	0	0	0	0	0	0	0	0	0	0	0	0	0	0	0	0	0	0	0	0	0	0	0	0	13888
7.5	8.0	0	0	0	0	0	0	0	0	0	0	0	0	0	0	0	0	0	0	0	0	0	0	0	0	13888
8.0	8.5	0	0	0	0	0	0	0	0	0	0	0	0	0	0	0	0	0	0	0	0	0	0	0	0	13888
8.5	9.0	0	0	0	0	0	0	0	0	0	0	0	0	0	0	0	0	0	0	0	0	0	0	0	0	13888
9.0	9.5	0	0	0	0	0	0	0	0	0	0	0	0	0	0	0	0	0	0	0	0	0	0	0	0	13888
9.5	10.0	0	0	0	0	0	0	0	0	0	0	0	0	0	0	0	0	0	0	0	0	0	0	0	0	13888
10.0	10.5	0	0	0	0	0	0	0	0	0	0	0	0	0	0	0	0	0	0	0	0	0	0	0	0	13888
10.5	11.0	0	0	0	0	0	0	0	0	0	0	0	0	0	0	0	0	0	0	0	0	0	0	0	0	13888
11.0	11.5	0	0	0	0	0	0	0	0	0	0	0	0	0	0	0	0	0	0	0	0	0	0	0	0	13888
11.5	12.0	0	0	0	0	0	0	0	0	0	0	0	0	0	0	0	0	0	0	0	0	0	0	0	0	13888
12.0	12.5	0	0	0	0	0	0	0	0	0	0	0	0	0	0	0	0	0	0	0	0	0	0	0	0	13888
12.5	13.0	0	0	0	0	0	0	0	0	0	0	0	0	0	0	0	0	0	0	0	0	0	0	0	0	13888
13.0	13.5	0	0	0	0	0	0	0	0	0	0	0	0	0	0	0	0	0	0	0	0	0	0	0	0	13888
13.5	14.0	0	0	0	0	0	0	0	0	0	0	0	0	0	0	0	0	0	0	0	0	0	0	0	0	13888
14.0	14.5	0	0	0	0	0	0	0	0	0	0	0	0	0	0	0	0	0	0	0	0	0	0	0	0	13888
14.5	15.0	0	0	0	0	0	0	0	0	0	0	0	0	0	0	0	0	0	0	0	0	0	0	0	0	13888
15.0	15.5	0	0	0	0	0	0	0	0	0	0	0	0	0	0	0	0	0	0	0	0	0	0	0	0	13888
15.5	16.0	0	0	0	0	0	0	0	0	0	0	0	0	0	0	0	0	0	0	0	0	0	0	0	0	13888
16.0	16.5	0	0	0	0	0	0	0	0	0	0	0	0	0	0	0	0	0	0	0	0	0	0	0	0	13888
16.5	17.0	0	0	0	0	0	0	0	0	0	0	0	0	0	0	0	0	0	0	0	0	0	0	0	0	13888
		2	28	448	1111	2303	2933	3060	2058	1059	519	203	105	33	20	5	1	0	0	0	0	0	0	0	0	0
		2	30	478	1589	3892	6825	9885	11943	13002	13521	13724	13829	13862	13882	13887	13888	13888	13888	13888	13888	13888	13888	13888	13888	13888

Table 0-7: Monthly Scatter Table after Tp randomization for the samples from year 1957-2014 (July)

Spectral Peak Period, Tp [s]

Lower	Upper	<	3	4	5	6	7	8	9	10	11	12	13	14	15	16	17	18	19	20	21	22	23	Cum. Sum
0.0	0.5	0	3	2	7	5	5	5	10	6	4	0	0	0	0	0	0	0	0	0	0	0	0	47
0.5	1.0	0	12	92	131	176	244	191	126	118	42	17	5	8	6	5	4	2	1	0	0	0	0	1180
1.0	1.5	0	0	105	284	301	497	634	439	281	180	76	20	19	13	8	2	5	2	1	0	0	0	2867
1.5	2.0	0	0	25	182	319	370	548	539	424	258	117	43	32	13	6	1	2	1	0	0	0	0	2881
2.0	2.5	0	0	1	40	174	268	375	386	330	246	141	58	32	18	11	3	2	0	0	0	0	0	2085
2.5	3.0	0	0	0	7	64	167	291	318	232	201	148	63	32	16	9	4	2	1	0	0	0	0	1555
3.0	3.5	0	0	0	0	11	69	191	250	206	154	105	44	27	13	7	3	0	0	0	0	0	0	1080
3.5	4.0	0	0	0	0	0	1	15	115	163	141	102	59	43	21	10	3	4	1	0	0	0	0	678
4.0	4.5	0	0	0	0	0	0	2	31	107	128	90	44	21	6	5	2	0	2	0	0	0	0	438
4.5	5.0	0	0	0	0	0	0	0	12	41	79	86	38	16	6	7	3	0	0	0	0	0	0	288
5.0	5.5	0	0	0	0	0	0	0	14	59	59	46	12	10	4	0	1	0	0	0	0	0	0	205
5.5	6.0	0	0	0	0	0	0	1	3	25	50	28	10	8	6	2	0	0	0	0	0	0	0	133
6.0	6.5	0	0	0	0	0	0	0	0	10	18	28	4	9	3	4	0	0	0	0	0	0	0	76
6.5	7.0	0	0	0	0	0	0	0	0	2	12	19	13	5	2	0	0	0	0	0	0	0	0	53
7.0	7.5	0	0	0	0	0	0	0	0	4	6	17	9	5	1	0	0	0	0	0	0	0	0	42
7.5	8.0	0	0	0	0	0	0	0	1	3	5	11	7	2	0	0	0	0	0	0	0	0	0	29
8.0	8.5	0	0	0	0	0	0	0	0	0	1	2	4	5	1	2	0	0	0	0	0	0	0	15
8.5	9.0	0	0	0	0	0	0	0	0	0	0	4	4	4	3	0	0	0	0	0	0	0	0	15
9.0	9.5	0	0	0	0	0	0	0	0	0	0	4	3	1	2	0	0	0	0	0	0	0	0	6
9.5	10.0	0	0	0	0	0	0	0	0	0	0	0	1	3	0	0	0	0	0	0	0	0	0	4
10.0	10.5	0	0	0	0	0	0	0	0	0	0	0	0	1	0	0	0	0	0	0	0	0	0	1
10.5	11.0	0	0	0	0	0	0	0	0	0	0	0	0	0	0	0	0	0	0	0	0	0	0	0
11.0	11.5	0	0	0	0	0	0	0	0	0	0	0	0	0	0	0	0	0	0	0	0	0	0	0
11.5	12.0	0	0	0	0	0	0	0	0	0	0	0	0	0	0	0	0	0	0	0	0	0	0	0
12.0	12.5	0	0	0	0	0	0	0	0	0	0	0	0	0	0	0	0	0	0	0	0	0	0	0
12.5	13.0	0	0	0	0	0	0	0	0	0	0	0	0	0	0	0	0	0	0	0	0	0	0	0
13.0	13.5	0	0	0	0	0	0	0	0	0	0	0	0	0	0	0	0	0	0	0	0	0	0	0
13.5	14.0	0	0	0	0	0	0	0	0	0	0	0	0	0	0	0	0	0	0	0	0	0	0	0
14.0	14.5	0	0	0	0	0	0	0	0	0	0	0	0	0	0	0	0	0	0	0	0	0	0	0
14.5	15.0	0	0	0	0	0	0	0	0	0	0	0	0	0	0	0	0	0	0	0	0	0	0	0
15.0	15.5	0	0	0	0	0	0	0	0	0	0	0	0	0	0	0	0	0	0	0	0	0	0	0
15.5	16.0	0	0	0	0	0	0	0	0	0	0	0	0	0	0	0	0	0	0	0	0	0	0	0
16.0	16.5	0	0	0	0	0	0	0	0	0	0	0	0	0	0	0	0	0	0	0	0	0	0	0
16.5	17.0	0	0	0	0	0	0	0	0	0	0	0	0	0	0	0	0	0	0	0	0	0	0	0
		0	15	225	651	1051	1637	2394	2396	2046	1512	894	385	240	125	62	22	16	5	2	0	0	0	Sum
		0	15	240	891	1942	3579	5973	8369	10415	11927	12821	13206	13446	13571	13633	13655	13671	13676	13678	13678	13678	13678	Sum

Significant Wave Height, Hs [m]

Table 0-9: Monthly Scatter Table after Tp randomization for the samples from year 1957-2014 (September)

Spectral Peak Period, Tp [s]

Lower	Upper	< 3	3	4	5	6	7	8	9	10	11	12	13	14	15	16	17	18	19	20	21	22	23	Cum. Sum
0.0	0.5	0	0	0	9	0	2	0	3	1	0	0	0	0	0	0	0	0	0	0	0	0	0	15
0.5	1.0	0	4	20	37	54	57	64	38	61	24	10	2	5	1	2	0	0	0	0	0	0	0	379
1.0	1.5	0	0	46	121	148	233	325	244	205	132	46	38	17	10	7	3	1	0	0	0	0	0	1576
1.5	2.0	0	0	17	133	231	198	439	471	398	245	146	69	28	19	6	2	0	3	4	0	0	0	2409
2.0	2.5	0	0	0	56	229	202	265	402	407	291	169	97	32	21	3	3	7	2	1	0	0	0	2187
2.5	3.0	0	0	0	2	80	180	237	308	398	351	214	111	64	32	9	2	5	1	1	0	0	0	1995
3.0	3.5	0	0	0	2	16	127	231	283	285	247	183	92	54	31	10	6	4	1	0	0	0	0	1572
3.5	4.0	0	0	0	0	6	32	183	227	236	230	151	81	43	28	17	7	3	1	1	0	0	0	1246
4.0	4.5	0	0	0	0	0	7	79	168	195	183	100	74	47	31	11	5	1	0	2	0	0	0	903
4.5	5.0	0	0	0	0	0	1	23	107	149	131	85	38	29	15	7	1	3	1	1	0	0	0	591
5.0	5.5	0	0	0	0	0	0	6	41	106	97	58	42	19	11	8	2	3	0	0	0	0	0	393
5.5	6.0	0	0	0	0	0	0	3	25	53	85	57	23	23	10	4	1	0	2	1	0	0	0	287
6.0	6.5	0	0	0	0	0	0	0	3	17	50	41	21	6	8	6	1	0	0	0	0	0	0	153
6.5	7.0	0	0	0	0	0	0	0	1	11	22	51	16	15	10	4	2	2	0	1	0	0	0	135
7.0	7.5	0	0	0	0	0	0	0	0	1	11	34	36	14	10	5	5	2	0	0	0	0	0	118
7.5	8.0	0	0	0	0	0	0	0	0	0	4	19	20	13	5	1	6	0	0	0	0	0	0	68
8.0	8.5	0	0	0	0	0	0	0	0	0	2	8	16	9	5	0	1	0	0	0	0	0	0	41
8.5	9.0	0	0	0	0	0	0	0	0	0	0	2	15	4	3	0	0	0	0	0	0	0	0	24
9.0	9.5	0	0	0	0	0	0	0	0	0	0	1	8	6	0	1	0	0	0	0	0	0	0	16
9.5	10.0	0	0	0	0	0	0	0	0	0	0	1	2	2	3	1	0	0	0	0	0	0	0	9
10.0	10.5	0	0	0	0	0	0	0	0	0	0	0	1	1	0	0	0	0	0	0	0	0	0	2
10.5	11.0	0	0	0	0	0	0	0	0	0	0	0	2	3	2	1	0	0	0	0	0	0	0	8
11.0	11.5	0	0	0	0	0	0	0	0	0	0	0	0	3	2	0	0	0	0	0	0	0	0	5
11.5	12.0	0	0	0	0	0	0	0	0	0	0	0	0	3	0	0	0	0	0	0	0	0	0	3
12.0	12.5	0	0	0	0	0	0	0	0	0	0	0	0	0	0	1	0	0	0	0	0	0	0	1
12.5	13.0	0	0	0	0	0	0	0	0	0	0	0	0	0	0	0	0	0	0	0	0	0	0	0
13.0	13.5	0	0	0	0	0	0	0	0	0	0	0	0	0	0	0	0	0	0	0	0	0	0	0
13.5	14.0	0	0	0	0	0	0	0	0	0	0	0	0	0	0	0	0	0	0	0	0	0	0	0
14.0	14.5	0	0	0	0	0	0	0	0	0	0	0	0	0	0	0	0	0	0	0	0	0	0	0
14.5	15.0	0	0	0	0	0	0	0	0	0	0	0	0	0	0	0	0	0	0	0	0	0	0	0
15.0	15.5	0	0	0	0	0	0	0	0	0	0	0	0	0	0	0	0	0	0	0	0	0	0	0
15.5	16.0	0	0	0	0	0	0	0	0	0	0	0	0	0	0	0	0	0	0	0	0	0	0	0
16.0	16.5	0	0	0	0	0	0	0	0	0	0	0	0	0	0	0	0	0	0	0	0	0	0	0
16.5	17.0	0	0	0	0	0	0	0	0	0	0	0	0	0	0	0	0	0	0	0	0	0	0	0
		0	4	83	360	764	1039	1855	2321	2523	2105	1376	804	440	258	103	47	31	11	12	14136	14136	0	Sum
		0	4	87	447	1211	2250	4105	6426	8949	11054	12430	13234	13674	13932	14085	14082	14113	14124	14136	14136	14136	0	Cum. Sum

Table 0-10: Monthly Scatter Table after Tp randomization for the samples from year 1957-2014 (October)

Spectral Peak Period, T_p [s]

Lower	Upper	< 3	3	4	5	6	7	8	9	10	11	12	13	14	15	16	17	18	19	20	21	22	23	Cum. Sum
0.0	0.5	0	0	0	0	0	0	0	0	0	0	0	0	0	0	0	0	0	0	0	0	0	0	0
0.5	1.0	0	1	8	19	17	40	26	27	18	25	13	8	1	1	1	1	3	3	2	0	0	0	213
1.0	1.5	0	2	15	67	90	175	236	144	93	59	38	31	17	14	6	5	5	1	0	0	0	0	998
1.5	2.0	0	0	12	132	144	161	294	330	292	202	121	76	26	20	10	7	5	2	0	0	0	0	1834
2.0	2.5	0	0	0	40	193	152	222	312	365	289	201	107	50	37	13	5	6	1	1	0	0	0	5039
2.5	3.0	0	0	0	9	113	245	178	265	394	321	244	125	80	40	11	17	10	0	0	0	0	0	2052
3.0	3.5	0	0	0	0	45	165	215	233	295	303	212	126	65	40	17	11	6	3	1	1	0	0	1738
3.5	4.0	0	0	0	0	7	68	236	220	223	249	207	114	59	42	14	8	5	0	0	0	0	0	1452
4.0	4.5	0	0	0	0	0	13	89	155	196	199	157	83	51	25	22	11	4	1	0	0	0	0	1006
4.5	5.0	0	0	0	0	0	0	36	96	138	143	113	56	33	25	16	10	7	0	2	0	0	0	675
5.0	5.5	0	0	0	0	0	0	12	57	100	103	97	44	23	16	11	5	6	0	0	0	0	0	474
5.5	6.0	0	0	0	0	0	0	2	17	46	102	94	50	27	15	7	4	6	0	0	0	0	0	370
6.0	6.5	0	0	0	0	0	0	0	3	25	72	75	48	15	17	5	1	4	0	0	0	0	0	265
6.5	7.0	0	0	0	0	0	0	0	1	12	48	69	42	15	7	2	2	2	0	0	0	0	0	200
7.0	7.5	0	0	0	0	0	0	0	0	3	22	39	35	19	5	3	2	3	0	0	0	0	0	131
7.5	8.0	0	0	0	0	0	0	0	1	7	28	37	21	8	0	2	2	3	0	1	0	0	0	108
8.0	8.5	0	0	0	0	0	0	0	0	0	3	8	31	16	8	0	1	3	0	0	0	0	0	70
8.5	9.0	0	0	0	0	0	0	0	0	0	0	1	12	10	5	0	0	0	0	0	0	0	0	28
9.0	9.5	0	0	0	0	0	0	0	0	0	0	1	8	10	6	2	1	0	0	0	0	0	0	28
9.5	10.0	0	0	0	0	0	0	0	0	0	0	2	3	3	5	3	0	0	0	0	0	0	0	16
10.0	10.5	0	0	0	0	0	0	0	0	0	0	0	1	2	4	1	0	0	0	0	0	0	0	8
10.5	11.0	0	0	0	0	0	0	0	0	0	0	0	0	3	0	2	0	0	0	0	0	0	0	5
11.0	11.5	0	0	0	0	0	0	0	0	0	0	0	1	1	1	2	0	0	0	0	0	0	0	5
11.5	12.0	0	0	0	0	0	0	0	0	0	0	0	0	0	0	0	0	0	0	0	0	0	0	0
12.0	12.5	0	0	0	0	0	0	0	0	0	0	0	0	0	0	0	1	0	0	0	0	0	0	0
12.5	13.0	0	0	0	0	0	0	0	0	0	0	0	0	0	0	2	0	0	0	0	0	0	0	2
13.0	13.5	0	0	0	0	0	0	0	0	0	0	0	0	0	1	0	0	0	0	0	0	0	0	1
13.5	14.0	0	0	0	0	0	0	0	0	0	0	0	0	0	1	0	1	0	0	0	0	0	0	1
14.0	14.5	0	0	0	0	0	0	0	0	0	0	0	0	0	0	1	0	1	0	0	0	0	0	2
14.5	15.0	0	0	0	0	0	0	0	0	0	0	0	0	0	0	0	0	1	0	0	0	0	0	1
15.0	15.5	0	0	0	0	0	0	0	0	0	0	0	0	0	0	0	0	0	0	0	0	0	0	0
15.5	16.0	0	0	0	0	0	0	0	0	0	0	0	0	0	0	0	0	0	0	0	0	0	0	0
16.0	16.5	0	0	0	0	0	0	0	0	0	0	0	0	0	0	0	0	1	1	0	0	0	0	2
16.5	17.0	0	0	0	0	0	0	0	0	0	0	0	0	0	0	0	0	0	0	0	0	0	0	0
		0	3	35	267	609	1019	1546	1860	2201	2147	1720	1038	547	343	150	99	80	10	5	1	0	0	13680
		0	3	38	305	914	1933	3479	5339	7540	9687	11407	12445	12992	13335	13485	13584	13664	13674	13679	13680	13680	0	13680

Significant Wave Height, H_s [m]

Table 0-11: Monthly Scatter Table after T_p randomization for the samples from year 1957-2014 (November)

Spectral Peak Period, T_p [s]

Lower	Spectral Peak Period, T_p [s]																							Cum. Sum
	Upper	< 3	3	4	5	6	7	8	9	10	11	12	13	14	15	16	17	18	19	20	21	22	23	
0.0	0.5	0	0	0	0	0	0	0	0	0	0	0	0	0	0	0	0	0	0	0	0	0	0	0
0.5	1.0	0	1	1	4	1	7	7	3	11	4	1	1	1	0	0	0	0	0	0	1	0	0	43
1.0	1.5	0	0	8	34	40	62	117	100	38	56	46	37	18	24	27	11	4	2	2	1	0	600	
1.5	2.0	0	0	7	86	108	99	214	251	142	130	130	118	76	57	26	10	5	0	1	1	1	1401	
2.0	2.5	0	0	0	27	153	179	178	318	298	240	183	134	76	50	28	8	5	2	2	3	0	1884	
2.5	3.0	0	0	0	9	100	219	182	254	349	316	215	150	103	71	34	10	7	1	0	0	3	2023	
3.0	3.5	0	0	0	2	35	136	156	213	274	310	267	151	111	66	35	23	11	5	2	0	1	1798	
3.5	4.0	0	0	0	0	7	62	144	189	253	245	228	123	91	57	32	17	18	3	1	0	0	1470	
4.0	4.5	0	0	0	0	0	16	126	140	192	193	216	141	75	64	36	23	14	0	2	0	0	1238	
4.5	5.0	0	0	0	0	0	5	44	137	191	164	144	101	75	61	32	19	7	0	0	0	0	980	
5.0	5.5	0	0	0	0	0	0	14	70	140	164	151	100	43	28	21	15	7	0	1	0	1	755	
5.5	6.0	0	0	0	0	0	0	3	42	76	120	110	81	34	34	9	6	9	0	0	0	0	524	
6.0	6.5	0	0	0	0	0	0	1	15	35	98	112	56	35	33	11	7	5	0	2	0	0	410	
6.5	7.0	0	0	0	0	0	0	0	5	20	58	110	51	32	23	7	2	9	1	0	0	1	319	
7.0	7.5	0	0	0	0	0	0	0	4	7	19	88	54	23	16	8	5	4	0	0	0	0	228	
7.5	8.0	0	0	0	0	0	0	0	2	13	46	34	20	17	4	2	7	0	0	0	0	0	145	
8.0	8.5	0	0	0	0	0	0	0	0	7	18	36	18	7	2	3	4	0	0	0	0	0	95	
8.5	9.0	0	0	0	0	0	0	0	0	1	7	20	18	12	3	5	1	0	0	0	0	0	67	
9.0	9.5	0	0	0	0	0	0	0	0	0	1	1	14	12	7	4	1	1	1	1	0	0	42	
9.5	10.0	0	0	0	0	0	0	0	0	0	1	11	22	2	2	3	1	4	0	0	0	0	44	
10.0	10.5	0	0	0	0	0	0	0	0	0	0	0	9	8	6	5	1	4	0	0	0	0	33	
10.5	11.0	0	0	0	0	0	0	0	0	0	0	0	1	8	2	0	4	2	0	0	0	0	17	
11.0	11.5	0	0	0	0	0	0	0	0	0	0	0	1	3	4	0	2	1	0	0	0	0	11	
11.5	12.0	0	0	0	0	0	0	0	0	0	0	0	0	1	1	1	1	1	0	0	0	0	6	
12.0	12.5	0	0	0	0	0	0	0	0	0	0	0	0	0	1	0	0	0	0	0	0	0	2	
12.5	13.0	0	0	0	0	0	0	0	0	0	0	0	0	0	1	0	0	0	0	0	0	0	1	
13.0	13.5	0	0	0	0	0	0	0	0	0	0	0	0	0	0	0	0	0	0	0	0	0	0	
13.5	14.0	0	0	0	0	0	0	0	0	0	0	0	0	0	0	0	0	0	0	0	0	0	0	
14.0	14.5	0	0	0	0	0	0	0	0	0	0	0	0	0	0	0	0	0	0	0	0	0	0	
14.5	15.0	0	0	0	0	0	0	0	0	0	0	0	0	0	0	0	0	0	0	0	0	0	0	
15.0	15.5	0	0	0	0	0	0	0	0	0	0	0	0	0	0	0	0	0	0	0	0	0	0	
15.5	16.0	0	0	0	0	0	0	0	0	0	0	0	0	0	0	0	0	0	0	0	0	0	0	
16.0	16.5	0	0	0	0	0	0	0	0	0	0	0	0	0	0	0	0	0	0	0	0	0	0	
16.5	17.0	0	0	0	0	0	0	0	0	0	0	0	0	0	0	0	0	0	0	0	0	0	0	
		0	1	16	162	444	785	1186	1741	2028	2139	2074	1424	872	614	313	170	128	15	13	4	7	Sum	
		0	1	17	179	623	1408	2594	4335	6363	8502	10576	12000	12872	13486	13799	13969	14097	14112	14125	14129	14136	Cum. Sum	

Table 0-12: Monthly Scatter Table after T_p randomization for the samples from year 1957-2014 (December)

Appendix -3: Total No. of Windows in Month wise

Year	No. Of Windows for Hs = 2 m, Duration = 6 hours											
	Jan	Feb	Mar	Apr	May	Jun	Jul	Aug	Sep	Oct	Nov	Dec
1958	26	43	91	50	78	110	98	114	84	20	10	54
1959	17	2	24	43	89	62	109	81	45	65	26	24
1960	35	18	58	38	102	97	118	103	76	94	39	19
1961	35	8	7	82	86	81	118	96	52	42	9	16
1962	18	11	58	50	90	83	100	111	70	10	41	17
1963	13	48	36	64	59	110	84	118	35	35	30	5
1964	1	36	70	79	69	73	70	92	57	28	11	8
1965	11	12	16	34	90	91	102	100	89	27	68	40
1966	33	46	29	96	72	117	94	105	42	74	15	7
1967	26	16	1	40	95	73	93	110	94	32	19	15
1968	14	35	8	68	98	107	119	109	91	41	54	8
1969	46	64	46	45	116	103	89	107	52	16	27	15
1970	20	31	51	84	81	99	91	116	59	41	31	12
1971	26	12	26	77	89	102	87	69	44	11	24	2
1972	29	42	25	53	96	87	109	79	58	31	16	5
1973	8	15	8	53	83	71	107	66	78	40	7	24
1974	0	12	53	53	100	95	97	97	57	65	56	2
1975	9	12	19	44	66	74	99	94	21	51	25	4
1976	11	13	28	34	93	87	101	91	70	50	25	34
1977	29	45	38	38	108	108	100	101	45	54	19	9
1978	19	46	26	67	97	97	109	99	59	17	2	34
1979	34	13	40	75	70	105	100	94	34	59	31	13
1980	27	18	60	37	98	105	116	100	63	40	36	8
1981	6	8	34	35	112	96	103	90	74	30	21	41
1982	27	0	20	16	78	111	65	84	25	47	19	0
1983	1	10	17	66	101	97	77	72	63	19	21	29
1984	18	8	55	57	97	79	120	100	89	33	37	6
1985	32	19	27	44	95	98	107	109	60	11	20	32
1986	40	58	15	68	75	84	112	119	52	5	5	28
1987	32	16	45	60	93	87	102	104	62	20	28	15
1988	12	22	50	53	100	100	93	96	46	39	10	3
1989	1	0	7	76	48	75	99	85	35	38	19	19
1990	4	0	0	33	95	104	107	101	62	40	29	0
1991	12	25	44	37	68	109	108	80	40	48	12	0
1992	3	2	15	53	71	74	105	117	76	60	16	0
1993	3	2	0	66	89	102	105	102	103	38	19	14
1994	13	34	4	42	90	68	104	111	71	27	41	1
1995	7	1	7	45	90	71	96	65	75	23	34	8
1996	28	10	42	49	82	70	105	106	80	35	38	38
1997	8	0	28	20	82	103	114	90	34	34	54	53
1998	9	3	8	99	81	95	117	86	81	50	46	8
1999	33	12	32	56	88	75	85	107	62	64	7	16
2000	1	6	16	51	77	68	109	97	80	31	47	21
2001	19	24	64	45	87	89	91	108	96	55	0	14
2002	1	1	30	62	87	93	107	99	70	54	49	36
2003	14	9	0	57	93	112	121	89	43	49	40	5
2004	8	13	25	62	73	91	120	106	21	58	19	2
2005	5	29	42	51	71	88	90	70	20	23	13	28
2006	6	11	41	54	85	86	90	105	67	42	14	4
2007	1	29	6	29	71	113	105	77	26	13	7	5
2008	13	0	27	66	108	88	98	93	51	8	11	26
2009	5	25	18	55	57	98	81	86	20	43	32	33
2010	36	43	34	45	97	94	80	102	89	11	61	32
2011	21	8	9	26	76	87	102	94	54	5	17	6
2012	12	0	2	59	67	103	102	100	52	63	18	55
2013	25	28	54	36	86	105	74	84	64	31	5	1
Min	0	0	0	16	48	62	65	65	20	5	0	0
Mean	17	19	29	53	86	92	100	96	59	37	26	17
Median	13.5	13	27	53	87.5	94.5	102	99	59.5	38	21	14
Max	46	64	91	99	116	117	121	119	103	94	68	55

Table 0-1: Total no. of windows available for the significant wave height from year 1958 to 2013 in month wise, duration 6 hours, Hs=2 m

Year	No. Of Windows for Hs = 2 m, Duration = 12 hours											
	Jan	Feb	Mar	Apr	May	Jun	Jul	Aug	Sep	Oct	Nov	Dec
1958	12	20	44	22	35	54	47	56	40	8	4	25
1959	6	1	11	19	43	30	53	40	20	30	12	10
1960	15	7	28	18	50	47	58	50	37	46	16	8
1961	16	4	1	38	42	39	58	47	24	21	3	7
1962	8	4	27	23	43	40	49	55	33	4	19	8
1963	5	23	17	30	28	54	40	59	16	15	13	1
1964	0	16	34	37	33	35	34	43	27	12	4	3
1965	5	5	7	14	43	45	50	48	42	12	32	19
1966	16	21	12	47	35	58	45	52	20	35	6	3
1967	11	6	0	19	46	36	44	54	45	14	8	6
1968	5	17	3	33	46	53	59	53	45	18	26	2
1969	22	30	19	20	57	50	43	53	26	8	11	7
1970	8	15	24	40	39	48	44	58	28	19	12	2
1971	13	4	12	36	43	50	42	33	20	5	10	0
1972	13	19	12	25	47	41	53	37	27	14	7	2
1973	4	7	3	25	40	34	53	32	37	17	1	9
1974	0	5	25	24	49	46	47	48	26	31	27	1
1975	3	6	8	21	32	34	49	46	9	24	11	1
1976	5	6	13	14	45	42	49	43	34	22	12	16
1977	13	19	16	17	53	53	49	49	21	25	8	4
1978	9	22	11	32	47	47	53	49	28	7	1	16
1979	16	5	16	35	33	51	47	46	15	29	14	6
1980	13	8	29	15	47	51	57	49	30	19	17	2
1981	3	3	15	16	55	46	51	44	35	14	10	18
1982	13	0	9	7	38	54	30	40	10	21	9	0
1983	0	4	7	31	49	47	37	34	30	8	9	14
1984	8	3	26	26	48	37	59	48	42	14	16	2
1985	14	8	13	21	44	48	52	53	29	5	9	14
1986	20	26	7	32	34	40	56	58	24	2	1	13
1987	15	7	21	29	45	41	50	50	28	8	12	7
1988	5	9	23	24	50	49	44	46	21	18	3	1
1989	0	0	3	37	23	36	47	40	16	17	7	9
1990	1	0	0	15	46	51	52	48	30	18	13	0
1991	5	12	19	17	31	53	53	39	19	22	5	0
1992	1	0	7	24	34	35	51	58	37	28	7	0
1993	1	1	0	30	42	49	51	49	49	18	8	6
1994	6	16	1	20	43	32	51	55	34	12	20	0
1995	3	0	3	21	43	32	47	31	36	10	16	3
1996	13	5	19	23	39	34	51	53	39	17	18	17
1997	3	0	13	8	39	51	56	43	15	14	26	25
1998	3	1	3	48	37	47	58	42	39	23	23	4
1999	15	5	15	25	42	36	40	52	30	30	3	6
2000	0	3	8	23	35	31	54	47	38	14	21	9
2001	7	11	29	21	43	43	44	51	46	26	0	6
2002	0	0	14	29	41	46	53	49	34	25	24	16
2003	6	4	0	27	45	56	60	43	21	21	19	2
2004	3	5	11	28	35	44	59	52	8	27	9	1
2005	2	14	19	24	34	42	43	33	9	11	6	12
2006	2	4	18	25	40	42	44	51	30	18	6	1
2007	0	14	3	14	33	56	51	36	11	6	2	2
2008	5	0	12	31	53	42	47	44	23	3	4	11
2009	2	11	6	25	27	48	39	40	8	20	15	13
2010	16	20	15	19	46	46	37	50	43	4	29	13
2011	9	3	4	11	37	42	49	45	25	1	8	2
2012	5	0	1	28	30	50	50	49	24	29	8	26
2013	10	11	25	15	42	51	35	42	31	13	2	0
Min	0	0	0	7	23	30	30	31	8	1	0	0
Mean	7	8	13	25	41	45	49	47	28	17	11	7
Median	5.5	5.5	12	24	42	46	49.5	48	28	17	9.5	6
Max	22	30	44	48	57	58	60	59	49	46	32	26

Table 0-2: Total no. of windows available for the significant wave height from year 1958 to 2013 in month wise, duration 12 hours, Hs=2 m

Year	No. Of Windows for Hs = 2 m, Duration = 24 hours											
	Jan	Feb	Mar	Apr	May	Jun	Jul	Aug	Sep	Oct	Nov	Dec
1958	5	8	20	9	15	25	23	27	17	3	2	11
1959	2	0	5	9	19	13	26	18	9	13	5	4
1960	4	1	13	8	24	22	29	23	17	21	6	3
1961	7	2	0	17	18	18	28	23	11	10	1	2
1962	2	2	12	9	21	20	24	27	15	1	6	4
1963	1	10	6	12	12	26	18	29	7	7	5	0
1964	0	7	15	17	16	15	16	21	12	6	1	0
1965	2	0	2	4	20	19	24	22	17	5	14	8
1966	7	9	4	22	16	28	20	25	9	16	0	0
1967	4	2	0	9	22	17	20	26	21	6	3	2
1968	2	8	0	15	21	26	29	26	22	8	12	1
1969	9	14	8	8	27	24	19	26	11	2	4	2
1970	3	6	10	18	18	22	20	29	12	7	5	0
1971	5	1	4	15	18	24	19	15	8	1	4	0
1972	5	9	4	11	23	19	25	17	13	5	3	1
1973	1	2	0	12	19	14	26	14	16	8	0	3
1974	0	2	11	11	24	22	22	23	11	14	12	0
1975	0	3	3	7	14	14	24	22	3	10	4	0
1976	2	2	5	5	20	20	24	19	16	9	5	7
1977	5	7	7	7	26	25	22	24	9	10	2	2
1978	3	10	3	15	23	22	25	23	12	2	0	6
1979	5	1	5	17	16	24	22	22	5	13	5	2
1980	4	3	13	7	23	25	27	23	13	8	7	0
1981	1	0	7	7	26	22	24	19	14	7	3	6
1982	6	0	4	2	18	26	13	19	4	9	4	0
1983	0	1	3	14	21	22	17	14	13	2	3	6
1984	2	1	12	11	23	16	29	22	19	5	6	1
1985	5	2	6	7	19	22	25	26	12	2	3	5
1986	8	10	3	14	15	20	27	28	10	0	0	5
1987	5	2	9	12	21	20	24	23	11	3	4	3
1988	1	2	10	11	23	24	21	22	8	7	0	0
1989	0	0	1	17	8	16	21	18	6	6	2	3
1990	0	0	0	6	22	25	25	22	15	8	6	0
1991	2	6	7	7	14	26	26	19	7	10	2	0
1992	0	0	3	10	16	16	25	28	16	12	3	0
1993	0	0	0	13	20	23	23	24	23	9	3	3
1994	2	6	0	9	20	15	24	27	17	4	9	0
1995	1	0	1	9	19	13	21	14	16	4	6	1
1996	5	2	8	10	15	15	25	24	18	8	7	5
1997	0	0	6	3	18	24	28	19	6	6	12	11
1998	0	0	0	22	16	22	29	17	18	11	11	1
1999	5	2	6	11	19	17	19	24	14	13	1	2
2000	0	1	2	9	14	13	26	21	17	6	9	4
2001	2	4	13	9	20	20	22	25	21	11	0	2
2002	0	0	6	14	18	21	26	22	15	10	11	7
2003	2	1	0	13	21	27	30	20	10	7	7	0
2004	1	1	5	12	16	21	29	25	3	10	4	0
2005	0	7	8	11	16	19	21	15	4	5	2	4
2006	1	0	7	11	18	20	20	25	12	8	2	0
2007	0	5	1	6	15	27	24	16	3	3	0	0
2008	2	0	5	14	25	19	22	21	8	1	1	5
2009	0	4	2	10	13	23	18	18	3	9	5	4
2010	7	8	5	8	23	22	15	23	19	1	14	5
2011	3	0	1	4	17	19	23	22	10	0	3	1
2012	2	0	0	11	11	24	23	23	11	13	3	12
2013	3	3	11	6	19	25	15	20	14	3	0	0
Min	0	0	0	2	8	13	13	14	3	0	0	0
Mean	3	3	5	11	19	21	23	22	12	7	5	3
Median	2	2	5	10.5	19	22	24	22	12	7	4	2
Max	9	14	20	22	27	28	30	29	23	21	14	12

Table 0-3: Total no. of windows available for the significant wave height from year 1958 to 2013 in month wise, duration 24 hours, Hs=2 m

Year	No. Of Windows for Hs = 2 m, Duration = 48 hours											
	Jan	Feb	Mar	Apr	May	Jun	Jul	Aug	Sep	Oct	Nov	Dec
1958	2	3	10	2	5	12	10	13	6	1	0	4
1959	0	0	2	3	8	6	11	8	3	5	2	1
1960	1	0	6	3	11	9	13	10	8	9	1	1
1961	2	0	0	7	7	8	13	10	4	4	0	0
1962	0	0	6	4	9	8	11	13	5	0	2	1
1963	0	4	1	4	5	13	7	14	2	2	1	0
1964	0	2	5	5	8	7	7	10	5	3	0	0
1965	0	0	1	1	9	7	12	10	7	2	6	2
1966	2	3	1	10	6	13	8	11	4	7	0	0
1967	1	0	0	4	10	8	9	13	9	2	1	0
1968	0	3	0	5	9	12	14	12	11	3	5	0
1969	3	6	3	2	13	11	8	12	4	1	1	1
1970	0	3	4	8	7	9	9	14	5	3	1	0
1971	1	0	1	5	7	11	8	7	4	0	1	0
1972	1	4	1	4	11	8	11	7	6	1	1	0
1973	0	0	0	5	7	6	12	6	5	3	0	0
1974	0	0	3	4	10	9	11	10	3	5	5	0
1975	0	1	1	2	5	5	9	9	1	4	0	0
1976	0	0	2	1	9	8	11	8	7	3	1	2
1977	1	2	3	2	12	11	9	11	3	3	0	0
1978	1	3	1	6	10	9	12	11	6	0	0	2
1979	1	0	2	7	5	11	10	11	1	6	1	0
1980	0	0	6	2	10	10	13	10	5	2	1	0
1981	0	0	3	2	11	10	10	7	5	2	1	1
1982	3	0	1	0	8	12	6	8	1	3	1	0
1983	0	0	1	6	10	10	7	5	6	0	1	2
1984	0	0	5	4	11	5	13	10	9	2	2	0
1985	2	1	2	2	9	9	11	12	4	0	1	1
1986	3	5	1	6	5	8	12	13	4	0	0	2
1987	1	0	3	5	9	8	11	10	3	1	1	0
1988	0	1	3	5	11	11	9	10	2	2	0	0
1989	0	0	0	6	2	7	8	8	1	1	1	1
1990	0	0	0	3	9	12	12	9	7	4	3	0
1991	0	2	1	2	4	11	11	9	3	4	1	0
1992	0	0	1	4	7	7	12	14	6	4	1	0
1993	0	0	0	6	8	10	9	12	10	4	1	1
1994	0	2	0	4	9	6	11	12	7	1	4	0
1995	0	0	0	4	7	5	9	6	7	0	1	0
1996	2	0	4	3	5	5	12	11	8	3	2	0
1997	0	0	2	1	8	11	14	9	2	2	6	4
1998	0	0	0	10	6	10	14	6	7	4	5	0
1999	1	0	2	4	7	7	8	11	5	5	0	0
2000	0	0	1	3	4	4	13	8	7	1	3	2
2001	0	0	6	3	8	8	9	11	9	4	0	0
2002	0	0	2	5	7	10	12	9	6	3	5	3
2003	1	0	0	6	10	12	15	9	3	1	2	0
2004	0	0	1	4	7	8	13	12	0	4	1	0
2005	0	3	3	5	7	7	9	5	1	2	0	0
2006	0	0	1	4	7	8	9	12	3	2	0	0
2007	0	1	0	1	7	13	11	7	0	1	0	0
2008	1	0	1	5	11	7	9	10	3	0	0	2
2009	0	1	0	2	5	10	8	6	0	3	1	1
2010	2	4	1	3	10	9	6	10	9	0	5	1
2011	1	0	0	2	8	8	10	11	4	0	0	0
2012	1	0	0	4	4	11	10	11	5	5	1	4
2013	0	0	4	3	8	10	5	9	6	0	0	0
Min	0	0	0	0	2	4	5	5	0	0	0	0
Mean	1	1	2	4	8	9	10	10	5	2	1	1
Median	0	0	1	4	8	9	10.5	10	5	2	1	0
Max	3	6	10	10	13	13	15	14	11	9	6	4

Table 0-4: Total no. of windows available for the significant wave height from year 1958 to 2013 in month wise, duration 48 hours, Hs=2 m

Installation Analyses of A Subsea Structure

Year	No. Of Windows for Hs = 2 m, Duration = 72 hours											
	Jan	Feb	Mar	Apr	May	Jun	Jul	Aug	Sep	Oct	Nov	Dec
1958	1	1	6	1	3	7	5	7	4	0	0	2
1959	0	0	1	2	4	2	6	4	2	2	0	1
1960	1	0	3	2	7	6	9	5	5	6	1	0
1961	1	0	0	5	3	5	9	6	2	2	0	0
1962	0	0	2	1	6	5	6	8	3	0	2	1
1963	0	3	1	2	2	7	4	9	1	1	1	0
1964	0	0	3	4	4	4	4	5	2	2	0	0
1965	0	0	0	1	5	4	6	5	4	1	3	0
1966	1	0	0	7	3	9	4	5	2	3	0	0
1967	1	0	0	3	6	5	4	8	5	0	0	0
1968	0	2	0	4	6	7	9	7	6	0	3	0
1969	1	4	2	1	6	7	3	8	3	0	0	0
1970	0	0	1	5	4	5	5	9	3	0	1	0
1971	0	0	0	3	4	7	5	3	1	0	1	0
1972	0	1	1	2	6	5	6	4	3	1	0	0
1973	0	0	0	1	4	3	8	3	3	1	0	0
1974	0	0	3	2	7	6	6	6	3	2	3	0
1975	0	1	1	1	4	3	6	6	0	1	0	0
1976	0	0	0	0	4	5	6	5	4	2	1	1
1977	0	1	1	2	6	7	5	7	2	2	0	0
1978	0	2	0	2	6	6	7	7	2	0	0	0
1979	1	0	0	4	2	6	6	7	0	3	1	0
1980	0	0	2	1	6	6	8	6	3	2	0	0
1981	0	0	1	1	7	6	7	4	3	1	0	0
1982	2	0	1	0	4	8	2	4	0	1	1	0
1983	0	0	0	2	5	7	4	3	2	0	0	1
1984	0	0	1	2	7	2	8	5	5	1	1	0
1985	0	0	2	1	4	6	6	8	2	0	0	0
1986	1	2	0	2	2	4	8	8	2	0	0	1
1987	1	0	1	2	4	5	7	5	2	0	0	0
1988	0	0	1	2	7	7	5	6	0	1	0	0
1989	0	0	0	4	0	3	4	3	1	0	0	0
1990	0	0	0	1	6	7	8	5	4	1	0	0
1991	0	1	0	1	2	7	6	4	2	2	0	0
1992	0	0	0	2	4	4	7	9	3	2	0	0
1993	0	0	0	3	5	6	6	5	5	1	1	0
1994	0	1	0	2	6	3	6	8	3	1	1	0
1995	0	0	0	2	5	3	5	2	4	0	1	0
1996	1	0	1	2	1	2	7	6	5	1	1	0
1997	0	0	1	1	3	6	9	4	1	1	3	2
1998	0	0	0	5	4	6	9	3	4	1	3	0
1999	1	0	0	2	4	4	5	7	4	3	0	0
2000	0	0	0	2	3	1	8	6	4	1	3	1
2001	0	0	3	2	6	5	6	7	4	2	0	0
2002	0	0	1	3	4	5	7	6	3	1	2	1
2003	0	0	0	3	5	8	9	5	2	1	1	0
2004	0	0	1	2	4	4	9	6	0	1	1	0
2005	0	1	2	2	2	4	6	4	0	0	0	0
2006	0	0	0	1	5	5	6	7	2	1	0	0
2007	0	1	0	1	4	8	6	4	0	0	0	0
2008	0	0	1	3	6	5	6	6	1	0	0	1
2009	0	0	0	1	3	5	5	4	0	2	0	0
2010	1	0	0	1	6	5	2	6	6	0	3	1
2011	0	0	0	0	5	5	5	5	0	0	0	0
2012	0	0	0	3	0	7	6	6	3	2	0	3
2013	0	0	2	0	4	6	3	6	3	0	0	0

Table 0-5: Total no. of windows available for the significant wave height from year 1958 to 2013 in month wise, duration 72 hours, Hs=2 m

Appendix -4: Duration to complete a operation in Month wise

Year	No. of days to complete a operation (Hs <= 2 m, Duration = 72 hours) starting at first day of a month											
	Jan	Feb	Mar	Apr	May	Jun	Jul	Aug	Sep	Oct	Nov	Dec
1958	3.0	8.5	12.5	3.3	5.8	3.0	3.0	9.0	3.0	0.0	0.0	17.4
1959	0.0	0.0	27.4	12.6	11.6	22.9	3.0	7.1	19.3	8.4	0.0	13.0
1960	13.0	0.0	12.6	3.0	4.6	4.8	3.0	3.0	4.9	3.0	21.3	0.0
1961	23.0	0.0	0.0	3.0	15.9	3.0	4.3	4.6	8.8	3.9	0.0	0.0
1962	0.0	0.0	23.9	19.4	3.0	5.4	5.8	3.0	3.0	0.0	10.3	30.6
1963	0.0	9.0	20.3	17.4	22.1	3.0	3.0	3.4	4.6	30.8	5.3	0.0
1964	0.0	0.0	5.3	3.0	19.6	10.6	6.1	4.4	4.9	14.5	0.0	0.0
1965	0.0	0.0	0.0	22.8	3.0	4.5	7.6	4.3	5.1	3.0	10.6	0.0
1966	14.6	0.0	0.0	4.3	8.5	3.0	7.3	3.0	4.4	10.9	0.0	0.0
1967	7.0	0.0	0.0	8.6	3.6	3.0	3.8	3.0	3.0	0.0	0.0	0.0
1968	0.0	3.8	0.0	16.4	3.9	3.5	4.5	5.9	3.9	0.0	8.5	0.0
1969	22.4	16.9	20.0	24.3	6.4	3.0	9.1	3.0	4.6	0.0	0.0	0.0
1970	0.0	0.0	9.6	4.5	5.8	7.4	3.0	3.5	13.8	0.0	15.6	0.0
1971	0.0	0.0	0.0	5.9	3.0	3.0	3.0	3.0	27.9	0.0	21.9	0.0
1972	0.0	8.3	9.3	9.3	3.0	7.1	3.0	3.0	13.1	28.6	0.0	0.0
1973	0.0	0.0	0.0	21.6	6.5	17.6	7.5	3.9	6.5	7.8	0.0	0.0
1974	0.0	0.0	12.4	25.1	6.5	9.3	3.0	3.0	3.0	3.9	3.0	0.0
1975	0.0	11.4	29.5	15.5	10.1	4.6	8.0	7.0	0.0	16.5	0.0	0.0
1976	0.0	0.0	0.0	0.0	3.1	3.0	4.1	4.0	14.4	3.0	10.3	11.4
1977	0.0	25.9	20.4	10.4	3.0	10.1	4.5	3.0	11.8	8.4	0.0	0.0
1978	0.0	9.4	0.0	22.9	3.0	3.0	3.0	3.0	3.0	0.0	0.0	0.0
1979	23.5	0.0	0.0	5.0	9.1	4.8	6.0	5.9	0.0	3.0	14.1	0.0
1980	0.0	0.0	24.5	27.1	3.0	3.0	3.0	3.0	10.9	14.0	0.0	0.0
1981	0.0	0.0	3.4	26.8	3.4	3.0	5.8	8.8	3.0	23.1	0.0	0.0
1982	4.3	0.0	20.0	0.0	16.0	3.5	3.0	3.0	0.0	11.6	28.9	0.0
1983	0.0	0.0	0.0	12.9	3.0	3.0	9.0	3.0	10.5	0.0	0.0	18.9
1984	0.0	0.0	26.0	7.0	3.0	4.5	3.0	5.5	4.1	4.9	18.5	0.0
1985	0.0	0.0	17.6	11.4	5.4	7.4	3.6	3.0	3.0	0.0	0.0	0.0
1986	3.0	3.0	0.0	16.9	7.9	18.5	3.0	3.0	13.0	0.0	0.0	23.0
1987	13.9	0.0	10.8	5.4	12.1	3.0	8.1	9.3	8.0	0.0	0.0	0.0
1988	0.0	0.0	6.4	24.6	3.0	4.4	7.9	4.1	0.0	21.3	0.0	0.0
1989	0.0	0.0	0.0	5.0	0.0	3.8	18.8	7.0	15.5	0.0	0.0	0.0
1990	0.0	0.0	0.0	5.8	6.1	6.6	3.0	10.0	3.0	25.0	0.0	0.0
1991	0.0	11.5	0.0	27.3	7.1	3.8	7.5	3.0	9.1	14.8	0.0	0.0
1992	0.0	0.0	0.0	3.1	20.8	3.0	3.0	3.4	19.6	3.0	0.0	0.0
1993	0.0	0.0	0.0	3.4	8.9	5.3	11.6	3.0	8.4	3.0	4.4	0.0
1994	0.0	23.1	0.0	10.0	11.9	19.0	4.6	3.0	3.0	30.4	9.5	0.0
1995	0.0	0.0	0.0	23.8	11.5	5.3	10.5	3.0	3.0	0.0	28.8	0.0
1996	24.0	0.0	17.9	13.9	23.0	16.5	3.6	7.6	5.9	18.8	20.9	0.0
1997	0.0	0.0	21.8	27.4	16.6	5.4	4.9	7.1	3.0	10.9	14.0	22.5
1998	0.0	0.0	0.0	3.3	11.0	3.5	3.0	8.5	3.0	5.8	3.8	0.0
1999	10.8	0.0	0.0	22.4	3.0	8.6	3.0	3.0	15.3	17.1	0.0	0.0
2000	0.0	0.0	0.0	3.6	15.4	26.3	4.6	3.0	5.1	3.0	6.4	28.9
2001	0.0	0.0	3.0	24.3	7.3	15.1	5.5	4.8	14.6	7.0	0.0	0.0
2002	0.0	0.0	15.1	5.4	6.4	5.1	3.0	3.1	9.5	6.5	16.4	14.8
2003	0.0	0.0	0.0	18.3	3.0	3.0	5.6	7.3	9.4	15.0	17.0	0.0
2004	0.0	0.0	25.0	21.6	8.6	3.0	3.0	3.0	0.0	16.8	23.3	0.0
2005	0.0	23.3	27.1	23.9	9.1	3.0	3.0	3.0	0.0	0.0	0.0	0.0
2006	0.0	0.0	0.0	19.9	6.9	6.8	4.9	3.0	3.0	6.6	0.0	0.0
2007	0.0	8.5	0.0	30.0	3.0	3.0	3.0	8.8	0.0	0.0	0.0	0.0
2008	0.0	0.0	28.1	12.9	3.0	3.0	3.4	6.6	6.8	0.0	0.0	4.8
2009	0.0	0.0	0.0	28.0	15.8	7.6	3.0	3.4	0.0	24.5	0.0	0.0
2010	13.9	0.0	0.0	22.5	6.5	6.5	25.0	3.1	3.0	0.0	15.8	25.5
2011	0.0	0.0	0.0	0.0	3.0	7.4	9.4	3.0	0.0	0.0	0.0	0.0
2012	0.0	0.0	0.0	15.9	0.0	6.6	3.0	4.3	20.4	11.8	0.0	7.6
2013	0.0	0.0	14.8	0.0	11.6	8.0	12.3	3.0	8.4	0.0	0.0	0.0

Table 0-1: Number of days to complete an operation (Hs<=2m, Duration =72 hours) starting at the first day of a month

Year	No. Of Windows for $H_s \leq 2$ m, Duration = 48 hours, 24 hours											
	Jan	Feb	Mar	Apr	May	Jun	Jul	Aug	Sep	Oct	Nov	Dec
1958	3.0	8.5	12.5	3.3	5.8	3.0	3.0	4.9	3.0	0.0	0.0	17.4
1959	0.0	0.0	25.4	12.6	5.8	5.5	3.0	5.1	4.1	8.4	23.3	13.0
1960	13.0	0.0	12.6	3.0	4.6	4.8	3.0	3.0	4.9	3.0	21.3	0.0
1961	8.1	0.0	0.0	3.0	13.9	3.0	4.3	4.6	6.8	3.9	0.0	0.0
1962	0.0	0.0	13.1	19.4	3.0	5.4	5.8	3.0	3.0	0.0	10.3	30.6
1963	0.0	9.0	20.3	7.9	20.1	3.0	3.0	3.4	4.6	14.4	5.3	0.0
1964	0.0	23.3	5.3	3.0	17.6	8.6	6.1	4.4	4.9	14.5	0.0	0.0
1965	0.0	0.0	0.0	22.8	3.0	4.5	5.6	4.3	5.1	3.0	10.6	8.9
1966	14.6	13.4	29.8	4.3	6.5	3.0	5.3	3.0	4.4	10.9	0.0	0.0
1967	7.0	0.0	0.0	8.6	3.6	3.0	3.8	3.0	3.0	10.9	7.0	0.0
1968	0.0	3.8	0.0	16.4	3.9	3.5	4.5	3.9	3.9	18.1	8.5	0.0
1969	20.4	16.9	20.0	24.3	4.4	3.0	7.1	3.0	4.6	0.0	15.1	0.0
1970	0.0	17.0	9.6	4.5	5.8	7.4	3.0	3.5	13.8	13.0	15.6	0.0
1971	17.1	0.0	27.5	5.9	3.0	3.0	3.0	3.0	14.0	0.0	21.9	0.0
1972	8.6	6.3	9.3	9.3	3.0	5.1	3.0	3.0	13.1	28.6	0.0	0.0
1973	0.0	0.0	0.0	11.8	6.5	17.6	5.5	3.9	6.5	7.8	0.0	0.0
1974	0.0	0.0	12.4	23.1	6.5	9.3	3.0	3.0	3.0	3.9	3.0	0.0
1975	0.0	11.4	29.5	15.5	10.1	4.6	8.0	7.0	0.0	14.5	0.0	0.0
1976	0.0	0.0	14.1	27.0	3.1	3.0	4.1	4.0	14.4	3.0	10.3	11.4
1977	21.3	16.5	18.4	10.4	3.0	10.1	4.5	3.0	11.8	8.4	0.0	0.0
1978	29.9	9.4	0.0	11.4	3.0	3.0	3.0	3.0	3.0	0.0	0.0	9.1
1979	23.5	0.0	23.0	5.0	9.1	4.8	6.0	5.9	7.9	3.0	14.1	0.0
1980	0.0	0.0	17.8	27.1	3.0	3.0	3.0	3.0	8.9	14.0	25.9	0.0
1981	0.0	0.0	3.4	26.8	3.4	3.0	5.8	6.8	3.0	21.1	29.5	19.3
1982	4.3	0.0	20.0	0.0	14.0	3.5	3.0	3.0	13.6	9.6	28.9	0.0
1983	0.0	0.0	0.0	7.1	3.0	3.0	7.0	3.0	4.4	0.0	26.5	18.9
1984	0.0	0.0	16.0	7.0	3.0	4.5	3.0	5.5	4.1	4.9	8.1	0.0
1985	14.5	0.0	17.6	11.4	5.4	7.4	3.6	3.0	3.0	0.0	0.0	10.3
1986	3.0	3.0	30.0	5.1	5.9	11.1	3.0	3.0	13.0	0.0	0.0	23.0
1987	13.9	0.0	10.8	5.4	3.6	3.0	6.1	7.3	8.0	0.0	25.3	0.0
1988	0.0	0.0	6.4	13.8	3.0	4.4	7.9	4.1	21.5	19.3	0.0	0.0
1989	0.0	0.0	0.0	5.0	14.1	3.8	7.6	5.0	15.5	0.0	0.0	0.0
1990	0.0	0.0	0.0	5.8	6.1	4.6	3.0	6.5	3.0	19.3	21.1	0.0
1991	0.0	11.5	0.0	27.3	7.1	3.8	3.3	3.0	9.1	14.8	0.0	0.0
1992	0.0	0.0	24.5	3.1	18.8	3.0	3.0	3.4	17.6	3.0	0.0	0.0
1993	0.0	0.0	0.0	3.4	4.9	5.3	11.6	3.0	6.4	3.0	4.4	0.0
1994	0.0	23.1	0.0	10.0	9.9	6.6	4.6	3.0	3.0	30.4	7.5	0.0
1995	0.0	0.0	0.0	23.8	11.5	5.3	8.5	3.0	3.0	0.0	28.8	0.0
1996	24.0	0.0	17.9	11.9	5.4	16.5	3.6	5.6	5.9	16.8	18.9	0.0
1997	0.0	0.0	21.8	27.4	11.0	5.4	4.9	5.1	3.0	10.9	12.0	17.9
1998	0.0	0.0	0.0	3.3	11.0	3.5	3.0	6.5	3.0	3.8	3.8	0.0
1999	10.8	0.0	9.8	4.4	3.0	8.6	3.0	3.0	15.3	15.1	0.0	0.0
2000	0.0	0.0	0.0	3.6	15.4	8.6	4.6	3.0	5.1	3.0	6.4	28.9
2001	0.0	0.0	3.0	24.3	7.3	15.1	3.5	4.8	4.4	7.0	0.0	0.0
2002	0.0	0.0	15.1	5.4	6.4	5.1	3.0	3.1	7.5	4.5	14.4	14.8
2003	0.0	0.0	0.0	16.3	3.0	3.0	3.6	7.3	9.4	15.0	17.0	0.0
2004	0.0	0.0	25.0	21.6	8.6	3.0	3.0	3.0	0.0	14.8	23.3	0.0
2005	0.0	23.3	27.1	18.8	7.1	3.0	3.0	3.0	10.1	23.1	0.0	0.0
2006	0.0	0.0	15.6	4.9	6.9	6.8	4.9	3.0	3.0	6.6	0.0	0.0
2007	0.0	8.5	0.0	30.0	3.0	3.0	3.0	8.8	0.0	0.0	0.0	0.0
2008	0.0	0.0	28.1	10.9	3.0	3.0	3.4	6.6	6.8	0.0	0.0	4.8
2009	0.0	15.1	0.0	28.0	15.8	7.6	3.0	3.4	0.0	24.5	12.3	0.0
2010	11.9	16.9	0.0	10.0	6.5	6.5	6.6	3.1	3.0	0.0	13.8	25.5
2011	13.1	0.0	0.0	29.0	3.0	7.4	4.3	3.0	3.9	0.0	0.0	0.0
2012	0.0	0.0	0.0	15.9	8.1	6.6	3.0	4.3	20.4	11.8	28.3	7.6
2013	0.0	0.0	14.8	7.9	7.9	6.0	12.3	3.0	8.4	0.0	0.0	0.0

Table 0-2: Number of days to complete the operations ($H_s \leq 2$ m, Duration = 48 hours + 24 hours) starting at the first day of a month

Year	No. Of Windows for Hs <= 2 m, Duration = 24+24+24 hours											
	Jan	Feb	Mar	Apr	May	Jun	Jul	Aug	Sep	Oct	Nov	Dec
1958	3.0	8.5	12.5	3.3	5.8	3.0	3.0	4.9	3.0	14.8	0.0	15.4
1959	0.0	0.0	25.4	12.6	5.8	5.5	3.0	5.1	4.1	6.4	23.3	13.0
1960	13.0	0.0	12.6	3.0	4.6	3.8	3.0	3.0	4.9	3.0	19.3	21.8
1961	5.8	0.0	0.0	3.0	6.5	3.0	4.3	3.6	6.8	3.9	0.0	0.0
1962	0.0	0.0	13.1	19.4	3.0	4.4	4.8	3.0	3.0	0.0	10.3	29.6
1963	0.0	9.0	18.3	7.9	11.1	3.0	3.0	3.4	3.6	7.0	4.3	0.0
1964	0.0	16.9	5.3	3.0	17.6	8.6	5.1	4.4	4.9	14.5	0.0	0.0
1965	0.0	0.0	0.0	22.8	3.0	4.5	5.6	4.3	4.1	3.0	10.6	5.4
1966	13.6	10.8	25.8	4.3	6.5	3.0	5.3	3.0	4.4	9.9	0.0	0.0
1967	7.0	0.0	0.0	8.6	3.6	3.0	3.8	3.0	3.0	8.0	7.0	0.0
1968	0.0	3.8	0.0	12.5	3.9	3.5	4.5	3.9	3.9	16.4	7.5	0.0
1969	12.1	14.9	19.0	22.3	4.4	3.0	7.1	3.0	4.6	0.0	15.1	0.0
1970	30.3	17.0	8.6	4.5	4.8	6.4	3.0	3.5	11.8	8.4	14.6	0.0
1971	15.4	0.0	22.1	4.9	3.0	3.0	3.0	3.0	14.0	0.0	20.9	0.0
1972	6.5	6.3	9.3	8.3	3.0	5.1	3.0	3.0	12.1	26.6	22.6	0.0
1973	0.0	0.0	0.0	11.8	6.5	16.6	5.5	3.9	5.5	7.8	0.0	23.8
1974	0.0	0.0	11.4	15.8	5.5	7.3	3.0	3.0	3.0	3.9	3.0	0.0
1975	0.0	11.4	29.5	13.5	9.1	3.6	7.0	6.0	12.6	10.0	18.1	0.0
1976	0.0	0.0	14.1	22.9	3.1	3.0	4.1	4.0	13.4	3.0	9.3	11.4
1977	16.9	14.6	18.4	10.4	3.0	4.9	4.5	3.0	10.8	8.4	0.0	0.0
1978	29.9	7.4	4.1	4.0	3.0	3.0	3.0	3.0	3.0	0.0	0.0	5.6
1979	22.5	0.0	23.0	5.0	8.1	3.8	6.0	5.9	6.4	3.0	13.1	0.0
1980	8.9	11.5	15.8	25.1	3.0	3.0	3.0	3.0	4.9	14.0	10.0	0.0
1981	0.0	0.0	3.4	16.1	3.4	3.0	4.8	6.8	3.0	21.1	29.5	13.3
1982	4.3	0.0	20.0	0.0	8.9	3.5	3.0	3.0	13.6	7.9	27.9	0.0
1983	0.0	0.0	24.4	5.1	3.0	3.0	7.0	3.0	4.4	0.0	26.5	18.9
1984	0.0	0.0	13.5	7.0	3.0	3.5	3.0	4.5	4.1	4.9	8.1	0.0
1985	14.5	0.0	17.6	11.4	5.4	6.4	3.6	3.0	3.0	0.0	22.4	6.8
1986	3.0	3.0	30.0	5.1	5.9	5.1	3.0	3.0	12.0	0.0	0.0	23.0
1987	11.9	0.0	9.8	5.4	3.6	3.0	3.3	3.8	7.0	22.0	25.3	19.3
1988	0.0	0.0	5.4	13.8	3.0	4.4	6.9	4.1	6.0	13.8	0.0	0.0
1989	0.0	0.0	0.0	5.0	11.9	3.8	5.1	5.0	13.5	19.1	0.0	14.4
1990	0.0	0.0	0.0	5.8	6.1	4.6	3.0	4.9	3.0	19.3	21.1	0.0
1991	0.0	10.5	6.5	25.3	5.1	3.8	3.3	3.0	9.1	12.8	0.0	0.0
1992	0.0	0.0	24.5	3.1	12.6	3.0	3.0	3.4	14.5	3.0	15.9	0.0
1993	0.0	0.0	0.0	3.4	4.9	4.3	8.0	3.0	3.9	3.0	4.4	26.6
1994	0.0	22.1	0.0	10.0	9.9	6.6	4.6	3.0	3.0	29.4	7.5	0.0
1995	0.0	0.0	0.0	22.8	9.5	4.3	8.5	3.0	3.0	28.0	10.8	0.0
1996	24.0	0.0	17.9	7.4	5.4	10.0	3.6	5.6	5.9	16.8	12.0	22.3
1997	0.0	0.0	20.8	27.4	11.0	4.4	4.9	5.1	3.0	10.9	12.0	12.0
1998	0.0	0.0	0.0	3.3	9.0	3.5	3.0	6.5	3.0	3.8	3.8	0.0
1999	10.8	0.0	9.8	4.4	3.0	7.6	3.0	3.0	14.3	9.0	0.0	0.0
2000	0.0	0.0	0.0	3.6	13.4	5.9	4.6	3.0	4.1	3.0	6.4	28.9
2001	0.0	24.8	3.0	22.3	6.3	10.0	3.5	4.8	4.4	7.0	0.0	0.0
2002	0.0	0.0	15.1	4.4	6.4	4.1	3.0	3.1	7.5	4.5	14.4	13.8
2003	0.0	0.0	0.0	13.5	3.0	3.0	3.6	7.3	8.4	13.0	15.0	0.0
2004	0.0	0.0	23.0	18.0	8.6	3.0	3.0	3.0	29.3	9.4	23.3	0.0
2005	0.0	22.3	25.1	18.8	7.1	3.0	3.0	3.0	7.1	23.1	0.0	26.1
2006	0.0	0.0	10.6	4.9	6.9	5.8	4.9	3.0	3.0	5.6	0.0	0.0
2007	0.0	8.5	0.0	23.5	3.0	3.0	3.0	8.8	9.0	5.3	0.0	0.0
2008	0.0	0.0	26.1	9.0	3.0	3.0	3.4	6.6	6.8	0.0	0.0	4.8
2009	0.0	7.4	0.0	14.0	13.8	6.6	3.0	3.4	14.0	22.5	10.0	23.9
2010	7.4	16.9	16.4	4.9	5.5	5.5	6.6	3.1	3.0	0.0	13.8	23.5
2011	13.1	0.0	0.0	29.0	3.0	7.4	4.3	3.0	3.9	0.0	18.8	0.0
2012	0.0	0.0	0.0	15.9	6.4	5.6	3.0	4.3	20.4	9.8	28.3	6.6
2013	20.8	22.6	13.8	7.9	7.9	3.9	11.3	3.0	8.4	26.5	0.0	0.0

Table 0-3: Number of days to complete the operations (Hs<=2m, Duration =24 + 24+24 hours) starting at the first day of a month

Appendix -5: Matlab Scripts

(Pages 39)

```

%------%
%Jonswap Spectrum
%------%
function [w,specJ,M0,M2,del_w]=Jonswap(Hs,Tp,gamma)

T= 60:-0.5:3.5; % Time in seconds

wp=2*pi()/Tp; %angular spectral peak frequency [rad/s]

w=2.*pi()./T; % angular frequency [rad/s]

f=w./(2.*pi()); % wave frequency [Hz]

%-----Pierson-Moskowitz spectrum-----%
specPM=(5/16)*(Hs^2)*(wp^4).*(w.^-5).*exp((-5/4).*(w/wp).^-4);
%------%

%-----input for Jonswap-----%
Agamma= 1-0.287*log(gamma);
sigma_a=0.07; sigma_b=0.09; %spectral width parameter
if w<=wp,
    sigma=sigma_a;
else
    sigma=sigma_b;
end

%-----Jonswap Spectrum-----%
specJ=Agamma.*specPM.*gamma.^exp(-0.5.*((w-wp)./(sigma*wp)).^2);
specJ_f=specJ.*2*pi();
%------%

% % xlsxwrite('motion.xlsx','w','spectrum','A1:A34');
% % xlsxwrite('motion.xlsx',specJ,'spectrum','B1:B34');
% % xlsxwrite('motion.xlsx','f','spectrum','C1:C34');
% % xlsxwrite('motion.xlsx',specJ_f,'spectrum','D1:D34');
% Angular_frequency = w';
% spectrum_rad=specJ';
% wave_frequency=f';
% spectrum_HZ=specJ_f';
% time_period=T';
% SpecTable=table(time_period,Angular_frequency,spectrum_rad,wave_frequency,spectrum_HZ);
% writetable(SpecTable,'spectrum.xlsx');
% % plot(w,specJ);
% % hold on
% % plot(w,specPM,'--')
% % hold off
% % legend ('specJ','specPM')
% % plot(f,specJ_f);
%------%
%Zero moment = variance of the spectrum
del_w = ( w(1,length(w)) - w(1,1) ) ./ (length(w)-1);

M0=sum(specJ.*del_w);
M1=sum(w.*specJ.*del_w);
M2=sum(w.^2.*specJ.*del_w);

end

```

```

%-----%
%Combined sea Spectrum
%-----%
function [w,specJ, specJw, specJs, M0,M2,del_w]=Jonswap_cross(Hs,Tp)

af=6.6; % for the fetch length of 370 km
Tpf=af*Hs^(1/3);

if Tp <=Tpf

T= 60:-0.5:3.5; % Time in seconds

wp=2*pi()/Tp; %angular spectral peak frequency [rad/s]

w=2.*pi()./T; % angular frequency [rad/s]

f=w./(2.*pi()); % wave frequency [Hz]

%-----%
%Primary Peak
a1=0.5;
a10=0.7;
ae=2;
Tl=ae*Hs^(1/2);
if Tp<Tl
    epl=1;
else
    epl=(Tpf-Tp)/(Tpf-Tl);
end

Rw= ((1-a10)*exp(-(epl/a1)^2 )) + a10;

Hw1=Rw*Hs;
Tpw1=Tp;

g=9.81;
sp=(2*pi()/g) * Hw1/Tpw1^2;
kg=35;
gammaw= kg*sp^(6/7);

[~,specJw,~,~,~]=Jonswap(Hw1,Tpw1, gammaw);

%-----%
%Secondary Peak
Hw2=((1-Rw^2)^(1/2))*Hs;
b1=2;
Tpw2=Tpf+b1;
gammass=1;

[~,specJs,~,~,~]=Jonswap(Hw2,Tpw2, gammass);

else
%-----%
% swell dominated sea

T= 60:-0.5:3.5; % Time in seconds

wp=2*pi()/Tp; %angular spectral peak frequency [rad/s]

w=2.*pi()./T; % angular frequency [rad/s]

f=w./(2.*pi()); % wave frequency [Hz]

    au=25;

```

```

Tu=au;
if Tp>Tu
    epu=1;
else
epu=(Tp-Tpf)/(Tu-Tpf);
end

a2=0.3;
a20=0.6;
Rs=((1-a20)*exp(-(epu/a2)^2 )) + a20;
Hs1=Rs*Hs;
Tps1=Tp;

g=9.81;
sf=(2*pi()/g)*Hs/Tpf^2;
kg=35;
gammaf=kg*sf^(6/7);
a3=6;
gamma1= gammaf *(1+a3*epu);

[~,specJs,~,~,~]=Jonswap(Hs1,Tps1, gamma1);

```

```

%-----%

```

```

%Secondary Peak

```

```

Hs2=((1-Rs^2)^(1/2))*Hs;
af=6.6;
Tps2=af*Hs2^(1/3);
gamma2=1;
[~,specJw,~,~,~]=Jonswap(Hs2,Tps2, gamma2);

```

```

end

```

```

specJ=specJw+specJs;
plot(w,specJs);
plot(w/(2*pi()), specJ.*2*pi());
hold on
plot(w/(2*pi()), specJw.*2*pi(), '-');
hold on
plot(w/(2*pi()), specJs.*2*pi(), '*');
hold off

```

```

%-----%

```

```

%Zero moment = variance of the spectrum

```

```

del_w = ( w(1,length(w)) - w(1,1) ) ./ (length(w)-1);

```

```

M0=sum(specJ.*del_w);
M1=sum(w.*specJ.*del_w);
M2=sum(w.^2.*specJ.*del_w);

```

```

end

```

```
%-----%
```

```
%comparing heave at a point having equal distance from cog at forward and  
%aft of vessel
```

```
%-----%
```

```
%calculating heave at a point 76 m from cog towards aft in the centre line
```

```
[w, heave_amp_aft_180,~] = cranetip ( -76, 0, 13 );
```

```
[w, heave_amp_aft_0, ~] = cranetip ( -76, 0, 1 );
```

```
%calculating heave at a point 76 m from cog towards fwd in the centre line
```

```
[w, heave_amp_fwd_180, ~] = cranetip ( 76, 0, 13 );
```

```
[w, heave_amp_fwd_0, ~] = cranetip ( 76, 0, 1 );
```

```
%calculating heave at cog
```

```
[w, heave_amp_cog_0, Hfd_amp] = cranetip ( 0, 0, 1 );
```

```
[w, heave_amp_cog_180, Hfd_amp] = cranetip ( 0, 0, 13 );
```

```
%plotting
```

```
freq_rad = w;
```

```
freq_HZ=2.*pi() .\ freq_rad;
```

```
%-----%
```

```
subplot(2,1,1);
```

```
plot (freq_HZ, heave_amp_aft_180,...
```

```
freq_HZ, heave_amp_fwd_180, '-','...'
```

```
freq_HZ, heave_amp_cog_180, '--', 'LineWidth', 2);
```

```
legend ('aft point head sea', 'fwd point head sea', 'at cog head sea');
```

```
grid;
```

```
title ('Heave Amplitude at points having equal distance from CoG at forward and aft of vessel', 'FontSize', 10, 'FontWeight', 'bold');
```

```
xlabel ('Frequency, f [Hz]', 'FontSize', 10, 'FontWeight', 'bold');
```

```
ylabel ('Heave amplitude, [m/m]', 'FontSize', 10, 'FontWeight', 'bold');
```

```
axis( [0 0.3 0 1.8]);
```

```
%-----%
```

```
subplot(2,1,2);
```

```
plot (freq_HZ, heave_amp_aft_0,'-',...
```

```
freq_HZ, heave_amp_fwd_0,'-',...
```

```
freq_HZ, heave_amp_cog_0,'--', 'LineWidth', 2);
```

```
legend ('aft point 0 deg sea', 'fwd point 0 deg sea', 'at cog 0 deg sea');
```

```
grid;
```

```
title ('Heave Amplitude at points having equal distance from CoG at forward and aft of vessel', 'FontSize', 10, 'FontWeight', 'bold');
```

```
xlabel ('Frequency, f [Hz]', 'FontSize', 10, 'FontWeight', 'bold');
```

```
ylabel ('Heave amplitude, [m/m]', 'FontSize', 10, 'FontWeight', 'bold');
```

```
axis( [0 0.3 0 1.8]);
```

```

%-----%
%Crane tip motion and dynamic tension transfer functions
%-----%
function [w, Htz_amp, Hfd_amp,Hfdm_amp,Htz_phase_deg, nmz0] = cranetip ( X, Y, wave_dir )
%cranetip motion transfer function
% [freq_rad,amplitude,phase]=rao(dof,wdir);
%phase given in degrees
%rotational motions in rad/m
%-----%
% reading the RAO data from the given file
[~,heave_amp_q, heave_phase_q]=rao('heave', wave_dir);
[~,pitch_amp_q, pitch_phase_q]=rao('pitch', wave_dir);
[~, roll_amp_q, roll_phase_q]=rao('roll', wave_dir);

T= [ 60.0 50.0 40.0 35.0 30.0 28.0 27.0 26.0 25.0 24.5 ...
     24.0 23.5 23.0 22.0 21.0 20.0 19.0 18.0 17.0 16.5 ...
     16.0 15.5 15.0 14.5 14.0 13.5 13.0 12.5 12.0 11.5 ...
     11.0 10.5 10.0 9.5 9.0 8.5 8.0 7.5 6.5 6.0 5.5 5.0 4.5 4.0 3.5];

w_q=(2.*pi ./ T)';

T_i = 60:-0.5:3.5;    w_i = ( 2.*pi ./ T_i)';

freq_rad = w_i;
%-----%
%interpolation to have the values for every 0.5 sec interval
heave_amp = interp1( w_q, heave_amp_q, w_i, 'linear', 'extrap' );
pitch_amp = interp1( w_q, pitch_amp_q, w_i, 'linear', 'extrap' );
roll_amp = interp1( w_q, roll_amp_q, w_i, 'linear', 'extrap' );
heave_phase = interp1( w_q, heave_phase_q, w_i, 'linear', 'extrap' );
pitch_phase = interp1( w_q, pitch_phase_q, w_i, 'linear', 'extrap' );
roll_phase = interp1( w_q, roll_phase_q, w_i, 'linear', 'extrap' );

%writing in complex form
heave_comp=heave_amp.*exp(1i.*heave_phase);
pitch_comp=pitch_amp.*exp(1i.*pitch_phase);
roll_comp=roll_amp.*exp(1i.*(roll_phase));

%-----%
%crane tip location from cog
xtip = X; ytip = Y;
% xtip = -33 ; ytip = 29; ( Crane pedestal center wrt to Global
% co-ordinate)
%-----%

%-----%
%crane tip motion transfer function
Htz_comp = heave_comp - (xtip.*pitch_comp) + (ytip.*roll_comp);
Re_Htz=real(Htz_comp);
Im_Htz=imag(Htz_comp);
Htz_amp = abs(Htz_comp);
Htz_phase = angle(Htz_comp);
Htz_phase_deg = (180.*angle(Htz_comp))./pi();
%-----%
% to write it in excel
% [w, Htz_amp] = cranetip ( 1 );
% xlsxwrite('motion.xlsx', w, 'cranetip', 'A1:A114');
% xlsxwrite('motion.xlsx', Htz_amp, 'cranetip', 'B1:B114');
% [w, Htz_amp] = cranetip ( 2 );
% xlsxwrite('motion.xlsx', Htz_amp, 'cranetip', 'C1:C114');
% [w, Htz_amp] = cranetip ( 3 );
% xlsxwrite('motion.xlsx', Htz_amp, 'cranetip', 'D1:D114');
% [w, Htz_amp] = cranetip ( 4 );
% xlsxwrite('motion.xlsx', Htz_amp, 'cranetip', 'E1:E114');

```

```

% [w, Htz_amp] = cranetip ( 5 );
% xlswrite('motion.xlsx', Htz_amp, 'cranetip', 'F1:F114');
% [w, Htz_amp] = cranetip ( 6 );
% xlswrite('motion.xlsx', Htz_amp, 'cranetip', 'G1:G114');
% [w, Htz_amp] = cranetip ( 7 );
% xlswrite('motion.xlsx', Htz_amp, 'cranetip', 'H1:H114');
% [w, Htz_amp] = cranetip ( 8 );
% xlswrite('motion.xlsx', Htz_amp, 'cranetip', 'I1:I114');
% [w, Htz_amp] = cranetip ( 9 );
% xlswrite('motion.xlsx', Htz_amp, 'cranetip', 'J1:J114');
% [w, Htz_amp] = cranetip ( 10 );
% xlswrite('motion.xlsx', Htz_amp, 'cranetip', 'k1:k114');
% [w, Htz_amp] = cranetip ( 11 );
% xlswrite('motion.xlsx', Htz_amp, 'cranetip', 'l1:l114');
% [w, Htz_amp] = cranetip ( 12 );
% xlswrite('motion.xlsx', Htz_amp, 'cranetip', 'm1:m114');
% [w, Htz_amp] = cranetip ( 13 );
% xlswrite('motion.xlsx', Htz_amp, 'cranetip', 'n1:n114');

%-----%
% Vertical motion of cranetip due to the heave components from dof for
% T=11.5 s)
%-----%
% [t,w,xi,elev]=wave(amplitude, Wave period);
[t,w,xi,elev]=wave(1, 11.5);
heave_heave=real((heave_amp(30))*exp(1i*(w.*t+heave_phase(30))));
heave_pitch= xtip.*real((pitch_amp(30))*exp(1i*(w.*t+pitch_phase(30))));
cranetip_heave= heave_heave-heave_pitch;

% subplot(4,1,2);
% plot(t,elev, t,heave_heave, t, heave_pitch,'--',t,cranetip_heave,'+');
% title('heave components on cranetip, wave period T=11.5 s');
% xlabel('Time (s)'); ylabel('amplitude (m/m)');
% legend('waveelev','heave due to heave', 'heave due to pitch', 'total cranetip heave');
% grid;
%-----%

%-----%
%plotting the heave components at cranetip
freq_HZ=2.*pi() .\ freq_rad;
pitch_amp_tip=(-xtip.*pitch_amp);
roll_amp_tip= (ytip.*roll_amp);
%-----%

%-----%
%for wave direction '13' in SIMA
T_sima =[20 15 12 11 10 8.5 8 7.5 7 6.5 6 4];
freq_HZ_sima =1./T_sima;
Htz_amp_sima =[0.96 0.92 0.64 0.52 0.39 0.12 0.16 0.22 0.21 0.14 0.035 0];
%-----%

%-----%
%Plotting Crane tip motion transfer function
%-----%
% subplot(3,1,1);
% plot( freq_HZ, heave_amp,'--', freq_HZ, pitch_amp_tip,'--', freq_HZ, roll_amp_tip,'--',freq_HZ_sima, Htz_amp_sima,'-dk',
'LineWidth', 2, 'MarkerSize', 5);
% legend ( 'heave amplitude at cranetip due to heave', 'heave amplitude at cranetip due to pitch',...
% 'heave amplitude at cranetip due to roll', 'Heave at cranetip by SIMA','Combined Heave Motion amplitude at cranetip');
% hold on
% plot( freq_HZ, Htz_amp, 'LineWidth', 2.5);
% title ('Crane tip motion transfer function, [Htz], at Head Sea ', 'FontName', 'times', 'FontSize', 12, 'FontWeight', 'bold');
% grid;
% xlabel ('Wave Frequency, [Hz]', 'FontName', 'times', 'FontSize', 11, 'FontWeight', 'normal');

```

```

% ylabel ('Amplitude, [m]', 'FontName', 'times', 'FontSize', 11, 'FontWeight', 'normal');
% axis ( [0 0.3 0 1.2]);
% hold off
%-----%
% 'Phase angle for Crane tip motion transfer function
%-----%
% plot( freq_HZ, Htz_phase_deg, 'LineWidth', 2.5);
% title ('Phase angle for Crane tip motion transfer function, [Htz], at Head Sea ', 'FontName', 'times', 'FontSize', 12, 'FontWeight',
'bold');
% grid;
% xlabel ('Wave Frequency, [Hz]', 'FontName', 'times', 'FontSize', 11, 'FontWeight', 'normal');
% ylabel ('Phase, [deg]', 'FontName', 'times', 'FontSize', 11, 'FontWeight', 'normal');
% axis ( [0 0.3 -180 180]);

%-----%
%Vertical motion of mass without weight of wire% Passive Heave Compensation
%-----%
w= freq_rad;
% k = 7690; %stiffness of crane 7690 kN/m
kc=880; % stiffness of passive heave comp kN/m
cc=1200; % damping coeff of passive heave comp in kN.s/m
k=kc+1i.*w*cc;

m= 2230; %mass of object m = 223 ton% taken 10 times for study
c=0; %damping is zero;
Hmz_comp=k./((-w.^2)*m+1i.*w*c+k);
Hmz_amp=abs(Hmz_comp);
Hmz_phase=angle (Hmz_comp);
Hmz_phase_deg = (180.*angle(Hmz_comp))./pi();
%-----%
%dynamic tension transfer function
%-----%
eta_tz= Htz_comp;
eta_mz=Hmz_comp.*eta_tz;
k=kc; %stiffness of PHC
Hfd_comp=k * ( eta_tz - eta_mz );
% Hfd_comp=k *0.5* ( eta_tz - eta_mz );
Hfd_amp=abs (Hfd_comp);
Hfd_phase=angle ( Hfd_comp );
Hfd_phase_deg = (180.*angle( Hfd_comp))./pi();
%-----%
%relative displacement
%-----%
rel_comp= eta_tz - eta_mz;
rel_amp=abs(rel_comp);

%-----%
%dynamic transfer function including mass of wire
%-----%
mw = 77.8*9.81/1000; %mass of wire per unit length in kN
kwire = 7690;
EA=kwire;
kw =w.*sqrt (mw/EA);

L=20;
x=20;

c1=1+( (mw.*tan(kw.*L)) ./ (kw*m) );

c2 = (mw./ (kw.*m))-tan(kw.*L);

c3= c1./c2;

```



```

Hfdm_comp = EA .*kw .*eta_tz .* ( -sin(kw*x) + c3 .* (cos(kw.*x)) );
Hfdm_amp=abs (Hfdm_comp);
Hfdm_phase=angle ( Hfdm_comp );

%-----%
% Response spectrum
%-----%
%calling out jonswap spectra
% Hs=4; Tp=10;
% [~,specJ,~,~,del_w]=Jonswap(Hs,Tp);
% spec_resp = (Hfdm_amp.^2).* specJ';
%-----%

% subplot(3,1,2)
% plot ( freq_HZ, heave_amp,'-', freq_HZ, Htz_amp, '--', freq_HZ, Hmz_amp, 'LineWidth', 2, 'MarkerSize', 5);
% title ('Heave at different points', 'FontName', 'times', 'FontSize', 12, 'FontWeight', 'bold');
% legend('Heave at Vessel CoG', 'Heave at crane tip', ' Heave at load' );
% grid;
% xlabel ('Wave Frequency, [Hz]', 'FontName', 'times', 'FontSize', 11, 'FontWeight', 'normal');
% ylabel ('Amplitude, [m]', 'FontName', 'times', 'FontSize', 11, 'FontWeight', 'normal');
% axis ([0 0.25 0 5]);
%
% plot ( freq_HZ, Htz_amp, '--', freq_HZ, Hmz_amp.*Htz_amp, 'LineWidth', 2, 'MarkerSize', 5);
% title ('Heave at different points', 'FontName', 'times', 'FontSize', 12, 'FontWeight', 'bold');
% legend('Heave at crane tip', ' Heave at load' );
% grid;
% xlabel ('Wave Frequency, [Hz]', 'FontName', 'times', 'FontSize', 11, 'FontWeight', 'normal');
% ylabel ('Amplitude, [m]', 'FontName', 'times', 'FontSize', 11, 'FontWeight', 'normal');
% axis ([0 0.25 0 3]);

nmz0=Hmz_amp.*Htz_amp;

% subplot(4,1,1)
% plot (freq_rad, specJ );
% title ('Wave Spectrum');
%
% subplot(3,1,3)
% plot (freq_HZ, Hfdm_amp, freq_HZ, 0.8.*Hfdm_amp, freq_HZ, 0.5.*Hfdm_amp, freq_HZ, 0.2.*Hfdm_amp,'LineWidth', 2);
% legend('No AHC', '80% Residual motion', '50% Residual motion', '20% Residual motion');
% title ('Dynamic Tension Transfer Function, [Hfd]', 'FontName', 'times', 'FontSize', 12, 'FontWeight', 'bold');
% xlabel ('Wave Frequency, [Hz]', 'FontName', 'times', 'FontSize', 11, 'FontWeight', 'normal');
% ylabel ('Dynamic Load Amplitude, [kN/m]', 'FontName', 'times', 'FontSize', 11, 'FontWeight', 'normal');
% grid;
% axis ([0 0.25 0 500]);
%
% subplot(4,1,4)
% plot (freq_rad, spec_resp);
% title ('Response spectrum');
%-----%
%Comparing Crane tip motion and Motion of load-Graph
%-----%
% plot( freq_HZ, Htz_amp, freq_HZ, nmz0, '--', 'LineWidth', 2.5);
% title ('Crane tip motion transfer function, [Htz], at Head Sea ', 'FontName', 'times', 'FontSize', 12, 'FontWeight', 'bold');
% grid;
% xlabel ('Wave Frequency, [Hz]', 'FontName', 'times', 'FontSize', 11, 'FontWeight', 'normal');
% ylabel ('Amplitude, [m]', 'FontName', 'times', 'FontSize', 11, 'FontWeight', 'normal');
% axis ( [0 0.3 0 1.2]);
%-----%
%Phase angle for motion of load - Graph
%-----%
% plot( freq_HZ, Hmz_phase_deg, 'LineWidth', 2.5);
% title ('Phase angle for Crane tip motion transfer function, [Htz], at Head Sea ', 'FontName', 'times', 'FontSize', 12, 'FontWeight', 'bold');

```

```

% grid;
% xlabel ('Wave Frequency, [Hz]', 'FontName', 'times', 'FontSize', 11, 'FontWeight', 'normal');
% ylabel ('Phase, [deg]', 'FontName', 'times', 'FontSize', 11, 'FontWeight', 'normal');
% axis ( [0 0.3 -180 180]);
%-----%
%Dynamic Tension Transfer function - Graph
%-----%
% plot (freq_HZ, Hfd_amp, 'LineWidth', 2);
% title ('Dynamic Tension Transfer Function, [Hfd]','FontName', 'times', 'FontSize', 12, 'FontWeight', 'bold');
% xlabel ('Wave Frequency, [Hz]', 'FontName', 'times', 'FontSize', 11, 'FontWeight', 'normal');
% ylabel ('Dynamic Load Amplitude, [kN/m]', 'FontName', 'times', 'FontSize', 11, 'FontWeight', 'normal');
% grid;
% axis ([0 0.25 0 500]);
%-----%
%Phase angle for dynamic tension of load - Graph
%-----%
% plot( freq_HZ, Hfd_phase_deg, 'LineWidth', 2.5);
% title ('Phase angle for Crane tip motion transfer function, [Htz], at Head Sea ', 'FontName', 'times', 'FontSize', 12, 'FontWeight', 'bold');
% grid;
% xlabel ('Wave Frequency, [Hz]', 'FontName', 'times', 'FontSize', 11, 'FontWeight', 'normal');
% ylabel ('Phase, [deg]', 'FontName', 'times', 'FontSize', 11, 'FontWeight', 'normal');
% axis ( [0 0.3 -180 180]);
%-----%
%Relative displacement - Graph
%-----%
% plot (freq_HZ, rel_amp, 'LineWidth', 2);
% title ('Dynamic Tension Transfer Function, [Hfd]','FontName', 'times', 'FontSize', 12, 'FontWeight', 'bold');
% xlabel ('Wave Frequency, [Hz]', 'FontName', 'times', 'FontSize', 11, 'FontWeight', 'normal');
% ylabel ('Dynamic Load Amplitude, [kN/m]', 'FontName', 'times', 'FontSize', 11, 'FontWeight', 'normal');
% grid;
% axis ([0 0.25 0 500]);
end

```

```
%-----%
%Response variance function with Jonswap spectrum
%-----%
%-----%
function [sigma_FD, variance_FD]=varience_resp(Hs,Tp,gamma, Hfd_amp)

[~,specJ,~,~,del_w]=Jonswap(Hs,Tp,gamma);

varience_resp = sum ((Hfd_amp.^2).*specJ' .*del_w);

variance_FD=varience_resp;
sigma_FD=sqrt (varience_resp);

end
%-----%
```

```

%-----%
%Response variance function with Combined sea spectrum
%-----%
%-----%
function [sigma_FD, variance_FD]=variance_resp_cross(Hs,Tp, Hfd_amp_w, Hfd_amp_s)

[w,specJ, specJw, specJs, M0,M2,del_w]=Jonswap_cross(Hs,Tp);

variance_resp_w = sum ((Hfd_amp_w.^2).*specJw' .*del_w);
variance_resp_s = sum ((Hfd_amp_s.^2).*specJs' .*del_w);

variance_FD=variance_resp_w+variance_resp_s;
sigma_FD=sqrt (variance_FD);

end
%-----%

```

```

%-----%
% Limiting sea state calculation based on deterministic wave
%-----%

[w, Htz_amp, Hfd_amp] = cranetip (-33, 29, 13);

T=60:-0.5:3.5;
H=0.5:0.5:15; % maximum height from wave data

%-----%
%allowable dynamic tension
FD_all = 76*9.81;
%-----%
Comb(:,:)=0; m=0;
Maxim(:,:)=0; n=0;

for i=1:length(T)

    for j=1:length(H)

        FD = H(j) .* Hfd_amp(i);

        if FD<=FD_all,

            m=m+1; Comb(m,1)=T(i); Comb(m,2)=H(j);
            else
                end
        end

        n=n+1;
        Maxim(n,1)=Comb(m,1);
        Maxim(n,2)=Comb(m,2);

    end

end

%-----%
%breaking limit for deterministic waves for deep water
Hb = 0.223.* T.^2;
x = Maxim(:,1); y = Maxim(:,2);
%-----%
%conversion to deterministic to stochastic
Hsd = min(y./1.86, Hb'./1.86);
% Hsd = y./1.86;
Tpd = T./0.9;
% gamma = 2;
% Tpd=T./ (0.6673+(0.05037*gamma) - (0.006230*gamma^2) + (0.0003341*gamma^3));

%-----%
plot(x,y,x,Hb,Tpd, Hsd, 'LineWidth',2);
legend('Limiting Wave Height', 'Breaking Wave Height limit for deep water', 'Significant Wave Height with Tp');
axis ([5 25 0 40]);
grid;
set(gca,'xtick', [5:1:25]);
set(gca,'ytick', [0:1:30]);
xlabel ('Wave Period, T or Spectral peak period Tp, [s]', 'FontName', 'times', 'FontSize', 10, 'FontWeight', 'normal');
ylabel ('Wave Height or Sig. wave height, H or Hs [m]', 'FontName', 'times', 'FontSize', 10, 'FontWeight', 'normal');
%-----%

```

```

%-----%
% Limiting sea state based on stochastic approach for total sea waves
%-----%
[w, Htz_amp, Hfd_amp] = cranetip ( -33, 29, 13 );

Tp=5:1:20;
Hs=0:0.5:15; % maximum height from wave data

%-----%
%allowable dynamic tension
FD_all = 76*9.81;
%probability of exceedance
q3h=0.01;
%-----%

Comb(:,:)=0; m=0;
Maxim(:,:)=0; n=0;

for i=1:length(Tp)

    for j=1:length(Hs)

        gamma=2;
        [Sigma_c_FD,Tz] = variance (FD_all, q3h, Hs(j),Tp(i),gamma);

        [sigma_FD, varience_FD1]=varience_resp (Hs(j),Tp(i),gamma, Hfd_amp);

        if sigma_FD<=Sigma_c_FD,

            m=m+1; Comb(m,1)=Tp(i); Comb(m,2)=Hs(j);
                else
                    end
        end

        n=n+1; Maxim(n,1)=Comb(m,1); Maxim(n,2)=Comb(m,2);

    end

end

x = Maxim(:,1); y = Maxim(:,2);

%-----%
%statistical 100 year waves from Sverre lecture notes
Hs100 = [3 8 14];
Tp100 = [5 10 15];
%-----%
% plot (Tpd,Hsd, x,y,Tp100, Hs100,'LineWidth',2 );
plot (x,y,Tp100, Hs100,'LineWidth',2 );
% legend('Limiting state from deterministic wave', 'Limiting state from stochastic wave', '100 yr statistical maximum wave limit');
legend('Limiting state from stochastic wave', '100 yr statistical maximum wave limit');
grid;
set(gca,'xtick', [5:1:20]);
set(gca,'ytick', [0:1:20]);
xlabel ('Spectral peak period, Tp [s]', 'FontName', 'times', 'FontSize', 10, 'FontWeight', 'normal');
ylabel ('Significant wave height, Hs [m]', 'FontName', 'times', 'FontSize', 10, 'FontWeight', 'normal');
axis([5 20 0 20]);
%-----%

```

```

%-----%
% Limiting sea state based on stochastic waves
%-----%
[w, Htz_amp, Hfd_amp_w] = crantip ( -33, 29, 13 );
[w, Htz_amp, Hfd_amp_s] = crantip ( -33, 29, 7 );

Tp=5:1:20;
Hs=0:0.5:15; % maximum height from wave data

%-----%
%allowable dynamic tension
FD_all = 76*9.81;
%probability of exceedance
q3h=0.01;
%-----%

%-----%
% Plotting Response spectrum
%-----%
% %calling out jonswap spectra
% Hs=2; Tp=9;
% [w,specJ, specJw, specJs, M0,M2,del_w]=Jonswap_cross(Hs,Tp);
% spec_respw = (Hfd_amp_w.^2).* specJw';
% spec_resps = (Hfd_amp_s.^2).* specJs';
% total_resp=spec_respw+spec_resps;
% plot(w,total_resp);
%-----%

Comb(:,:)=0; m=0;
Maxim(:,:)=0; n=0;

for i=1:length(Tp)

    for j=1:length(Hs)

        [Sigma_c_FD,Tz] = variance_cross (FD_all, q3h, Hs(j),Tp(i));

        [~, variance_FD]=variance_resp_cross (Hs(j),Tp(i), Hfd_amp_w,Hfd_amp_s);

        sigma_FD=sqrt(variance_FD);

        if sigma_FD<=Sigma_c_FD,

            m=m+1; Comb(m,1)=Tp(i); Comb(m,2)=Hs(j);
            else
            end
        end

        n=n+1; Maxim(n,1)=Comb(m,1); Maxim(n,2)=Comb(m,2);

    end

end

x = Maxim(:,1); y = Maxim(:,2);

%-----%
%statistical 100 year waves from Sverre lecture notes
Hs100 = [3 8 14];
Tp100 = [5 10 15];
%-----%
% plot (Tpd,Hsd, x,y,Tp100, Hs100,'LineWidth',2 );
plot (x,y,Tp100, Hs100,'LineWidth',2 );
% legend('Limiting state from deterministic wave', 'Limiting state from stochastic wave', '100 yr statistical maximum wave limit');

```

```
legend('Limiting state from stochastic wave', '100 yr statistical maximum wave limit');
grid;
set(gca,'xtick', [5:1:20]);
set(gca,'ytick', [0:1:14]);
xlabel ('Spectral peak period, Tp [s]', 'FontName', 'times', 'FontSize', 10, 'FontWeight', 'normal');
ylabel ('Significant wave height, Hs [m]', 'FontName', 'times', 'FontSize', 10, 'FontWeight', 'normal');
axis([5 20 0 16]);
%-----%
```



```
%-----%
%Critical variance function for Stochastic Approach
%-----%
%-----%
function [Sigma_c_FD,Tz]=variance(FD_all, q3h, Hs,Tp,gamma)
%Critical variance
% probability of exceedance

[w,specJ,M0,M2,~]=Jonswap(Hs,Tp,gamma);

Tz=2*pi()*sqrt(M0/M2);

n3h= 10800/Tz;% number of zero crossing cycles per 3 hours

Sigma_c_FD=FD_all / sqrt(-2*log(1-(1-q3h)^(1/n3h)));

end
%-----%
```

```
%-----%
%Critical variance function for Combined sea spectrum
%-----%
%-----%
function [Sigma_c_FD,Tz]=variance_cross(FD_all, q3h, Hs,Tp)
%Critical variance
% probability of exceedance

[w,specJ, specJw, specJs, M0,M2,del_w]=Jonswap_cross(Hs,Tp);

Tz=2*pi()*sqrt(M0/M2);

n3h= 10800/Tz;% number of zero crossing cycles per 3 hours

Sigma_c_FD=FD_all / sqrt(-2*log(1-(1-q3h)^(1/n3h)));

end
%-----%
```

```

%-----%
% Wind Speed correction & Spectral Peak period randomisation & Annual
% Scatter Plot
%-----%
[YEAR,M,D,H,WSP,DIR,HS,TP,TM,DIRP,DIRM,HS1,TP1,DIRP1,HS2,TP2,DIRP2] = hindcast('Heidrun_WAM10_6529N_0732E.txt',5,
166057);

%-----%
WSP(WSP>15) = WSP(WSP>15) + 0.2.*(WSP(WSP>15) -15);
hindcast_corrected = [YEAR,M,D,H,WSP,DIR,HS,TP,TM,DIRP,DIRM,HS1,TP1,DIRP1,HS2,TP2,DIRP2];
%-----%

%-----%
%before correction
% subplot(2,1,1);
% scatter(TP, HS, '.');
% grid
% x=[2 3 4 5 6 7 8 9 10 11 12 13 14 15 16 17 18 19 20 21 22 23];
% set(gca,'XTick', x);
% title('Annual Scatter Diagram before Randomizing Tp', 'FontName', 'times', 'FontSize', 10, 'FontWeight', 'bold');
% xlabel('Spectral Peak Period, Tp [s]', 'FontName', 'times', 'FontSize', 10, 'FontWeight', 'normal');
% ylabel('Significant Wave Height, Hs [m]', 'FontName', 'times', 'FontSize', 10, 'FontWeight', 'normal');
% axis([2 23 0 20]);
% hold on;
%-----%
i = round (1. + ((log(TP ./ 3.244)) ./ 0.09525));
%after randomizing
Tp = 3.244.*exp(0.09525.*( i-0.5- rand (size(i)) ));
% %-----%
% subplot(2,1,2);
scatter(Tp,HS, '.!');
grid
x=[2 3 4 5 6 7 8 9 10 11 12 13 14 15 16 17 18 19 20 21 22 23];
set(gca,'XTick', x);
title('Annual Scatter Diagram after Randomizing Tp', 'FontName', 'times', 'FontSize', 10, 'FontWeight', 'bold');
xlabel('Spectral Peak Period, Tp [s]', 'FontName', 'times', 'FontSize', 10, 'FontWeight', 'normal');
ylabel('Significant Wave Height, Hs [m]', 'FontName', 'times', 'FontSize', 10, 'FontWeight', 'normal');
axis([2 23 0 20]);
% hold off;
%-----%

```

```

%-----%
%Annual Scatter Plot for Swell
%-----%
%-----%
[YEAR,M,D,H,WSP,DIR,HS,TP,TM,DIRP,DIRM,HS1,TP1,DIRP1,HS2,TP2,DIRP2] = hindcast('Heidrun_WAM10_6529N_0732E.txt',5,
166057);

hcb= [YEAR,M,D,H,WSP,DIR,HS,TP,TM,DIRP,DIRM,HS1,TP1,DIRP1,HS2,TP2,DIRP2] ;

i = round (1.+ ((log(TP1 ./ 3.244)) ./ 0.09525));
%after randomizing
Tp1 = 3.244.*exp(0.09525.*( i-0.5- rand (size(i)) ));

hcc = [YEAR,M,D,H,WSP,DIR,HS,TP,TM,DIRP,DIRM,HS1,TP1,DIRP1,HS2,TP2,DIRP2] ;
%-----%
i = round (1.+ ((log(TP2 ./ 3.244)) ./ 0.09525));
%after randomizing
Tp2 = 3.244.*exp(0.09525.*( i-0.5- rand (size(i)) ));

hccs = [YEAR,M,D,H,WSP,DIR,HS,TP,TM,DIRP,DIRM,HS1,TP1,DIRP1,HS2,TP2,DIRP2] ;
%-----%
Hsw=hcc(:,12);
Tpw=hcc(:,13);
Hss=hccs(:,15);
Tps=hccs(:,16);
%-----%
subplot(2,1,1);
scatter(Tpw, Hsw, '!');
grid
x=[1 2 3 4 5 6 7 8 9 10 11 12 13 14 15 16 17 18 19 20];
set(gca,'XTick', x);
title('Annual Scatter Diagram for Wind Sea', 'FontName', 'times', 'FontSize', 10, 'FontWeight', 'bold');
xlabel('Spectral Peak Period, Tp [s]', 'FontName', 'times', 'FontSize', 10, 'FontWeight', 'normal');
ylabel('Significant Wave Height, Hs [m]', 'FontName', 'times', 'FontSize', 10, 'FontWeight', 'normal');
axis([0 20 0 18]);
%-----%
subplot(2,1,2);
scatter(Tps, Hss, '!');
grid
x=[1 2 3 4 5 6 7 8 9 10 11 12 13 14 15 16 17 18 19 20 21 22 23 24 25];
set(gca,'XTick', x);
title('Annual Scatter Diagram for Swell Sea', 'FontName', 'times', 'FontSize', 10, 'FontWeight', 'bold');
xlabel('Spectral Peak Period, Tp [s]', 'FontName', 'times', 'FontSize', 10, 'FontWeight', 'normal');
ylabel('Significant Wave Height, Hs [m]', 'FontName', 'times', 'FontSize', 10, 'FontWeight', 'normal');
axis([0 25 0 12]);
%-----%

```

```
%-----%  
%Scatter Table in month wise  
%-----%
```

```
function [scatter] =scattable(month)
```

```
[YEAR,M,D,H,WSP,DIR,HS,TP,TM,DIRP,DIRM,HS1,TP1,DIRP1,HS2,TP2,DIRP2] = hindcast('Heidrun_WAM10_6529N_0732E.txt',5, 166057);
```

```
hcb= [YEAR,M,D,H,WSP,DIR,HS,TP,TM,DIRP,DIRM,HS1,TP1,DIRP1,HS2,TP2,DIRP2] ;
```

```
i = round (1.+ ((log(TP ./ 3.244)) ./ 0.09525));
```

```
%after randomizing
```

```
TP = 3.244.*exp(0.09525.*( i-0.5- rand (size(i)) ) );
```

```
hcc = [YEAR,M,D,H,WSP,DIR,HS,TP,TM,DIRP,DIRM,HS1,TP1,DIRP1,HS2,TP2,DIRP2] ;
```

```
%Annual Scatter Table
```

```
scatter (,:) = 0; m = 0; n =0;
```

```
mo=hcc(:,2);
```

```
hccm = hcc((mo==month),:,:);
```

```
t=2:1:22;
```

```
h=0:0.5:16.5;
```

```
for i= 1:length(t)
```

```
    n =n+1;
```

```
    Tp=hccm(:,8);
```

```
    Tpg = hccm(Tp> t(i), :);
```

```
    Tp=Tpg(:,8);
```

```
    Tpl = Tpg(Tp<= t(i)+1, :);
```

```
for j = 1:length(h)
```

```
    HS=Tpl(:,7);
```

```
    Hsg =Tpl(HS>h(j), :);
```

```
    HS= Hsg(:,7);
```

```
    Hsl =Hsg (HS<=h(j)+0.5, :);
```

```
    HS= Hsl(:,7);
```

```
    m=m+1;
```

```
if m<=length(h)
```

```
    m;
```

```
else
```

```
    m=m-length(h);
```

```
    end
```

```
    scatter(m,n)=length(HS);
```

```
    end
```

```
end
```

```
end
```

```

%-----%
% Monthly Scatter Plot from Hindcast Data
%-----%
%-----%
[TP, HS] = Scattermonth (1);
subplot(6,2,1);
scatter(TP, HS, '.');
grid
x=[2 3 4 5 6 7 8 9 10 11 12 13 14 15 16 17 18 19 20 21 22 23];
y=[0:5:20];
set(gca,'XTick', x);
set(gca,'YTick', y);
title('January');
xlabel('Tp [s]', 'FontSize', 10);
ylabel('Hs [m]', 'FontSize', 10);
axis([2 23 0 20]);
%-----%
[TP, HS] = Scattermonth (2);
subplot(6,2,3);
scatter(TP, HS, '.');
grid
x=[2 3 4 5 6 7 8 9 10 11 12 13 14 15 16 17 18 19 20 21 22 23];
y=[0:5:20];
set(gca,'XTick', x);
set(gca,'YTick', y);
title('February');
xlabel('Tp [s]', 'FontSize', 10);
ylabel('Hs [m]', 'FontSize', 10);
axis([2 23 0 20]);
%-----%
%-----%
[TP, HS] = Scattermonth (3);
subplot(6,2,5);
scatter(TP, HS, '.');
grid
x=[2 3 4 5 6 7 8 9 10 11 12 13 14 15 16 17 18 19 20 21 22 23];
y=[0:5:20];
set(gca,'XTick', x);
set(gca,'YTick', y);
title('March');
xlabel('Tp [s]', 'FontSize', 10);
ylabel('Hs [m]', 'FontSize', 10);
axis([2 23 0 20]);
%-----%
[TP, HS] = Scattermonth (4);
subplot(6,2,7);
scatter(TP, HS, '.');
grid
x=[2 3 4 5 6 7 8 9 10 11 12 13 14 15 16 17 18 19 20 21 22 23];
y=[0:5:20];
set(gca,'XTick', x);
set(gca,'YTick', y);
title('April');
xlabel('Tp [s]', 'FontSize', 10);
ylabel('Hs [m]', 'FontSize', 10);
axis([2 23 0 20]);
%-----%
[TP, HS] = Scattermonth (5);
subplot(6,2,9);
scatter(TP, HS, '.');
grid
x=[2 3 4 5 6 7 8 9 10 11 12 13 14 15 16 17 18 19 20 21 22 23];
y=[0:5:20];
set(gca,'XTick', x);

```

```

set(gca,'YTick', y);
title('May');
xlabel('Tp [s]', 'FontSize', 10);
ylabel('Hs [m]', 'FontSize', 10);
axis([2 23 0 20]);
%-----%
[TP, HS] = Scattermonth (6);
subplot(6,2,11);
scatter(TP, HS, '.');
grid
x=[2 3 4 5 6 7 8 9 10 11 12 13 14 15 16 17 18 19 20 21 22 23];
y=[0:5:20];
set(gca,'XTick', x);
set(gca,'YTick', y);
title('June');
xlabel('Tp [s]', 'FontSize', 10);
ylabel('Hs [m]', 'FontSize', 10);
axis([2 23 0 20]);
%-----%
[TP, HS] = Scattermonth (7);
subplot(6,2,2);
scatter(TP, HS, '.');
grid
x=[2 3 4 5 6 7 8 9 10 11 12 13 14 15 16 17 18 19 20 21 22 23];
y=[0:5:20];
set(gca,'XTick', x);
set(gca,'YTick', y);
title('July');
xlabel('Tp [s]', 'FontSize', 10);
ylabel('Hs [m]', 'FontSize', 10);
axis([2 23 0 20]);
%-----%
[TP, HS] = Scattermonth (8);
subplot(6,2,4);
scatter(TP, HS, '.');
grid
x=[2 3 4 5 6 7 8 9 10 11 12 13 14 15 16 17 18 19 20 21 22 23];
y=[0:5:20];
set(gca,'XTick', x);
set(gca,'YTick', y);
title('August');
xlabel('Tp [s]', 'FontSize', 10);
ylabel('Hs [m]', 'FontSize', 10);
axis([2 23 0 20]);
%-----%
[TP, HS] = Scattermonth (9);
subplot(6,2,6);
scatter(TP, HS, '.');
grid
x=[2 3 4 5 6 7 8 9 10 11 12 13 14 15 16 17 18 19 20 21 22 23];
y=[0:5:20];
set(gca,'XTick', x);
set(gca,'YTick', y);
title('Septemper');
xlabel('Tp [s]', 'FontSize', 10);
ylabel('Hs [m]', 'FontSize', 10);
axis([2 23 0 20]);
%-----%
[TP, HS] = Scattermonth (10);
subplot(6,2,8);
scatter(TP, HS, '.');
grid
x=[2 3 4 5 6 7 8 9 10 11 12 13 14 15 16 17 18 19 20 21 22 23];
y=[0:5:20];

```

```

set(gca,'XTick', x);
set(gca,'YTick', y);
title('October');
xlabel('Tp [s]', 'FontSize', 10);
ylabel('Hs [m]', 'FontSize', 10);
axis([2 23 0 20]);
%-----%
[TP, HS] = Scattermonth (11);
subplot(6,2,10);
scatter(TP, HS, '.');
grid
x=[2 3 4 5 6 7 8 9 10 11 12 13 14 15 16 17 18 19 20 21 22 23];
y=[0:5:20];
set(gca,'XTick', x);
set(gca,'YTick', y);
title('November');
xlabel('Tp [s]', 'FontSize', 10);
ylabel('Hs [m]', 'FontSize', 10);
axis([2 23 0 20]);
%-----%
[TP, HS] = Scattermonth (12);
subplot(6,2,12);
scatter(TP, HS, '.');
grid
x=[2 3 4 5 6 7 8 9 10 11 12 13 14 15 16 17 18 19 20 21 22 23];
y=[0:5:20];
set(gca,'XTick', x);
set(gca,'YTick', y);
title('December');
xlabel('Tp [s]', 'FontSize', 10);
ylabel('Hs [m]', 'FontSize', 10);
axis([2 23 0 20]);

```



```

%-----%
%Function for Scatter plot in monthwise
%-----%
function [TP, HS] = Scattermonth (month)

[YEAR,M,D,H,WSP,DIR,HS,TP,TM,DIRP,DIRM,HS1,TP1,DIRP1,HS2,TP2,DIRP2] = hindcast('Heidrun_WAM10_6529N_0732E.txt',5,
166057);

%-----%
WSP(WSP>15) = WSP(WSP>15) + 0.2.*(WSP(WSP>15) -15);

i = round (1.+ ((log(TP) ./ 3.244) ./ 0.09525));
%after randomizing
Tp = 3.244.*exp(0.09525.*( i-0.5- rand (size(i)) ));

hindcast_corrected = [YEAR,M,D,H,WSP,DIR,HS,Tp,TM,DIRP,DIRM,HS1,TP1,DIRP1,HS2,TP2,DIRP2];

hc = hindcast_corrected;

hc_scatter_month = hc(hc(:,2)==month, :);

%total sea Tp & HS

TP = hc_scatter_month (:,8);
HS = hc_scatter_month (:,7);

end

```

```

%-----%
% Matlab Script for Annual Scatter Table%
%-----%

[YEAR,M,D,H,WSP,DIR,HS,TP,TM,DIRP,DIRM,HS1,TP1,DIRP1,HS2,TP2,DIRP2] = hindcast('Heidrun_WAM10_6529N_0732E.txt',979,
166057);

hcb= [YEAR,M,D,H,WSP,DIR,HS,TP,TM,DIRP,DIRM,HS1,TP1,DIRP1,HS2,TP2,DIRP2] ;

i = round (1.+ ((log(TP ./ 3.244)) ./ 0.09525));
%after randomizing
Tp = 3.244.*exp(0.09525.*( i-0.5- rand (size(i)) ) );
%
hcc = [YEAR,M,D,H,WSP,DIR,HS,TP,TM,DIRP,DIRM,HS1,TP1,DIRP1,HS2,TP2,DIRP2] ;

%Annual Scatter Table
scatter (,:)= 0;      m = 0; n =0;

t=2:1:22;
h=0:0.5:16.5;

for i= 1:length(t)

    n =n+1;

    Tp=hcc(:,8);
    Tpg = hcc(Tp> t(i), :);

    Tp=Tpg(:,8);
    Tpl = Tpg(Tp<= t(i)+1, :);

    for j = 1:length(h)

        HS=Tpl(:,7);
        Hsg =Tpl(HS>h(j), :);

        HS= Hsg(:,7);
        Hsl =Hsg (HS<=h(j)+0.5, :);

        HS= Hsl(:,7);

        m=m+1;

        if m<=length(h)
            m;
        else
            m=m-length(h);
            end
        scatter(m,n)=length(HS);

    end

end
end

```

```

%-----%
%Calculating percentage of time seastates below particular level
%-----%
[YEAR,M,D,H,WSP,DIR,HS,TP,TM,DIRP,DIRM,HS1,TP1,DIRP1,HS2,TP2,DIRP2] = hindcast('Heidrun_WAM10_6529N_0732E.txt',5,
166057);

hcb= [YEAR,M,D,H,WSP,DIR,HS,TP,TM,DIRP,DIRM,HS1,TP1,DIRP1,HS2,TP2,DIRP2] ;

i = round (1.+ ((log(TP ./ 3.244)) ./ 0.09525));
%after randomizing
Tp = 3.244.*exp(0.09525.*( i-0.5- rand (size(i)) ) );

hcc = [YEAR,M,D,H,WSP,DIR,HS,TP,TM,DIRP,DIRM,HS1,TP1,DIRP1,HS2,TP2,DIRP2] ;

%Annual Scatter Table
percentage (:,:) = 0;      m = 0; n =0;

mo=hcc(:,2);

month =1:1:12;

h=0.5:0.5:15;

for i= 1:length(month)

    n =n+1;

    hccm = hcc((mo==month(i)),:,:);
    hrs_total = 3.* length (hccm);

    for j = 1:length(h)

        HS= hccm (:,7);
        Hs_p=hccm (HS<=h(j), :);

        HS=  Hs_p (:,7);

        m=m+1;

        if m<=length(h)
            m;
        else
            m=m-length(h);
        end
        hrs_hs=3.*length(HS);
        percentage (m,n)= 100.* hrs_hs ./ hrs_total;
        end

end

end

```

```

%-----%
% Duration calculation to complete an operation & Average Duration
% calculation
%-----%
function [noofwin_year, count, whours, time, atime] = noofw_month_duration(duration, hs)

%-----%
[YEAR,M,D,H,WSP,DIR,HS,TP,TM,DIRP,DIRM,HS1,TP1,DIRP1,HS2,TP2,DIRP2] = hindcast('Heidrun_WAM10_6529N_0732E.txt',5,
166057);

hcb= [YEAR,M,D,H,WSP,DIR,HS,TP,TM,DIRP,DIRM,HS1,TP1,DIRP1,HS2,TP2,DIRP2] ;

i = round (1.+ ((log(TP ./ 3.244)) ./ 0.09525));
%after randomizing
Tp = 3.244.*exp(0.09525.*( i-0.5- rand (size(i)) ));

hcc = [YEAR,M,D,H,WSP,DIR,HS,TP,TM,DIRP,DIRM,HS1,TP1,DIRP1,HS2,TP2,DIRP2] ;
%-----%
y=1958:1:2013;
noofwin_year(:,,:)=0;
ym=0;
time(:,:)=0;
atime(:,:)=0;

for yi = 1:length(y)
ym =ym +1;
noofwin_year(ym,1) = y(yi);
time(ym,1)=y(yi);

hccyear=hcc(YEAR==y(yi), :);
M=hccyear(:,2);

mo=1:1:12;
noofwin_month(:,:)=0;
mm=0;

for mi = 1:length(mo)
mm =mm +1;
noofwin_month(mm,1) = mo(mi);

hccmonth=hccyear(M==mo(mi), :);
    if isempty (hccmonth)
        break
    end
HS=hccmonth(:,7);
D =hccmonth(:,3);
H=hccmonth(:,4);
YE=hccmonth(:,1);
%-----%

m=0; n=1;
i=1; l=0;
count(:,:)=0;
x=length(HS);
timem(:,:)=0;

if HS(i) <=hs

    while HS(i) <=hs
        i=i+1;
        k=i-1;

                if i==1+x;
                    m=m+1;

```

```

        count(m,1) =k-l;
        break
    end

if HS(i) > hs
    m=m+1;
    count(m,1) =k-l;

    while HS(i) >hs
        i=i+1;

        if i==1+x;
            l=i-1;
            count(m,2) = i-1-k;
            break
        end

        end
        l=i-1;
        count(m,2) = i-1-k;

else

end
    if i==1+x;
        break
    end
end
else

while HS(i) >hs
    i=i+1;
    k=i-1;

    if i==1+x;
        m=m+1;
        count(m,2) =k-l;
        break
    end

if HS(i) <= hs
    m=m+1;
    count(m,2) =k-l;

    while HS(i) <=hs
        i=i+1;

        if i==1+x;
            l=i-1;
            count(m+1,1) = i-1-k;
            break
        end

        end
        l=i-1;
        count(m+1,1) = i-1-k;

else

end
    if i==1+x;
        break
    end
end

```

```

        end
end
end

whours = 3.*count;
noofwin= (whours-mod(whours, duration))./duration;
tot_noofwin=sum(noofwin(:,1));
avgduration = mean(whours(whours(:,1)~=0));
%-----%
% [row]=find(whours(:,1)>=72);
% timev=[row];
% if isempty(timev)
%     timem=0;
% elseif timev(1)==1
%     timem=72;
% else
%     rn=timev(1);
%     bm=whours(1:rn-1, :);
%     timem=72+sum(sum(bm));
% end
% timep(mm,1)=timem;

%-----%
[row]=find(whours(:,1)>=48);
timev=[row];
if isempty(timev)
    timem=0;
elseif timev(1)==1 && whours(1) < 72
    rn=1;
    if whours(rn,1) >=48 && whours(rn,1) <72
        cm=whours(rn+1:end, :);
        [rowcm]=find(cm(:,1)>=24);
        timew=[rowcm];

        if isempty(timew)
            timem=0;
        else
            rnc=timew(1) +timev(1);
            bm=whours(1:rnc-1, :);
            timem=24+sum(sum(bm));
        end
    end
else
    end

elseif timev(1)==1 && whours(1) >= 72
    timem=72;

elseif timev(1) > 1
    rn=timev(1);
    if whours(rn,1) >=72
        bm=whours(1:rn-1, :);
        timem=72+sum(sum(bm));
    elseif whours(rn,1) >=48 && whours(rn,1) <72
        cm=whours(rn+1:end, :);
        [rowcm]=find(cm(:,1)>=24);
        timew=[rowcm];

        if isempty(timew)
            timem=0;
        else
            rnc=timew(1) +timev(1);
            bm=whours(1:rnc-1, :);
            timem=24+sum(sum(bm));
        end
    end
end
end
end

```

```

    end
  else
  end
else
end
timep(mm,1)=timem;
%-----%
noofwin_month(mm,2) = tot_noofwin;
% totno_month = length (hccmonth(D==10 & H==6, :));
% noofwin_month(mm,3) =totno_month;
% noofwin_month(mm,4) = round(tot_noofwin ./ totno_month);
aa=noofwin_month(:,2);
bb=timep(:,1)./24;
avgdurationtable(mm,2)=avgduration;
cc=avgdurationtable(:,2);
end

noofwin_year(y,2) = aa(1);
noofwin_year(y,3) = aa(2);
noofwin_year(y,4) = aa(3);
noofwin_year(y,5) = aa(4);
noofwin_year(y,6) = aa(5);
noofwin_year(y,7) = aa(6);
noofwin_year(y,8) = aa(7);
noofwin_year(y,9) = aa(8);
noofwin_year(y,10) = aa(9);
noofwin_year(y,11) = aa(10);
noofwin_year(y,12) = aa(11);
noofwin_year(y,13) = aa(12);

time(y,2) =bb(1);
time(y,3) =bb(2);
time(y,4) =bb(3);
time(y,5) =bb(4);
time(y,6) =bb(5);
time(y,7) =bb(6);
time(y,8) =bb(7);
time(y,9) =bb(8);
time(y,10) =bb(9);
time(y,11) =bb(10);
time(y,12) =bb(11);
time(y,13) =bb(12);

atime(y,2) =cc(1);
atime(y,3) =cc(2);
atime(y,4) =cc(3);
atime(y,5) =cc(4);
atime(y,6) =cc(5);
atime(y,7) =cc(6);
atime(y,8) =cc(7);
atime(y,9) =cc(8);
atime(y,10) =cc(9);
atime(y,11) =cc(10);
atime(y,12) =cc(11);
atime(y,13) =cc(12);

```

```

end

% plot(mo, noofwin_year(:,2:end));
% grid;
% x=[1 2 3 4 5 6 7 8 9 10 11 12];
% set(gca,'XTick', x);
% axis([1 12 0 30]);
% xlabel ('Month');
% ylabel ('No of Windows in a month of a year');

%------%
%mean value

% cc= time(:,2:end);
% cc(cc==0)=35;
% nonz(1)=nnz(cc(:,1));
% nonz(2)=nnz(cc(:,2));
% nonz(3)=nnz(cc(:,3));
% nonz(4)=nnz(cc(:,4));
% nonz(5)=nnz(cc(:,5));
% nonz(6)=nnz(cc(:,6));
% nonz(7)=nnz(cc(:,7));
% nonz(8)=nnz(cc(:,8));
% nonz(9)=nnz(cc(:,9));
% nonz(10)=nnz(cc(:,10));
% nonz(11)=nnz(cc(:,11));
% nonz(12)=nnz(cc(:,12));
%
% mean=sum(cc)./nonz;
%
%
% plot(mo,cc);
% grid;
% x=[1 2 3 4 5 6 7 8 9 10 11 12];
% set(gca,'XTick', x);
% axis([1 12 0 35]);
% xlabel ('Month');
% ylabel ('No of days in a month of a year');
% hold on
% plot(mo, mean, mo, max(time(:,2:end)), mo, min(cc),'LineWidth', 2)
% hold off
end

```



```

%-----%
% Number of windows in year
%-----%
function [noofwin_year] =noofwyear(hslimit)

%-----%
[YEAR,M,D,H,WSP,DIR,HS,TP,TM,DIRP,DIRM,HS1,TP1,DIRP1,HS2,TP2,DIRP2] = hindcast('Heidrun_WAM10_6529N_0732E.txt',5,
166057);

hcb= [YEAR,M,D,H,WSP,DIR,HS,TP,TM,DIRP,DIRM,HS1,TP1,DIRP1,HS2,TP2,DIRP2] ;

i = round (1.+ ((log(TP ./ 3.244)) ./ 0.09525));
%after randomizing
Tp = 3.244.*exp(0.09525.*( i-0.5- rand (size(i)) ));

hcc = [YEAR,M,D,H,WSP,DIR,HS,TP,TM,DIRP,DIRM,HS1,TP1,DIRP1,HS2,TP2,DIRP2] ;
%-----%
y=1958:1:2013;
noofwin_year(:,:)=0;
ym=0;

for yi = 1:length(y)
ym =ym +1;
noofwin_year(ym,1) = y(yi);

hccyear=hcc(YEAR==y(yi), :);
HS=hccyear(:,7);

%-----%

m=0; n=1;
i=1; l=0;
count(:,:)=0;
x=length(HS);

if HS(i) <=hslimit

while HS(i) <=hslimit
    i=i+1;
    k=i-1;

        if i==1+x;
            m=m+1;
            count(m,1) =k-l;
            break
        end

if HS(i) > hslimit
    m=m+1;
    count(m,1) =k-l;

while HS(i) >hslimit
    i=i+1;

        if i==1+x;
            l=i-1;
            count(m,2) = i-1-k;
            break
        end

end
l=i-1;

```

```

        count(m,2) = i-1-k;

    else

    end

        if i==1+x;
            break
        end
end
else
    while HS(i) > hslimit
        i=i+1;
        k=i-1;

        if i==1+x;
            m=m+1;
            count(m,2) = k-l;
            break
        end

        if HS(i) <= hslimit
            m=m+1;
            count(m,2) = k-l;

            while HS(i) <= hslimit
                i=i+1;

                if i==1+x;
                    l=i-1;
                    count(m,1) = i-1-k;
                    break
                end

            end

            l=i-1;
            count(m,1) = i-1-k;

        else

    end

        if i==1+x;
            break
        end
end
end

whours = 3.*count;
noofwin= (whours-mod(whours,12))/12;
tot_noofwin=sum(noofwin(:,1));

noofwin_year(y,2) = tot_noofwin;
end
end

```

```

%-----%
% Number of windows in monthwise
%-----%
function [noofwin_year, count, whours, time] = noofw_month(duration, hs)

%-----%
[YEAR,M,D,H,WSP,DIR,HS,TP,TM,DIRP,DIRM,HS1,TP1,DIRP1,HS2,TP2,DIRP2] = hindcast('Heidrun_WAM10_6529N_0732E.txt',5,
166057);

hcb= [YEAR,M,D,H,WSP,DIR,HS,TP,TM,DIRP,DIRM,HS1,TP1,DIRP1,HS2,TP2,DIRP2] ;

i = round (1.+ ((log(TP ./ 3.244)) ./ 0.09525));
%after randomizing
Tp = 3.244.*exp(0.09525.*( i-0.5- rand (size(i)) ));

hcc = [YEAR,M,D,H,WSP,DIR,HS,TP,TM,DIRP,DIRM,HS1,TP1,DIRP1,HS2,TP2,DIRP2] ;
%-----%
y=1958:1:2013;
noofwin_year(:,:)=0;
ym=0;
time(:,:)=0;

for yi = 1:length(y)
ym =ym +1;
noofwin_year(ym,1) = y(yi);
time(ym,1)=y(yi);

hccyear=hcc(YEAR==y(yi), :);
M=hccyear(:,2);

mo=1:1:12;
noofwin_month(:,:)=0;
mm=0;

for mi = 1:length(mo)
mm =mm +1;
noofwin_month(mm,1) = mo(mi);

hccmonth=hccyear(M==mo(mi), :);
    if isempty (hccmonth)
        break
    end
HS=hccmonth(:,7);
D =hccmonth(:,3);
H=hccmonth(:,4);
YE=hccmonth(:,1);
%-----%

m=0; n=1;
i=1; l=0;
count(:,:)=0;
x=length(HS);
timem(:,:)=0;

if HS(i) <=hs

    while HS(i) <=hs
        i=i+1;
        k=i-1;

        if i==1+x;
            m=m+1;
            count(m,1) =k-l;
            break

```

```

                end

if HS(i) > hs
    m=m+1;
    count(m,1) =k-l;

    while HS(i) >hs
        i=i+1;

                if i==1+x;
                l=i-1;
                count(m,2) = i-1-k;
                break
                end

        end
        l=i-1;
        count(m,2) = i-1-k;

else

end

        if i==1+x;
        break
        end

end
else

while HS(i) >hs
    i=i+1;
    k=i-1;

    if i==1+x;
        m=m+1;
        count(m,2) =k-l;
        break
    end

if HS(i) <= hs
    m=m+1;
    count(m,2) =k-l;

    while HS(i) <=hs
        i=i+1;

                if i==1+x;
                l=i-1;
                count(m+1,1) = i-1-k;
                break
                end

        end
        l=i-1;
        count(m+1,1) = i-1-k;

else

end

        if i==1+x;
        break
        end

end
end

```

end

```
whours = 3.*count;
noofwin= (whours-mod(whours, duration))./duration;
tot_noofwin=sum(noofwin(:,1));
%------%
%72 hour operation in one go
%------%
% [row]=find(whours(:,1)>=72);
% timev=[row];
% if isempty(timev)
%     timem=0;
% elseif timev(1)==1
%     timem=72;
% else
%     rn=timev(1);
%     bm=whours(1:rn-1, :);
%     timem=72+sum(sum(bm));
% end
% timep(mm,1)=timem;
%------%
%48+24 hour operation split
%------%
% [row]=find(whours(:,1)>=48);
% timev=[row];
% if isempty(timev)
%     timem=0;
% elseif timev(1)==1 && whours(1) < 72
%     rn=1;
%     if whours(rn,1) >=48 && whours(rn,1) < 72
%         cm=whours(rn+1:end, :);
%         [rowcm]=find(cm(:,1)>=24);
%         timew=[rowcm];
%
%         if isempty(timew)
%             timem=0;
%         else
%             rnc=timew(1) +timev(1);
%             bm=whours(1:rnc-1, :);
%             timem=24+sum(sum(bm));
%         end
%     else
%         end
%
% elseif timev(1)==1 && whours(1) >= 72
%     timem=72;
%
% elseif timev(1) > 1
%     rn=timev(1);
%     if whours(rn,1) >=72
%         bm=whours(1:rn-1, :);
%         timem=72+sum(sum(bm));
%     elseif whours(rn,1) >=48 && whours(rn,1) < 72
%         cm=whours(rn+1:end, :);
%         [rowcm]=find(cm(:,1)>=24);
%         timew=[rowcm];
%
%         if isempty(timew)
%             timem=0;
%         else
%             rnc=timew(1) +timev(1);
%             bm=whours(1:rnc-1, :);
%             timem=24+sum(sum(bm));
%         end
%     end
% end
```

```

% else
% end
% else
% end
% timep(mm,1)=timem;
%------%
%24+24+24 hour operation split
%------%
[row]=find(whours(:,1)>=24);
timev=[row];
if isempty(timev)
    timem=0;
elseif timev(1)==1 && whours(1) < 72
    rn=1;
    if whours(rn,1) >=48 && whours(rn,1) <72
        cm=whours(rn+1:end, :);
        [rowcm]=find(cm(:,1)>=24);
        timew=[rowcm];

        if isempty(timew)
            timem=0;
        else
            rnc=timev(1) +timev(1);
            bm=whours(1:rnc-1, :);
            timem=24+sum(sum(bm));
        end
    else
        cm=whours(rn+1:end, :);
        [rowcm48]=find(cm(:,1)>=48);
        [rowcm24]=find(cm(:,1)>=24);
        time48=[rowcm48];
        time24=[rowcm24];

        if (isempty(time24) && ~isempty(time48))
            timex= [rowcm48];
            rnc=timev(1) +timev(1);
            bm=whours(1:rnc-1, :);
            timem=48+sum(sum(bm));
        elseif ~isempty(time48) && time48(1) <= time24(1)
            timex= [rowcm48];
            rnc=timev(1) +timev(1);
            bm=whours(1:rnc-1, :);
            timem=48+sum(sum(bm));
        else
            timex1= [rowcm24];
            if isempty(timex1)
                timem=0;
            else
                rns=timex1(1);
                cms=whours(rn+rns+1:end, :);
                [rowcms]=find(cms(:,1)>=24);
                timex=[rowcms];
                if isempty(timex)
                    timem=0;
                else
                    rnc= timex(1)+timex1(1) +timev(1);
                    bm=whours(1:rnc-1, :);
                    timem=24+sum(sum(bm));
                end
            end
        end
    end
end
elseif timev(1)==1 && whours(1) >= 72

```

```

timem=72;

elseif timev(1) >1
    rn=timev(1);
    if whours(rn,1) >=72
        bm=whours(1:rn-1, :);
        timem=72+sum(sum(bm));
    elseif whours(rn,1) >=48 && whours(rn,1) <72
        cm=whours(rn+1:end, :);
        [rowcm]=find(cm(:,1)>=24);
        timew=[rowcm];

        if isempty(timew)
            timem=0;
        else
            rnc=timew(1) +timev(1);
            bm=whours(1:rnc-1, :);
            timem=24+sum(sum(bm));
        end
    else
        cm=whours(rn+1:end, :);
        [rowcm48]=find(cm(:,1)>=48);
        [rowcm24]=find(cm(:,1)>=24);
        time48=[rowcm48];
        time24=[rowcm24];

        if (isempty(time24) && ~isempty(time48))
            timex= [rowcm48];
            rnc=timex(1) +timev(1);
            bm=whours(1:rnc-1, :);
            timem=48+sum(sum(bm));
        elseif ~isempty(time48) && time48(1) <= time24(1)
            timex= [rowcm48];
            rnc=timex(1) +timev(1);
            bm=whours(1:rnc-1, :);
            timem=48+sum(sum(bm));
        else
            timex1= [rowcm24];
            if isempty(timex1)
                timem=0;
            else
                rns=timex1(1);
                cms=whours(rn+rns+1:end, :);
                [rowcms]=find(cms(:,1)>=24);
                timex=[rowcms];
                if isempty(timex)
                    timem=0;
                else
                    rnc= timex(1)+timex1(1) +timev(1);
                    bm=whours(1:rnc-1, :);
                    timem=24+sum(sum(bm));
                end
            end
        end
    end
end
else
end
timep(mm,1)=timem;
%-----%
noofwin_month(mm,2) = tot_noofwin;
% totno_month = length (hccmonth(D==10 & H==6, :));
% noofwin_month(mm,3) =totno_month;
% noofwin_month(mm,4) = round(tot_noofwin ./ totno_month);

```

```
aa=noofwin_month(:,2);
bb=timep(:,1)./24;
```

```
end
```

```
noofwin_year(ym,2) = aa(1);
noofwin_year(ym,3) = aa(2);
noofwin_year(ym,4) = aa(3);
noofwin_year(ym,5) = aa(4);
noofwin_year(ym,6) = aa(5);
noofwin_year(ym,7) = aa(6);
noofwin_year(ym,8) = aa(7);
noofwin_year(ym,9) = aa(8);
noofwin_year(ym,10) = aa(9);
noofwin_year(ym,11) = aa(10);
noofwin_year(ym,12) = aa(11);
noofwin_year(ym,13) = aa(12);
```

```
time(ym,2) = bb(1);
time(ym,3) = bb(2);
time(ym,4) = bb(3);
time(ym,5) = bb(4);
time(ym,6) = bb(5);
time(ym,7) = bb(6);
time(ym,8) = bb(7);
time(ym,9) = bb(8);
time(ym,10) = bb(9);
time(ym,11) = bb(10);
time(ym,12) = bb(11);
time(ym,13) = bb(12);
```

```
end
```

```
% plot(mo, noofwin_year(:,2:end));
% grid;
% x=[1 2 3 4 5 6 7 8 9 10 11 12];
% set(gca,'XTick', x);
% axis([1 12 0 30]);
% xlabel ('Month');
% ylabel ('No of Windows in a month of a year');
```

```
%-----%
```

```
end
```